Mechanism and mediated mechanistic analysis of HIV Nef

Thesis

UNRESTRICTED.

Molecular and mechanistic analysis of HIV Nef

Alison Simmons

Thesis submitted in partial requirement for degree of Doctor of Philosophy, Open University, 2003.

[Sponsor: Weatherall Institute of Molecular medicine]

Submission date: 10 April 2003
Award date: 25 February 2004

ProQuest LLC.
789 East Eisenhower Parkway
P.O. Box 1346
Ann Arbor, MI 48106 – 1346

Molecular and Mechanistic Analysis of HIV Nef

Abstract

The *nef* gene of HIV is required for complete viral pathogenicity. As an accessory gene with no known paradigm its principle function has been enigmatic. Nef is capable of a variety of in vitro effects including CD4 downregulation, MHC I downregulation, alteration of T cell signalling activity and enhancement of viral infectivity. The effect of Nef on host CD4 T cell signalling paths is intriguing as it is the earliest expressed HIV gene and because HIV replicates to high levels in activated host cells. An effect of Nef on T cell activation state could dictate host T cell fate tipping the balance between productive viral infection and post-integration latency. Although Nef can form in vitro interactions with a variety of T cell signalling proteins in vivo evidence for signalling path activation has been inconclusive mainly due to the limitations of the experimental systems used to address the question.

An in vivo role for Nef in alteration of T cell activation state should lead to gene expression changes in the host cell. Large scale gene expression profiling was used to monitor T cell gene expression after controlled expression of Nef using the tetracycline inducible system. Nef induces a widespread transcriptional program in T cells. Comparison of this profile with reference T cell activation states reveals a strong identity to the gene expression profile of Jurkat activated by anti-CD3 cross-linking. Gene expression profiling was used to explore the mechanism by which Nef mediates this effect. After cyclosporin treatment the profile was attenuated. A similar effect was observed after Nef expression in Jurkat T cells genetically deficient in ZAP-70 and functionally deficient in TCRζ. Expression of a mutant defective in a functional SH3 binding domain had a stronger effect on attenuation of gene induction. Thus gene expression profiling demonstrates definitively Nef is capable of activating T cells at the transcriptional level and that this effect is initiated high in the T cell signalling path.

Within the Nef expression profile differential expression of multiple genes with the ability to affect viral replication was noted. In a few instances it was possible to demonstrate the Nef mediated changes in mRNA levels were functionally significant. Proteomic analysis of Nef effect on T cells was initiated. 2D gel analysis of T cell lysates after Nef expression demonstrated a differential regulation of proteins in T cell lysates. The mechanism by which Nef initiates T cell signalling was explored using a similar approach. The proteins interacting with Nef in lipid rafts were identified after immunoprecipitation of HA tagged Nef from this subcellular compartment. 2D gel analysis reveals the presence of Nef changes the content of lipid rafts and that Nef co-immunoprecipitates with several proteins in the raft fraction. The identity of these interactors obtained by peptide microsequencing should give insight into the molecular mechanism by which Nef induces a CD4 T cell transcriptional programme.

Acknowledgements

I am indebted to my supervisor Andrew McMichael for making this work possible and to colleagues at the Weatherall Institute of Molecular Medicine in Oxford and Laboratory of Molecular Biology in Cambridge.

CONTENTS

CHAPTER 6: DISCUSSION AND CONCLUSIONS

ABBREVIATIONS

APS	ammonium persulphate
ATP	adenosine triphosphate
bp	basepair(s)
cDNA	complementary DNA
Ci	Curie
CTP	cytidine triphosphate
d	deoxy
Da	Dalton
dH_2O	Distilled water
DNase	deoxyribonuclease
DRB	5, 6-dichloro-1-β-D-ribofuranosylbenzimidazole
DTT	dithiothreitol
EDTA	ethylenediamine tetra-acetic acid
g	gram
GTP	guanosine triphosphate
HEPES	N-2-hydroxyethylpiperazine-N'-ethanesulphonic acid
HIV-1	Human Immunodeficiency Virus type 1
k	kilo
l	litre
LTR	long terminal repeat
U	micro
M	mili
M	molar
Mol	mole(s)
MOPS	3-[N-morpholino] propanesulphonic acid
Mr	relative molecular weight
mRNA	messenger RNA
N	any nucleotide
NTP	nucleoside triphosphate

OD	optical density
PAGE	polyacrylamide gel electrophoresis
PBS	phosphate buffered saline
PCR	polymerase chain reaction
PMSF	phenylmethylsulphonyl flouride
pol	polymerase
poly(A)	polyadenyl or polyadenylation
Rnase	ribonuclease
rRNA	ribosomal RNA
RT	room temperature
TAR	Tat activation response element
TEMED	N, N, N', N',-tetramethylethylinediamine
TTP	Thymidine triphosphate
UTP	uridine triphosphate
UTR	untranslated region
UV	ultraviolet
V	volts
W	watts

Chapter 1

1.1 Introduction

Acquired Immune Deficiency Syndrome (AIDS) was first described in 1982 after observation of illnesses experienced by clusters of patients in New York and San Francisco consisting of opportunistic infections and tumours in the context of a low CD4 count. Human Immunodeficiency Virus type 1 (HIV-1) was first isolated from the blood of AIDS patients in 1983-4 (Barre-Sinoussi et al., 1983, Popovic et al., 1984, Levy et al., 1984). Initially the infection appeared to be contained within a few high "risk groups" however within a few years it became clear the virus was spreading rapidly. Currently over 40 million people are infected with HIV-1 throughout the world and the epidemic is increasing.

The origins of HIV infection in humans remain somewhat enigmatic. Mathematical modelling of viral diversification has been used to estimate when HIV became a human infection. This is possible as HIV possesses inherent variability due to lack of proof reading in the viral reverse transcriptase (Roberts et al., 1988) and as the virus replicates rapidly (Perelson et al., 1997). Viral diversification modelling has utilised sequence data and time of sampling to estimate the minimum amount of time HIV has been a human infection. It has been proposed that the main (M) group of HIV-1 strains currently infecting the human population began to diversify around 1930 (Korber et al., 2000, Korber et al., 2001). It has been postulated HIV spread to humans from a closely related primate species. In the case of HIV-2 (a retrovirus strain sharing 40-60% homology with HIV-1) there is a high degree of homology with SIV strains infecting sooty mangabeys (SIV sm) in the same part of West Africa (Gao et al., 1992). The origin of HIV-1 is possibly from SIV infecting a chimpanzee species whose habitat overlaps with the central African area from where the M group of HIV-1 originated (Gao et al., 1999). The majority of people infected with HIV-2 will not die of this virus in contrast to HIV-1 where an inevitable decline in CD4

count is observed. Lentiviral infection in natural hosts likewise largely results in little evidence of disease although persistent infection is present. Sooty mangabeys and African Green Monkeys infected with SIVsm or SIVagm appear healthy (Broussard et al., 2001, Kaur et al., 1998, Rey-Cuille et al., 1998). In addition many chimpanzees infected with HIV-1 remain immunologically intact over decades. An exception is that SIV strains can rapidly kill macaques (Daniel et al., 1987).

1.2 HIV enters human cells via CD4 and chemokine receptors

HIV infects CD4+ T-helper cells as well as other CD4 bearing cells such as macrophages and dendritic cells. The CD4 molecule was shown to be a high affinity receptor for the virus in 1984 (Dalgleish et al., 1984, Klatzmann et al., 1984). In addition to CD4, coreceptors are required for HIV entry. Transfection of CD4 alone into many mammalian cell lines does not make them permissive for HIV infection. HIV coreceptors belong to the family of seven transmembrane spanning chemokine receptors. Several members of this family can function as coreceptors though at physiological levels of infection the main ones utilised are CXCR4 and CCR5. CXCR4 is the receptor for strains of HIV often found in late stage disease (syncytium inducing (SI) or T cell tropic (Feng et al., 1996). Strains that establish primary infection are termed macrophage tropic or non-syncytium inducing (NSI). It was demonstrated that the chemokine receptor binding three HIV suppressing CC-chemokines (MIP-1α, MIP-1β and RANTES) was the major coreceptor for macrophage tropic HIV (Dragic et al., 1996, Deng et al., 1996). In vivo observations of HIV tropism were explained following these observations and the terms NSI/SI were superseded by defining the co-receptor usage (R5 or X4) for a particular isolate. Primary HIV infection generally requires CCR5 to become established. During the course of the infection viral tropism widens as a result of envelope V3 loop mutations. In late disease the infecting viral quasispecies changes tropism predominantly from CCR5 to CXCR4 and this is often coincident with a decline in CD4 cells (Connor et al., 1997). CCR5 is largely

expressed on memory T cells of the Th-1 type (Loetscher et al., 1998) and is induced on T cell activation. CXCR4 possesses a wider distribution particularly on naïve T-cells (Bleul et al., 1997). The parameters controlling this HIV tropism change during disease evolution are not known.

1.3 HIV depletes CD4 T cells

The hallmark of HIV disease is the decline in CD4 count that is coincident with susceptability to AIDS defining opportunistic infections and malignancies. The mechanism by which this occurs is not clear. Measurements of infected T cells in the circulation recorded low values that seemed at odds with the extent of observed helper T cell dysfunction. However analysis of infected lymphoid tissue revealed infected CD4 T cells were being trapped in the follicular dendritic cell network of lymph nodes (Spiegel et al., 1992). The characteristic T cell abnormality is a loss of T cell help to HIV itself and to recall antigens. HIV-1 preferentially infects HIV antigen-specific CD4 T cells (Douek et al., 2002). Extrapolation of this observation suggests subsequent recruitment and activation of other lymphocyte populations responding to intercurrent infections would lead to their infection and deletion leading to impairment of other antigen specific responses.

1.4 HIV evasion of the host immune response

HIV is effective in evading the host cell immune response in a number of ways apart from the failure of specific CD4 T cell help. A vigorous antibody response is observed to HIV however antibodies rarely neutralise primary HIV strains. In addition the virus mutates quickly to escape antibody responses (Poignard et al., 1999). A strong CD8 T cell response to the virus is invariably observed. Measurement of antigen specific T cells in the blood using peptide-HLA tetrameric complexes has demonstrated a rise in virus-specific CTL concomitant with a fall in plasma viremia in acute HIV infection (Wilson et al., 2000). The magnitude and specificity of the CTL reponse has shown no clear relationship

with decline in CD4 count or clinical outcome (Addo et al., 2003). In addition to mutation mediated escape from antibody responses the virus mutates rapidly from very early on to escape from CTL responses (Price et al., 1997). A correlation has been observed between host HLA haplotype and viral sequence demonstrating adaption of the virus to immune pressure (Moore et al., 2002).

1.5 HIV Retrovirology

The HIV-1 genome encodes nine open reading frames (Figure 1a). Three of these encode the Gag, Pol, and Env polyproteins, which are subsequently proteolyzed into individual proteins common to all retroviruses. The three Pol proteins Protease, Reverse transcriptase and Integrase provide essential enzymatic function and are also present in the virion. The Gag proteins Matrix, Capsid, Nucleocapsid, p6 and Env proteins surface gp120 and gp41 are structural proteins making up the virion core and viral envelope.

Figure 1a. Diagrammatic representation of the HIV genome.

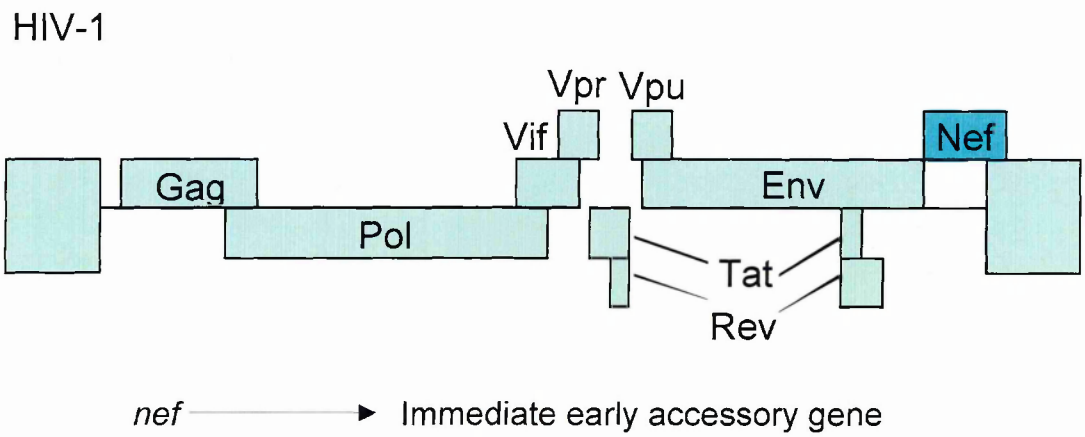

Lentiviruses differ from other retroviruses in that they encode six genes in addition to the three prototypic retroviral genes *gag, pol* and *env.* Two of the six additional open reading frames, *tat* and *rev*, encode factors essential for viral replication. The Tat protein that transactivates the HIV long terminal repeat and the Rev protein which co-ordinates HIV splicing. The four remaining genes are *nef, vpr, vpu* and *vif.* They have been termed accessory genes, as their inactivation does not completely terminate viral replication in vitro. But studies in vivo suggest viruses failing to express any of the accessory genes are disabled with decreased replicative capacity in SIV infected monkeys and HIV infected humans.

1.6 Lentiviral Life Cycle

A 9 kilobase (kb) RNA encodes the retroviral genome. This is packaged in duplicate in the viral particle. A diagrammatic representation of the viral life cycle is illustrated in Figure 1b. Virions bind target cells in an interaction that involves virion gp120 and CD4 and chemokine receptors on host cells. Following binding gp41 undergoes a conformational change that promotes virus-cell membrane fusion, facilitating entry of the core into the cell. Uncoating of the virion core occurs and the viral nucleoprotein complex consisting of Matrix, Reverse Transcriptase, Integrase, Vpr and RNA is exposed. The genomic RNA is reverse transcribed to form a cDNA copy. The complex known as the preintegration complex (PIC) is subsequently transported to the nucleus. Integrase then catalyses integration of the viral DNA into the host chromosome and the DNA is repaired. Viral transcripts are expressed from the promoter located in the 5' long terminal repeat (LTR), coordinated by the viral transactivator Tat. Rev coordinates splicing of RNA transcripts. Multiply spliced or genomic length transcripts are exported to the cytoplasm where they are translated or packaged. Following translation, the Gag and Gag-Pol polyproteins become localised to the cell membrane. The Env mRNA is translated at the ER. The core particle is assembled and an immature virion buds from the host cell surface. During

budding the virion undergoes a morphological change (maturation) that involves proteolytic processing of the Gag and Gag-Pol polyproteins by protease. The mature virion is then ready to infect the next cell.

Fig 1b. Diagrammatic representation of the HIV Life Cycle

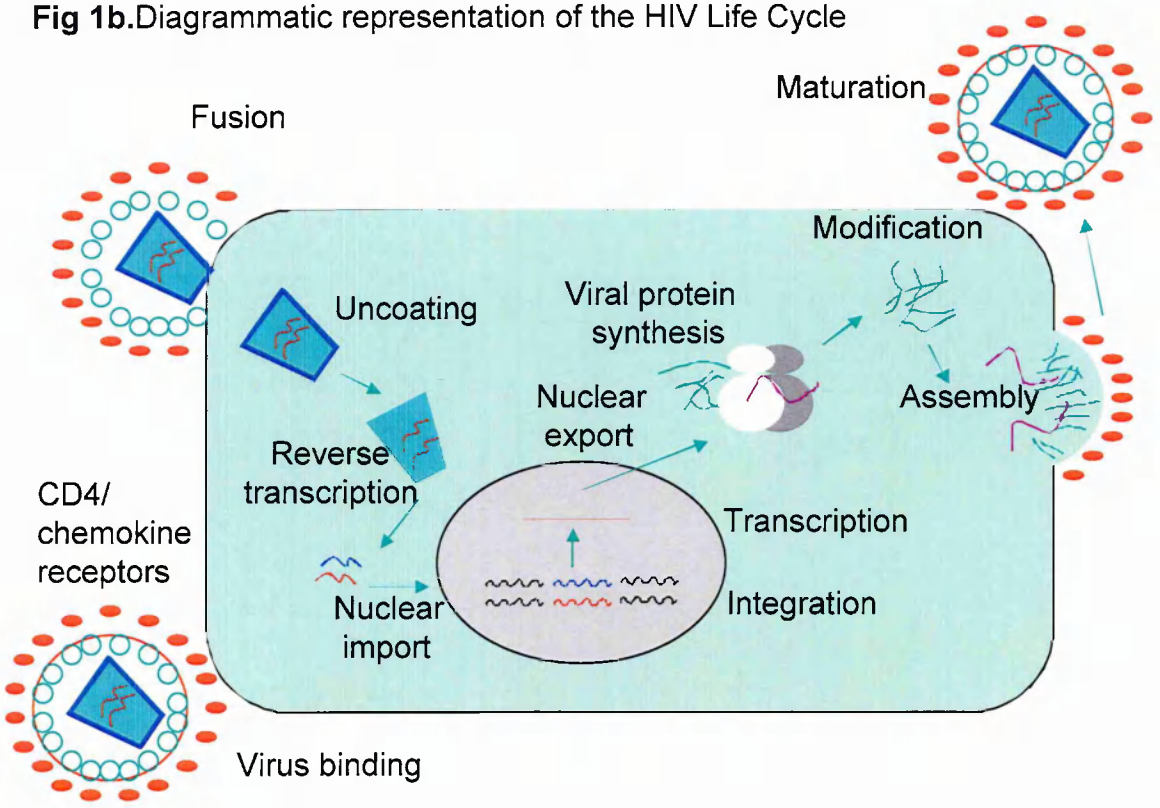

1.7 HIV RNA

The HIV transcript is approximately 9 kilobases (kb). The first 55 nucleotides form the transactivating response element (TAR), the RNA stem loop structure required for Tat transactivation. A binding site for primer is located at nucleotides 182-199 which can anneal to a cellular tRNA and initiate transcription. Genomic RNA is incorporated into the virion via a packing signal located at nucleotides 240-350. This binds Nucleocapsid and is critical for incorporation of genomic RNA into the virion (Clever and Parslow., 1997). Between nucleotides 248 and 271 lies a dimerisation site that facilitates incorporation of two genomic RNAs

into the virion (Paillart et al., 1996, Laughrea et al., 1997). At around nucleotide 290 is a major donor splice site required for generation of spliced transcripts. Rev, responsible for HIV splicing binds at nucleotides 7362-7596 at the Rev response element. Splice acceptor sites at nucleotides 5358 and 7971 in particular allow production of an increased number of spliced transcripts. A Gag-Pol frameshifting region comprises an RNA hairpin and slippery sequence facilitating –1 ribosomal frame shifting. This translates a fused Gag-Pol polyprotein at around 5-10% frequency (Cassan et al., 1994). A polyadenylation signal generates the 3' end of the HIV RNA.

1.8 Function of Individual HIV genes

1.8i Tat

Transcription complexes initiated at the HIV-1 promoter require the Tat protein to enhance the processivity of transcribing polymerases and in some instances increase the rate of transcription initiation. Tat is essential for viral replication increasing the production of viral mRNAs around 100 fold. The HIV-1 promoter contains sites for several transcription factors upstream of the start site including NFAT, NF-κB, SP1 and TBP (Jones and Peterlin, 1994). Studies substituting promoters suggest the TATA box and downstream sequences are important in reducing transcription efficiency (Jones and Peterlin, 1994). Tat functions in transcription complexes that phosphorylate the C terminal domain of RNA polymerase II. The catalytic component in such complexes in CDK9 and Tat appears to direct recruitment of CDK9 to such complexes (Zhou and Sharp, 1996, Parada and Roeder 1996, Yang et al., 1996, Garcia-Martinez et al., 1997, Cujec et al., 1997). To function Tat binds TAR, the RNA hairpin located at the 5' end of nascent viral transcripts.

NMR studies of Tat in complex with the TAR loop indicate an arginine rich Tat domain help binding to a three nucleotide bulge region of TAR with one arginine being primarily responsible for recognition (Puglisi et al., 1992, Aboul-ela et al., 1995). Contact is made between bases in the side chain and a guanine in the

RNA minor groove and stabilised with additional contacts with the phosphate backbone. NMR studies of full length Tat indicate the molecule is relatively disordered but contains a short hydrophobic core.

1.8ii Rev

Viral RNAs are doubly spliced and encode Tat, Rev and Nef when first produced. Subsequently singly spliced and unspliced transcripts occur. Rev coordinates this process by binding the Rev response element in the *env* coding region. Rev may function to enhance the nuclear export of unspliced mRNAs (Hope et al., 1997). Rev is required to export unspliced RNAs that contain a Rev response element (Fischer et al., 1995). Rev binding is thought to target the attached mRNA to the nuclear export machinery. Rev contains a leucine-rich nuclear export signal enabling nuclear-cytoplasmic shuttling and that interacts with hRip/Rab located at the nuclear pore (Meyer and Malim., 1994, Fritz et al., 1995, Bogerd et al., 1995). CRM1, a nuclear export factor bridges this interaction to facilitate nuclear export (Ullman et al., 1997). Mutagenesis of the RRE eliminates Rev activity indicating that entry into the splicing pathway may also be important for Rev function. Compensatory mutations in U1 snRNA which binds at 5' splice sites can restore activity in this context (Lu et al., 1990). Rev can inhibit splicing by preventing entry of additional snRNPs during the later stages of spliceosome assembly (Kjems et al., 1993).

1.8iii Matrix

Matrix is 132 amino acids long and lines the inner surface of the virion membrane in the mature virion. Matrix is the N-terminal portion of the Gag polyprotein and enables Gag and Gag-Pol precursor polyproteins to target to the plasma membrane before assembly of the virion. N terminal myristoylation of Matrix is required for membrane localisation. The first 50 residues also appear to be important in this regard. Residues 1 to 104 produce 5 α-helices capped by a three-stranded β mixed sheet in the matrix crystal structure (Hill et al., 1996). Three monomers are arranged as a triskelion and trimerisation appears to be

required for biological function as mutations in trimerisation residues abrogate viral assembly. In addition lysines 26, 27, 30 and 32 implicated in membrane localisation are arranged on the membrane-binding surface of the trimer. The structure of Matrix would suggest it inserts into the membrane using the myristoylation sites and interactions between the basic residues of the membrane binding surface and phospholipid head groups.

Matrix plays a role in infection of nondividing cells, a phenomenon peculiar to lentiviruses. The role of Matrix in viral entry is not fully elucidated. Initial studies implicating a nuclear localisation signal in Matrix that interacts with Rch1 (a member of the karyopherin-α family (Gallay et al., 1995)) have not been reproduced (Freed et al., 1995, Bukrinskaya et al., 1996, Freed et al., 1997, Fouchier et al., 1997).

1.8iv Capsid

Capsid forms the core of the viral particle. Around 2000 molecules of Capsid are contained in each virion. The N-terminal domain of Capsid is required for infectivity of viral particles by participating in viral uncoating by interaction with a cellular protein Cyclophilin A (Luban et al., 1993). Cyclophilin A acts as a chaperone. Capsid C-terminus functions in assembly and is important for Capsid dimerisation and Gag oligomerisation. Crystal structures of domains of Capsid in complex with cyclophilin A have been solved. The C-terminal domain consists of an extended strand followed by 4 α-helices. These demonstrate an extensive dimer interface (Gamble et al., 1997). A 20 amino acid sequence that is highly conserved within all Gag proteins (the major homology region) adopts a compact fold in which the four most conserved residues form a stabilising hydrogen bond network. Additional hydrophobic residues from the major homology region contribute to the hydrophobic core. The major homology region is required for viral particle assembly and via interaction with Gag may help incorporate Gag-Pol precursors (Srinivasakumar et al., 1995).

1.8v Nucleocapsid

Nucleocapsid coats the viral genomic RNA in the virion. It is 55 residues long and contains two zinc finger domains. Nucleocapsid binds and delivers full length viral RNAs into the assembling virion after binding the packaging signal. The packaging signal appears to consist of three RNA hairpins located around the major splice donor site (Clever and Parslow.,1997, Laughrea et al., 1997). Nucleocapsid is a basic protein that binds single stranded nucleic acids nonspecifically leading to coating of the genomic RNA that protects it from nucleases and insulates it within the core. This non-specific binding activity enhances other steps in the viral life cycle. These include stimulation of integration, promoting annealing of the tRNA primer, melting of RNA secondary structures, or by DNA strand exchange reactions during reverse transcription (Huang et al., 1997, Guo et al., 1997, Cameron et al., 1997, Carteau et al., 1997). The NMR structure of nucleocapsid has been determined (Summers et al., 1992, Morellet et al., 1992). This shows two well-ordered zinc finger domains and a flexible linker in the absence of RNA. Residues important for RNA binding in vitro include arginine 7, 32 and lysine 33 however mutagenesis of these residues indicates that they have little effect on RNA packaging (Poon and Aldovini 1996). The importance of the zinc finger domains has been highlighted by treatment with disulfide-substituted benzamide compounds that specifically remove zinc (Rice et al., 1995). These compounds inhibit viral replication.

1.8vi p6

The 51 C-terminal residues of Gag, termed p6 is required for incorporation of Vpr during viral assembly. This interaction is mediated by a predicted α helical structure located near the N-terminus of Vpr and residues 32-39 within p6 (Kondo and Gottlinger 1996, Lu et al., 1995, Checrone et al., 1996). P6 also appears to play a role in viral particle release, amino acids 7-10 being implicated in this function (Huang et al., 1995).

1.8vii Reverse transcriptase

Reverse transcriptase is responsible for converting the viral RNA genome into duplex DNA. Reverse transcriptase contains an RNase H domain that cleaves the RNA portion of the RNA-DNA hybrids generated during the reaction. Reverse transcriptase possesses both RNA-dependant and DNA-dependant polymerase activity. Activity is initiated from the 3' end of a $tRNA_3^{Lys}$ primer annealed to the primer binding site near the 5' end of genomic RNA (Oude Essink et al., 1996). After tRNA-primed initiation, reverse transcription involves two DNA strand transfer reactions that are catalysed by Reverse transcriptase and are required for priming the synthesis of both plus and minus strands (Katz and Skalka 1994, Peliska and Benkovic, 1992). Reverse transciptase displays different properties during initiation and elongation. It becomes highly processive during elongation, post-transcriptional modifications of $tRNA_3^{Lys}$ increasing the formation of initiation complexes (Lanchy et al., 1996). $tRNA_3^{Lys}$ appears to play a role similar to σ factor in transcription complexes in this instance.

The crystal structure of unliganded Reverse transcriptase, Reverse transcripase-DNA complex and Reverse transcriptase-inhibitor complexes have been solved (Rodgers et al., 1995, Esnouf et al., 1995, Hsiou et al., 1996, Jacobo-Molina et al., 1993, Kohlstaedt et al., 1992, Ren et al., 1995). Reverse transcriptase exists as a heterodimer of residues p66 and p51. Each subunit contains a polymerase domain composed of four subdomains named fingers, palm, thumb, and connection. Residue p66 contains an extra RNase H domain. The polymerase subdomains are arranged differently in the two subunits. P66 forms an active site cleft while in contrast p51 forms an inactive closed structure (Wang et al., 1991).

Reverse transcriptase inhibitors in current use include nucleoside analogues that bind to the polymerase active site. The structure of a non-nucleoside inhibitor-Reverse transcriptase complex show a hydrophobic binding site near to the polymerase active site that rearranges to fit the particular drug and lock Reverse transcriptase into an inactive conformation (Kohldstaedt et al., 1992, Ren et al., 1995). Reverse transcriptase variants resistant to inhibitors have mutations in and around the active site and DNA binding cleft suggesting more indirect effects

as well as simply altering the binding site occur (Ren et al 1995, Tantillo et al., 1994). Substantial variability in the position of the p66 thumb subdomain is revealed by structural studies (Rodgers et al., 1995, Esnouf et al., 1995, Hsiou et al., 1996). This could enable conformational rearrangements to occur after ligand binding which could facilitate reverse transcription by allowing translocation of Reverse transcriptase along nucleic acid or positioning RNase H in active sites.

1.8viii Protease

Immature viral particles are not infectious. Protease cleaves Gag and Gag-Pol polyproteins resulting in conformational changes before the viral particle is mature. Protease cleaves at several polyprotein sites to produce the final Matrix, Capsid, Nucleocapsid and p6 proteins from Gag and Protease, Reverse transcriptase and Integrase proteins from Pol. Ribosomal frameshifting determines the amount of Gag-Pol incorporated to the virion; usually about 5-10% Gag. Factors that influence protease activity have a large effect on virion production as assembly and maturation need to be well coordinated. Protease activity depends on the concentration of Gag-Pol and the rate of autoprocessing that can be influenced by adjacent p6 sequences (Zybarth and Carter 1995). Cleavage efficiencies vary among sites controlling the order of appearance of processed proteins (Dunn et al., 1994). Overexpression of protease can lead to disordered processing and reduced infectivity (Luukkonen et al., 1995). Crystal structures of protease in complex with inhibitors have been solved. The dimer interface comprises the enzyme active site with each monomer contributing a catalytically essential aspartate. A conserved triad Asp-Thr-Gly similar to that of other aspartyl proteases is present. The dimer contains flexible flaps that descend around the active site on substrate binding. Hydrophobic pockets in protease bind amino acid side chains around the active site (Wlodower and Erickson.,1993). HIV mutants resistant to multiple protease inhibitors contain mutations located within the inhibitor-binding pocket and at distant sites. Some of these mutants show reduced catalytic activity (Condra et al., 1995).

1.8ix Integrase

Integrase is a component of the pre-integration complex responsible for catalysing a series of reactions facilitating integration of the viral cDNA into the host genome. The actual biochemical mechanism of integration is well described and is notable due to its close similarity to VDJ recombination. Prior to the initiation of the integration process there is assembly of viral DNA on Integrase. HIV Integrase recognises specific sequences in the LTRs of viral DNA. Integrase removes two nucleotides from each 3' cDNA end (referred to as 3' processing). This occurs by site-specific endonuclease activity. For this initial 3'-processing step, Integrase apparently activates the phosphodiester bond towards cleavage. The tailored viral DNA is joined in the next step to host cell DNA in the nucleus through an esterification reaction. Here Integrase positions the 3'-OH end of the viral DNA for nucleophilic attack on the phosphodiester bond in the host DNA. Host cell enzymes catalyse the repair of the resulting gapped intermediate although a role here for Integrase is also possible.

The host cell factors required for successful repair of DNA after HIV integration are less well understood. Some evidence has recently suggested components of the non-homologous end-joining (NHEJ) path of DNA repair are involved. Infections of cells mutant in components of the NHEJ path generate reduced viral titres due to increased apoptosis of infected cells. In addition Integrase mutant viruses are toxic. Also studies with the Reverse transcriptase inhibitor nevirapine reveal that synthesis of viral cDNA is required to generate the pro-apoptotic signal in these contexts. Bushman and coworkers have recently shown that the 2-LTR circular form of viral cDNA is absent in infected cells mutant in components of the NHEJ pathway (Bushman et al., 2000). In addition NHEJ component Ku has been identified in PICS.

Integrase is active as an oligomer, probably a tetramer (Rice et al., 1996). The monomer consists of three domains. NMR studies indicate the N-terminal domain contains a binding site for zinc and forms a dimer with a largely hydrophobic interface (Miller et al., 1995). Each monomer contains a helix-turn-helix structure with close similarity to those found in DNA binding proteins. The catalytic domain

of Integrase contains a D, D (35), E motif conserved among Integrases and required for processing and joining reactions. It is proposed to bind the active site metal ion (Rice et al., 1996). The crystal structure of the catalytic domain reveals a dimeric structure with each monomer containing a five-stranded β-sheet and 6 α-helices. This structure is similar to that of other polynucleotide transfer enzymes (Dyda et al., 1994). As the two active sites are too far apart to permit five base pair staggered cleavage of the DNA target either a large conformational change occurs on catalysis or Integrase functions in an oligomeric form (most likely tetramer) during some reaction steps (Rice et al., 1996, Cai et al., 1997). The C-terminal domain forms a dimer of parallel monomers and displays non-specific DNA binding activity. Each monomer is similar to SH3 domains with a five-stranded β barrel with a saddle-shaped groove likely to incorporate double stranded DNA (Eijkelenboom et al., 1995, Lodi et al., 1995).

1.8x Vif

HIV-1 virions contain around 10-100 molecules of Vif per average particle (Camaur et al., 1996, Fouchier et al., 1996, Liu et al., 1995). Vif mutant viruses display attenuated viral DNA synthesis and produce unstable replicative intermediates (Cohen et al., 1996, Simon and Malim., 1996). Vif defective viruses show defects in infectivity when produced in certain cell types only. These observations prompted speculation that it was possible permissive cells produce a factor that compensates for a lack of Vif expression or that expression of Vif in permissive cells blocks an inhibitor of viral infectivity. Recently a cDNA subtraction approach in which the non-permissive cell line served as the "tester" and the permissive sample was used as the "driver" revealed a gene, *CEM15,* whose transient expression in cells that do not normally express this recreates the non-permissive phenotype. The presence of Vif overcomes this phenotype (Sheehy et al., 2002). Interestingly *CEM15* displays homology to Apobec-1 and Phorbolin-1. Apobec-1 is the cytidine deaminase that is the catalytic subunit of the mammalian Apolipoprotein B mRNA editing enzyme (Teng et al., 1993). Apobec-1 binds to and edits RNA (Macginnitie et al., 1995) and Vif has been

reported to bind genomic viral RNA and also to depend on this interaction for incorporation into virions (Dettenhofer et al., 2000, Khan et al., 2001, Zhang et al., 2000). It is possible CEM15 may affect *vif* deleted virions through their RNA components leading to inability to accumulate reverse transcripts and establish provirus in susceptible target cells.

Interestingly the RNA editing enzymes have recently been demonstrated to exhibit an addition function to that of RNA editing. Differential gene expression studies of somatic hypermutation in B cells have revealed expression of activation-induced cytidine deaminase (AID) exclusively in hypermutating cell lines (Mutamatsu et al., 2000). AID exhibits sequence homology to RNA editing enzymes such as APOBEC1. AID has also been implicated in immunoglobulin class switching and in gene conversion (Nagaoka et al., 2002). Indications that these three gene diversification processes might be initiated by a common type of DNA lesion and the proposal there is a first phase of hypermutation that targets dC/dG pairs suggested AID might function directly at dC/dG pairs. In support of this expression of AID in *E.coli* gives a mutator phenotype that yields nucleotide transitions at dC/dG in a context dependant manner. This AID induced mutation is accentuated by a deficiency in uracil-DNA glycosylase indicating that AID functions by deaminating dC residues in DNA (Petersen-Mahrt et al., 2002, Di Noia et al., 2002). Following on from these studies it has been shown APOBEC1, the catalytic component of an RNA editing complex and its homologues APOBEC3C and APOBEC3G demonstrate DNA mutator activity in an *E.coli* assay. This occurs via dC deamination, each protein exhibiting distinct local target sequence specificity (Harris et al., 2002). It is attractive to hypothesise that *CEM15* is acting in a similar manner on HIV cDNA, perhaps as part of an in built host defence mechanism rendering viral replication defective in the absence of *vif.*

1.8xi Vpu

Vpu is another of the HIV accessory genes whose function is not fully delineated. Vpu is an 81 amino acid oligomeric integral membrane protein. So far roles of

CD4 degradation, stimulation of virion release and function as an ion channel (Lamb and Pinto., 1997) have been assigned to Vpu. Vpu mutant viruses display retention of viral particles at the cell surface or localised to intracellular membranes (Cohen et al., 1996, Lamb and Pinto., 1997). As Vpu can also promote release of heterologous viral particles the mechanism is likely to be non-specific. Enhancement of particle release requires the N-terminal domain and is not influenced by serine phosphorylation (Cohen et al., 1996, Lamb and Pinto., 1997).

Vpu mediated CD4 degradation occurs in complexes with newly synthesised Env glycoproteins (gp160) in the endoplasmic reticulum. Vpu promotes degradation of CD4 in these complexes, allowing Env to travel to the cell surface for viral particle assembly. The C-terminal of Vpu is important for this effect as well as putative α helices in the cytoplasmic tail of CD4 (Tiganos et al., 1997). Vpu may interact directly with CD4 in achieving this effect as there be appears to be a direct correlation between the extent of Vpu association and relative levels of CD4 degradation (Bour et al., 1995). CD4 degradation by Vpu may involve the proteosome as lactacystein blocks the effect (Fujita et al., 1997). In addition serine phosphorylation of Vpu by a casein kinase–2 related protein is implicated (Cohen et al., 1996).

1.8xii Vpr

Vpr, another HIV accessory gene is required for nuclear localisation in non-dividing cells. Vpr contains a nuclear localisation signal that directs nuclear transport in the absence of nuclear envelope breakdown (Cohen et al., 1996). In addition to its function in nuclear localisation Vpr can induce cell cycle arrest at G2M prior to nuclear envelope breakdown and nuclear condensation. Sustained Vpr expression causes apoptosis of host cells. Vpr acts before dephosphorylation of Cdc2 by Cdc25, a prerequisite for initiation of cell division (Emerman 1996). Amino acids required to initiate G2 arrest are located in the C terminus of Vpr. The 65kDa regulatory subunit of Protein phosphatase 2A, a serine threonine phosphatase that regulates the transition from G2 to mitosis has

been shown to bind Vpr (Emerman 1996). Vpr has been shown to influence mutation rates during viral DNA synthesis (Mansky 1996) and in addition function as an ion channel (Lamb and Pinto, 1997).

1.8xiii Env

HIV-1 particles have a surface of densely arranged envelope spikes. Each spike is formed of a trimer of heterodimers of the gp120 surface and the gp41 transmembrane glycoproteins. The entry of human immunodeficiency virus (HIV) into cells requires the sequential interaction of the viral exterior envelope glycoprotein, gp120, with the CD4 glycoprotein and a chemokine receptor on the cell surface. These interactions initiate a fusion of the viral and cellular membranes. Env is synthesised as a fusion incompetent precursor (gp160) that is then proteolytically cleaved into two subunits (the surface subunit gp120 and the transmembrane subunit gp41). The surface subunits are responsible for recognizing and binding to specific receptors on the host cell. The transmembrane subunits contain the fusion peptide at their amino terminus and are anchored into the viral membrane via hydrophobic spanning helices. The entry event of HIV is accomplished at the cell surface at neutral pH. In common with other virus fusion proteins, the N-terminal fusion peptide of the gp41 ectodomain is followed by a 4,3 hydrophobic (heptad) repeat, characteristic of coiled coils (Delwart et al., 1990). The two-heptad repeat sequences form a helical core trimer of antiparallel dimers as a six-helix bundle (Chan et al., 1997). The N terminal helices form an inner-coiled trimer, whereas the C terminal helices align in an antiparallel fashion into three hydrophobic grooves on the surface of the trimeric core. This six-helix bundle is the fusogenic conformation of gp41 and is only formed after HIV-1 gp120 binds to CD4 receptor (Jiang et al., 1998).

Although gp120 can elicit virus-neutralizing antibodies, HIV eludes the immune system. The X-ray crystal structure of an HIV-1 gp120 core complexed with a two-domain fragment of human CD4 and an antigen-binding fragment of a neutralizing antibody that blocks chemokine-receptor binding has been solved.

The structure reveals a cavity-laden CD4-gp120 interface and a conserved binding site for the chemokine receptor. The structure provides evidence for a conformational change upon CD4 binding, the nature of a CD4-induced antibody epitope, and specific mechanisms for immune evasion.

Due to progress made in understanding the mechanism by which gp41 implements membrane fusion approaches for therapeutic intervention have been revealed. Synthetic C terminal peptides have been tested and are potent inhibitors of HIV-1 infection at nanomolar levels (Jiang et al., 1993, Wild et al., 1994). Based on the structural characteristics of the fusogenic confirmation of gp41, these C peptides most probably act through a dominant-negative mechanism (Chan et al., 1997, Wild et al., 1994, Furuta et al., 1998). C peptides probably act after the non-fusogenic state has undergone a conformational change but in advance of the formation of the stable core structure. This 'intermediate' stage must be in existence long enough for the C peptides to bind and act in a dominant-negative manner. The wide range of activity of C peptides against different HIV-1 isolates is explained by the conserved nature of the hydrophobic groove to which these peptides bind. At the distal end of this groove is a deep cavity, normally occupied by three hydrophobic residues from the C helix. In principle, this cavity is a good target for inhibitors, although peptides that do not fill this cavity are still potent inhibitors. A 36-amino acid C peptide (DP178, T-20; Trimeris Inc., Durham, USA) is a particularly potent inhibitor of HIV-1 infection and is currently undergoing clinical trials (Kilby et al., 1998, Kilby et al., 1999). The generation of mutant viruses that escape T-20 inhibition revealed amino acid changes in the N peptide region of gp41 (Rimsky et al., 1998), and it is worthy of note that whereas such cavity-binding inhibitors do not yet exist, it is considerably more difficult to select viruses resistant to a C peptide that contains the cavity-binding region (Rimsky et al., 1998). These observations imply that high-affinity ligands targeting the highly conserved coiled coil, and particularly the cavity, will have broad-spectrum anti-HIV-1 activity with a reduced propensity to develop resistance (Chan et al., 1998). The search for such inhibitors is the subject of intense current activity.

1.9 The HIV *nef* accessory gene

1.9i Role of Nef in viral pathogenesis

Nef is a major determinant of HIV virulence. A large deletion in *nef* attenuates HIV pathogenicity in rhesus macaques (Kestler et al., 1991). A similar situation is observed in human disease. A cohort of haemophiliac patients infected with *nef*-deleted HIV by blood transfusion are long term non-progressors (Deacon et al., 1995, Kirchhoff et al., 1995, Learmont et al., 1999). A strong selection pressure to maintain an intact *nef* reading frame is observed in both humans and animal models. Following infection of macaques with SIV encoding *nef* with a premature stop codon, the virus rapidly reverts to full-length *nef*. In humans reversion to full length *nef* correlates with disease progression.

Mouse models corroborate these findings. HIV-1 infection of SCID-hu mice transplanted with human thymus leads to the massive depletion of double positive thymocytes (Bonyhadi et al., 1993). Here full-length viruses replicate faster leading to higher viral loads and faster depletion of thymocytes than *nef* deleted viruses (Jamieson et al., 1994). Transgenic mice expressing *nef* under control of CD4 promoter suggest *nef* directly mediates pathology associated with HIV disease. Transgenics expressing full length *HIV* or *nef* alone experienced an AIDS like disease and died within weeks in contrast to transgenics expressing HIV without *nef* that remained healthy (Hanna et al., 1998).

Nef consists of a single open reading frame that overlaps with the HIV-1, HIV-2 and SIV 3' LTR (Cullen et al., 1994). Nef is expressed to highest levels immediately after HIV entry. It is the earliest detectable HIV transcript and can even be detected in latently infected primary CD4 T cells. Nef is expressed from a multiply spliced message and is a myristoylated phosphoprotein of around 206 amino acids in HIV and 263 amino acids in SIV. This myristoylation has been shown to be essential for Nef functions (Chowers et al., 1994, Sawai et al., 1995, Aiken et al., 1994). Subcellular localisation studies have demonstrated Nef throughout the cytoplasm but in high concentration at the perinuclear region and

the inner face of the plasma membrane. Recently Nef has been shown to localise to lipid rafts in T cells (Wu et al., 2001). In addition Nef has been found in viral cores (Kotov et al., 1999).

1.9ii Functions of Nef

Questions concerning the biological function of Nef have been intensively investigated. Nef bears little resemblance to any other protein of known function and has no orthologs. Early studies suggested a role in the suppression of viral replication however these were not reproduced. As a result Nef was christened with an acronym for negative factor. Since then Nef has been shown to exert four main in vitro functions: CD4 downregulation, MHC 1 downregulation, enhancement of virion infectivity and alteration of signalling activity in cells in which it is expressed.

1.9iii Nef CD4 downregulation

The ability of Nef to reduce surface expression of CD4 was demonstrated in 1986 (Garcia and Miller, 1991). CD4 is the primary receptor of HIV and SIV. It is expressed on thymocytes, T helper lymphocytes and cells of the monocyte/macrophage lineage. A function for this action of Nef was initially suggested to prevent deleterious super-infection of HIV infected cells. Recently two studies have demonstrated that high levels of CD4 on the surface of HIV producing cells inhibit infectivity of released virions by trapping viral envelope (Lama et al., 1999, Ross et al., 1999). Other suggested benefits to the virus might include the release of Lck that accompanies Nef binding to the CD4 cytoplasmic tail. Increased levels of free Lck could augment T cell activation, creating a milieu favourable for viral gene expression.

Nef downregulates CD4 in all cell lines tested. This effect is not dependant on phosphorylation of serine in the CD4 cytoplasmic tail (Garcia and Miller, 1991). Nef redirects some CD4 from the Golgi to lysosomes, triggers accelerated endocytosis from the cell surface and inhibits CD4 recycling to the cell surface targeting it instead to lysosomes.

The ability of Nef to downregulate CD4 depends on a di-leucine motif in its cytoplasmic tail. The fact HIV-1 and SIV Nef do not require identical amino acid sequences to downregulate the receptor implies that the receptor may make a direct association with its cellular target. This has been demonstrated in several systems including the yeast-two hybrid, CD4 capture assays using Nef column as bait, and after transfection of insect cells. In addition NMR studies reveal Nef binds to a CD4 derived peptide via a di-leucine motif (Grzesiek et al., 1996). This was one of the first trafficking interactions to be analysed at a structural level and encompasses the 13 amino acid residues in the cytoplasmic tail of CD4 (aa 407-419). The di-leucine motif is located at amino acids 413 and 414. Mapping of the interaction to the surface of Nef identifies a binding region that forms a hydrophobic patch of 10 residues encompassing W57, G96, R106, and I109. The side chains of the W57, L58 and L110 residues are most strongly affected by CD4 binding. These residues are highly conserved among Nef variants.

A mechanism for CD4 downregulation has been suggested to involve enhanced internalisation of the receptor from the cell surface. Chimeras containing the CD4 extracellular domain and trans-membrane domain with Nef as the cytoplasmic tail are rapidly internalised via clathrin-coated pits and degraded in lysosomes. Nef does not contain known CD4 internalisation motifs. It is therefore likely that Nef contains motifs capable of forming interactions with components of the vesicular trafficking pathways. This appears to be the case as Nef has been shown to be capable of forming an interaction with the μ chain of adaptor complexes in the yeast-2-hybrid system and in vitro using recombinant proteins. Adaptor proteins are hetero-tetrameric complexes that recruit clathrin to the cytoplasmic tail of receptors containing endocytosis signals. Several classes of adaptors have been documented. AP-1 and AP-2 mediate protein sorting in the *trans*-Golgi network and the plasma membrane. In contrast AP-3 participates in direct transport from the Golgi to the lysosomes. AP complexes recognise specific motifs in the cytoplasmic tail of surface receptors and direct their internalisation. These are either YxxC (where Y is tyrosine, x any amino acid and C a hydrophobic amino acid). The component of APs recognising di-leucine

motifs is not clear with studies supporting evidence for interactions with both μ and β chains. The μ chain however is known to interact with YxxC motifs. No binding to other subunits apart from μ has been demonstrated for Nef.

Nef mutants that cannot recruit AP do not show enhanced endocytosis either in trans or when fused to the extracellular and transmembrane domains of the receptor. In the case of SIV, Nef mutants in this domain display dominant negative characteristics (Piguet et al., 1998). Adaptor protein complexes appear to be a major downstream target for Nef in the context of CD4 downregulation.

Additional Nef binding proteins have been described that appear to influence CD4 downregulation. NBP-1 was identified using yeast-2-hybrid. It is capable of forming interactions with AP-2 and is probably recruited in clathrin-coated pits in addition to blocking CD4 recycling. This protein has homology with the yeast vacuolar ATPase (V-ATPase). It is the mammalian homologue of yeast Vma13p. This protein can form interactions with the adaptor AP-2 so may be part of a multi-protein complex directing CD4 internalisation. Nef also interacts with a Thioesterase, an enzyme cleaving thioester bonds. Consequently it is capable of altering palmitoyl chains on CD4 and facilitating CD4 recruitment in adaptor containing structures. Differences in studies determining Nef binding partners implicated in trafficking may have arisen due to low affinities between proteins participating in in endocytic trafficking (Marsh and McMahon 1999).

1.9iv Nef MHC I downregulation

Nef can also affect surface expression of MHC 1. This effect is incomplete and is limited to HLA A and B alleles. Nef enhances internalisation of these alleles via the YxxL motif in their cytoplasmic tail. It therefore does not affect downregulation of HLA C alleles that lack this particular motif. This allows Nef to mediate escape from NK cell lysis in addition to evasion from CTL attack. The mechanism of Nef mediated MHC 1 downregulation is less well explored than that of CD4 downregulation. It has not been possible to demonstrate a direct interaction between Nef and the cytoplasmic tail of MHC 1. In addition motifs in Nef other than that required for CD4 downregulation are required for MHC 1

downregulation. The SH3 binding domain in the central region of Nef and a series of N terminal residues are required. The exact biochemical basis by which Nef mediates this effect is a subject of further investigation. It has not been possible to demonstrate a change in tyrosine phosphorylation of the tyrosine residue in the MHC 1 cytoplasmic tail in the presence of Nef. Furthermore tyrosine kinase inhibitors cannot prevent this phenomenon. Recently it has been reported Nef may bind to PACS-1 (Piguet et al., 2000) to mediate retention of MHC 1 in the *trans*-Golgi. Endosome to Golgi trafficking of Furin and the Mannose-6-phosphate receptor is controlled by PACS-1. The Nef PACS-1 interaction is formed with four glutamic acid residues in Nef ($EEEE_{62}$). The recognition domain for PACS-1 has been shown to be quite promiscuous in that many proteins to which PACS-1 binds contain additional phosphorylated residues with respect to the defined binding motif (Molloy et al., 1999). HIV-1 Nef does not contain sites which can be phosphorylated around this motif. In contrast SIV Nef contains an acidic cluster region in the flexible loop that correlates well with known PACS-1 interaction motifs. The PACS-1 Nef interaction serves to usurp the ARF6 endocytic pathway by a PI3K-dependant process facilitating localisation of cell surface MHC 1 in the *trans*-Golgi (Blagoveshchenskaya et al., 2002).

1.9v Nef and apoptosis

Nef appears to be capable of subverting pathways of apoptosis in the T cell. Viral infection can be expected to trigger apoptosis via several routes. Unscheduled DNA synthesis and signals from the cell surface through death receptors TNFR1/2 and Fas could activate death programs. HIV gp120 ligation of CXCR4 on macrophages upregulates membrane bound TNF, which subsequently leads to cell death via TNFR in CD8 cells (Herbein et al., 1998). In addition Fas ligand upregulation on infected cells could induce death in an autocrine manner through Fas ligation.

Nef subverts these responses in different ways. Nef can associate with and inhibit the activity of apoptosis signalling regulating kinase 1 (ASK1). ASK1 links

the TNFR and Fas mediated signals via Fas ligand and TNFα to the JNK/p38 MAPK pathways. Overexpression of ASK1 causes apoptosis and expression of dominant negative ASK1 will block receptor induced death signals. Thioredoxin can inhibit ASK1. Thioredoxin is a redox regulator protein and it seems Nef blocks the stimulus dependant release of Thioredoxin from ASK1.

Nef can also block signals regulated by the Bcl family. Pro-apoptotic members of the family (Bad, Bax, Bak, Bid for example) form heterodimers with members of the same family serving to inactivate them (such as Bcl2, Bcl-X_L, Bcl-w). The pro-apoptotic factors such as Bad are phosphorylated on serine residues releasing Bcl-2 for pro-survival activity (Gross et al., 1996). Ligation of growth factor receptors or cytokines results in activation of PI3-K and Akt kinases that can directly phosphorylate Bad. Middle T antigen of Polyoma virus activates this pathway of anti-apoptotic signalling (Wolf et al., 2001). Nef binds and activates PI3-K like middle T antigen to activate the Nef associated PAK kinase. The Nef –PI-3-PAK complex phosphorylates Bad resulting in a block of apoptosis induced by serum starvation and HIV replication itself. Nef anti-apoptotic signalling increases viral particle release and enhances viral replication.

1.9vi Nef enhancement of virion infectivity

Two mechanisms have been proposed for the effect of Nef on HIV infectivity. One of these is the downregulation of CD4 that results in decreased sequestration of virion Env. Nef stimulates HIV-1 infectiousness in a CD4 dependant manner (Chowers et al., 1995). Nef defective viruses produced from CD4 negative cells are about ten times less infectious in single round infectivity assays as their wild type counterparts. Nef mutated virions demonstrate a severe growth defect in PBMC infected while resting and subsequently activated (Spina et al., 1994, Millar et al., 1994).

Analyses performed on single rounds of infection reveal that Nef promotes the events that immediately follow viral entry, thereby stimulating the efficiency of HIV proviral DNA synthesis. A recent study has revealed that *nef* transcripts can be detected even prior to proviral nuclear translocation and integration. The route

by which the virus infects cells appears to be important in this effect. HIV-1 particles pseudotyped with the G protein of vesicular stomatitis virus do not require *nef* to achieve similar levels of infection as the *nef* positive virus. This suggests direct targeting to the endocytic path may play a role. Possibilities include that Nef stabilises the reverse transcription complex or influences events associated with viral uncoating.

Different domains are required for this effect of Nef from those implicated in CD4 downregulation. These include a sequence between amino acids 17 and 26, the SH3 binding domain and the PAK kinase recruitment domain. This di-arginine motif contributes to CD4 dependent and independent enhancement of virion infectivity. Another explanation for Nef enhancement of infectivity has been described. Nef has a proteolytic cleavage site for the viral protease. About 60-200 copies of Nef are incorporated in each virion-usually the cleaved form. The C-terminal domain of Nef incorporated in viral particles is liberated from the N-terminal domain. Mutants in the proteolytic cleavage site (WL58) retain the ability to increase infectivity. Replacing HIV-1 Nef in trans by SIV Nef which is not cleaved by the HIV-1 protease does not affect infectivity. Therefore it is unclear what roles the virion incorporation of Nef and its cleavage by the viral protease plays in the life cycle.

1.9vii Nef alteration of T cell signalling

Nef is the earliest expressed HIV transcript and can be detected before HIV integration indicating a role in the earliest stages of the viral life cycle. The HIV long terminal repeat (LTR) contains transcriptional regulatory elements identical to those of T cell inducible genes. It has been hypothesised if Nef could affect signal transduction paths normally activated after T cell stimulation it might affect HIV replicative capacity as HIV replicates to high levels in activated T cells. Despite many studies addressing this question definitive evidence for a role for Nef in this context has been lacking.

Nef contains a conserved poly-proline motif that acts as an SH3 binding domain. Nef recognises the SH3 domain of Hck and Lyn PTKs via this domain (Lee et al.,

1996, Lee et al., 1995, Saksela et al., 1995). It has been reported to interact with Lck via its central domain and N-terminus (Baur et al., 1997, Collette et al., 1996, Greenway et al., 1996). In addition Nef is capable of sequestering Lck into the cytoplasm away from the CD4 cytoplasmic tail in the process of CD4 downregulation (Aiken et al., 1994, Baur et al., 1997). Nef also forms interactions with PAK1 and PAK2 (Sawai et al., 1994, Sawai et al., 1995, Lu et al., 1996, Nunn et al., 1996). PAK kinases induce cytoskeletal alterations, bind to GTPases cdc42 and RAC1 and signal through the MAP kinase cascade. In addition interaction of Nef with protein kinase C θ has been reported (Smith et al., 1996).

Despite the documentation of these multiple interactions it has not been possible to demonstrate a definitive functional effect of Nef on T cell signalling. Several Nef transgenics have been engineered. Nef-expressing transgenic thymocytes show enhanced calcium flux and increased mitogenic responses to anti-CD3 T cell stimulation. A Nef transgenic where *nef* was expressed under control of the CD4 promoter enhancer element demonstrated thymocyte hyperactivation with increased tyrosine phosphorylation of LAT and MAPK after T cell stimulation. In addition rare mature peripheral cells showed increased expression of activation markers. CD8-Nef chimeras were used to study Nef affect on signalling in Jurkat T cells. Surface expression of such chimeras resulted in induction of NFκB luciferase activity, accumulation of tyrosine phosphorylated proteins and surface expression of T cell activation markers. Furthermore prolonged expression of these chimeras on the T cell surface resulted in cell death by apoptosis (Baur et al., 1994). Not all CD8-Nef accumulated at the cell surface. In cells where it was sequestered in the cytoplasm inhibition of T cell signalling was observed.

Monkey models have lent further support for a function of Nef in T cell activation. SIV Nef variants containing amino acid sequences acting as functional immunoreceptor tyrosine-based activation motifs (ITAMS) replicated to high levels in unstimulated PBMC (Du et al., 1995). A study in an IL2-dependant rhesus monkey T lymphoid cell line infected with herpes virus demonstrated in the absence of IL2 SIV strains containing *nef* from SIV or HIV grew 100 times

more efficiently than *nef* deleted counterparts. In addition the *nef* positive viruses could induce IL2 in this context (Alexander et al., 1997).

More recently Nef has been shown to localise to lipid rafts in T cells via its myristoylated N terminus (Wu et al 2001, Schrager et al., 2000). Lipid rafts accumulate signalling mediators after T cell activation and are thought to represent a platform for initiation and maintenance of T cell activation signalling cascade. Two studies have demonstrated a priming role for Nef in T cells. In the presence of Nef, activity of NFκB, NFAT and AP1 luciferase reporters is significantly increased after exogenous stimulation in comparison to cells lacking Nef. In contrast other studies have inferred Nef can inhibit activation (Collette et al., 1996, Bandres et al., 1994, Carreer et al., 1994, Collette et al., 1996, Collette et al., 1996, Iafrate et al., 1997, Neidermann et al., 1993, Neidermann et al., 1992).

1.9viii Nef structural studies

It has not been possible to determine the complete structure of HIV Nef however components have been solved by either NMR or crystallography. Nef consists of a highly conserved and well-folded core domain of around 120 residues and a genetically diverse and structurally flexible N-terminal arm of around 70 residues. The core domain adopts a stable tertiary fold. This core forms an α-β domain in which a central anti-parallel β sheet of four strands (βA-βD) is surrounded N-terminally by two long anti-parallel α helices (αA and αB) and C-terminally by two short a helices (αC and αD). The proline rich sequence is located upstream of αA and adopts a left-handed helix of the type two polyproline II. The structure of this core domain has been solved by both NMR and crystallography and by crystallography in complex with Src kinases. Most signalling molecules capable of forming interactions with Nef require this domain for binding. Nef has a high (nanomolar) affinity for the SH3 domains of Hck and Lyn, and a lesser (micromolar) affinity for the SH3 domains of Lck, Fyn and Src. The functional outcome of interactions with the SH3 domains of various kinases does not appear to correlate with kinase activity. Nef has been shown to activate Hck but

not Lyn or Src. It has also been shown to decrease kinase activity of Lck and Fyn.

The core domain of Nef has been shown to mediate oligomerisation and Nef dimers and trimers have been demonstrated in vivo and in vitro. Their significance is unclear. Oligomerisation has been shown to mediate signalling and endocytosis in other contexts and as such may be important for Nef function. The quaternary structure of Nef might facilitate functional connections with signalling or vesicular trafficking components.

The core domain is involved with interactions with PAK kinase, TCRζ and the Thioesterase. Another feature of the Nef structure are the two flexible regions that comprise 50% of the polypeptide chain. These occur in the core domain and the N-terminal arm. This loop connects with three binding motifs a di-leucine based internalisation motif is found to the middle of the loop and associates with Adaptins. Closer to the N-terminal of the loop a di-acidic sequence has been shown to be necessary for the association with Nef and β-COP. Finally a C-terminally located cluster is required to localise Nef with both AP complexes and the v-ATPase. As the core domain sequence is divergent in sequence but conserved in length a proposed function is the presentation of these motifs at a defined distance from the folded core domain.

An unusual feature of Nef structure is the presence of several flexible regions that is not common for a cytoplasmic protein. This could explain so many of the diverse reported interactions of Nef as the flexible regions can provide an extensive accessible surface.

1.10 T cell activation and signalling

T cell activation following ligand recognition is a central part of the immune response. T cell receptor (TCR) heterodimers mediate this process. These resemble antibodies in their ability to create vast numbers of different variable (V) region sequences through DNA rearrangement. Most T cell types recognize specific fragments of antigens bound to major histocompatibility complex (MHC)

molecules displayed on the surface of other cells. This ability to survey degradation products of antigens makes for a detection system that is intrinsically difficult for pathogens to avoid, as all proteins must eventually be degraded. Very few peptide-MHC complexes on an antigen-presenting cell are needed to trigger a T cell response allowing for a high degree of sensitivity. In order to understand how engagement of the TCR to a ligand activates a T cell, attention has focused on the CD3 molecules (CD3 ε, γ, δ and ζ) that are assembled together with the TCR heterodimer and possess ITAM motifs that are phosphorylated on activation These phosphoryalted ITAMS may subsequently interact with SH2 domains (Reth, 1989). The TCR polypeptides themselves have very short cytoplasmic tails, and it appears that all proximal signalling events are mediated through the CD3 molecules. TCRs are organized in dimeric units (Terhorst et al., 1996), and evidence also indicates there are two TCR heterodimers per unit (Fernandez-Miguel et al., 1999, Terhorst et al., 1996). The variety and apparent redundancy of these polypeptides probably relate to the varying signals that a T cell must receive in order to mature and survive. In particular, immature T cells are heavily selected in the thymus both for a successful TCR rearrangement (the pre-TCR-CD3 complex) and later for complete TCRs that react weakly to self-peptide-MHC complexes, which is important for avoiding selection of self-reactive T cells. The selected T cells then require additional stimulation in the periphery from such ligands in order to survive. This selection and maintenance process is apparently necessary to establish a TCR repertoire that is both predisposed toward a particular MHC complement and in a high state of readiness to respond to the appropriate foreign antigen when it comes along.

For many years it has been thought that the principal trigger for T cell activation is the tyrosine phosphorylation of CD3 molecules, particularly CD3, brought about by TCR crosslinking and mediated by Lck (Kane et al., 1999). However it has recently been shown a slightly earlier event involving a conformational change and subsequent exposure of a proline-rich region of the cytoplasmic tail of CD3 may be involved (Gil et al., 2002). Exposure of this region allows the adaptor protein Nck to bind. This can occur in isolated TCR-CD3 complexes, with

stimulation by monovalent antibodies, and independent of early tyrosine phosphorylation. The association of Nck to CD3 appears to be necessary for proper T cell activation, as a dominant negative construct of Nck inhibits the ability of T cells to form conjugates to other cells in response to antigen, and disrupts aspects of synapse formation, cytoskeletal reorganization, and cytokine production. Thus, it appears that there are at least two distinct pathways whereby TCR engagement triggers activation in T cells: tyrosine phosphorylation of ITAMs by Lck and Fyn, and a conformational change in CD3 leading to Nck recruitment, with both of these occurring within seconds of TCR engagement with ligand. These signals probably converge at some point downstream, with a likely point of convergence being the one of the signalling molecules SLP76 or LAT both essential for T cell activation.

1.11 Functional genomics and microarray technology

Completion of the human genome sequencing project has paved the way for studying biological phenomena on a genome wide basis. Various methodologies are being evolved with this aim in mind. DNA microarrays provide a means of analysing transcriptional responses on a large scale. At present no whole genome chip exists for the human genome although it is inevitable this will be developed.

Microarrays consist of precisely positioned DNA fragments (probes) at high density on a solid support. Three main types of microarray are filter arrays, spotted glass slide arrays and in situ synthesised oligonucleotide arrays. In gene expression microarrays either synthetic oligonucleotides or cDNA fragments are used as probes. Ideally probes should be sequence validated, possess unique sequence, show minimal cross-hybridisation to related sequences and provide a comprehensive representation of the expressed fraction of a genome including splice variants. Sources of probe fragments used for arraying have been bacterial cDNA or bacterial artificial chromosome (BAC) clone sets, although sets of long oligonucleotides are increasingly becoming a viable alternative. There

have been many shortcomings in libraries for complex organisms. For example libraries available for mice and humans contain a certain amount of redundancy, contamination and misannotation. Many initial cDNA clone sets were compromised by contamination with T1 phage, by containing multiple clones in individual wells and by incorrect sequence assignment (Halgren et al., 2001). For some microarray applications such as the sensitive detection of genomic losses in tumour cells large insert clones such as BACS are more appropriate than cDNAs. Human BAC clone sets were generated as part of the human genome sequencing project. These libraries contain as much as a tenfold redundancy across genomes, requiring individual clones to be selected to reduce clonal overlap for microrraying purposes.

DNA for arraying is typically prepared from clone sets by high throughput PCR rather than purification of individual plasmids. There are considerable logistical difficulties in handling large numbers of bacterial clones making the use of oligonucleotide arrays an attractive alternative. The design of oligonucleotides for arraying is not simple (Relogio et al., 2002, Rouillard et al., 2002). In practise the use of commercially available arrays is favoured due to cost considerations and yield of full length long oligonucleotides which can be suboptimal.

Spotted arrays are mostly printed on glass. Glass slides are the favoured solid support for probe immoblisation as they allow a variety of surface chemical modifications, are resistant to high temperature, are cost effective, possess low fluorescence, are transparent and rigid. Many initial arrays contained poly-L-lysine as the substrate due to low cost and ease of manufacture. The type of substrate used can affect the signal intensity, degree of background and durability of the slide. Substrate choice is often dependent on whether cDNAs or oligonucleotides are being printed.

The main application of microarrays has been that of comparitive expression profiling in different contexts. Examples would be comparisons of diseased versus normal tissues (Lock et al., 2002), studying gene regulation during development (Miki et al., 2001), following changes after cell stimulation (Iyer et al., 1999) and profiling neoplastic lesions (Alizadeh et al., 2000, Bittner et al.,

2000, Dhanasekaran et al., 2001). Microarrays have also been used to screen for mutations (Ahrendt et al., 1999), comparative genomic hybridisation (Pollack et al., 1999), chromatin immunoprecipitation (Lo et al., 2001, Shannon and Rao., 2002), genotyping (Lindblad-Toh et al., 2000) and for localised cell transfection (Ziauddin and Sabatini, 2001). Experiments using glass slide microarrays involving competitive hybridisation of two targets are often carried out by labelling each target (test and reference) with a specific fluorescent dye (Cy3 or Cy5). Experiments may involve individual pairwise comparisons or compare one sample against all others. Labelling protocols are based on the reverse transcription of mRNA either from highly purified poly(A) mRNA or total RNA extracts. Many protocols have been developed for the extraction of high quality RNA that remove contaminating polysaccharide, protein and RNases. Initial protocols involved direct labelling. Here a poly(dT) primer is used to prime mRNA in the presence of fluorescently labelled nucleotides (typically Cy3 or Cy5 conjugated dCTP or dUTP) or radioactive isotopes. As Cy3 and Cy5 are bulky their incorporation using standard enzymes is rather inefficient. It has also been noted that rates of incorporation can differ between dyes resulting in biases between dye incorporation (Yang et al., 2002). The development of reverse transcriptases that allow more efficient incorporation of flourescently labelled oligonucleotides should bypass this problem. Other methods of sample labelling include amino allyl labelling. Here an amino modifed dUTP is used instead of a prelabelled nucleotide. After reverse transcription the free amine group on the amino allyl modified dUTP can be coupled to a reactive *N*-hydroxysuccinimydl ester flourescent dye. This technique has benefits of better sensitivity and absence of dye biases, but requires more time. A large amount of RNA is required for sample labelling. RNA amplification protocols have been developed to overcome this limitation. Many of the methods are based on "Eberwine" amplification (Van Geler et al., 1990).

Conventional methods of hybridising arrays such as under coverslips or in chambers can give variable results. This can be due to problems with probe distribution resulting in differences in gene expression dependent on spatial

position on the array (Colantuoni et al., 2002). Newly designed commercial instruments have the potential to undertake automated hybridisation improving reproducibility. After hybridisation microarrays are scanned using using either a scanning confocal laser or charge coupled device camera based reader.

Microarray experiments are providing unprecedented quantities of genome-wide data on gene-expression patterns. The completion of the sequencing of a large number of prokaryotic and eukaryotic genomes facilitates attempts to functionally classify predicted genes. Microarray analysis promises to contribute to the functional annotation of genomes and has already provided a wealth of genome-wide expression data. Much attention has been focused on experimental protocols for microarray studies, but the strategies for data analysis have a profound effect on the interpretation of the results. Expression data from each experiment must first be normalized to account for systematic experimental variation, including unequal dye incorporation and detection efficiencies. Normalisation of microarray data represents a key component of data analysis. It is not uncommon for a certain amount of systematic variation to exist in the data produced from experiments owing to the complex process of production and hybridisation of spotted microarrays. Various normalisation algorithms are available for analysis and the choice of that used is based on the type and degree of systematic biases that are encountered in a particular experiment. These could be biases in dye incorporation during labelling, variations in probe distribution during hybridisation, topographical slide variation or scanner induced bias (Karsten et al., 2002). Microarray analysis software incorporates options for normalisation. At present there are few normalisation algorithms that adjust for irregular spatial distribution across the surface of an array. After correction of biases toward a particular channel and global variation in mean expression has been adjusted for there can remain evidence of a nonrandom distribution of the differentially expressed genes present. Two options are available for addressing this. The SNOMAD method attempts to correct both intensity and spatial bias (Colantuoni et al., 2002). Pin-group normalisation uses information obtained from the grids and sub-grid layout to carry out a LOWESS based transformation of the

data. Both are implemented in the open-source R statistical language. It is hoped further development of normalisation techniques will improve correction for systematic variation. For comparison between experiments, data is often first filtered to select a subset or to exclude genes for which there is much missing data. A distance metric must then be chosen, which determines how similarity is measured between gene-expression patterns. Genes and experiments can then be grouped using various computational methods. Each step can influence how the expression data are grouped. Clustering algorithms, which are the most widely used approaches to analysing gene expression, can be classified as hierarchical or non-hierarchical (self-organizing maps (SOMs), *k*-means clustering and principal component analysis), agglomerative (hierarchical) or divisive (*k*-means, SOMs), and supervised (support vector machine) or non-supervised (hierarchical and *k*-means clustering, SOMs). The choice of data analysis strategy is determined by the purpose of the microarray experiment and the available knowledge of the biology of the system under investigation.

1.12 Proteomics

With complete genome sequences now available for several prokaryotic and eukaryotic organisms molecular and cellular functions for these genes must be assigned. The field of proteomics has evolved to address this and includes in its goals the development and application of methods for genome wide analysis of protein expression and function. The creation of systems for rapid analysis of proteins will accelerate the process of 'functionalisation' of these biomolecules. While proteomics can be conceptually viewed as the protein equivalent of genomics a myriad of technical problems exist for the scientific investigation of proteins that present challenges beyond that encountered in genomics. For example unlike RNA or DNA proteins do not inherently possess well defined high-affinity and/or selectivity of binding partners. Gene microarray technology utilises the interactions oligonucleotides share with their anti-sense partners. Protein microarrays however must be designed to use a specific capture reagent

for each protein. Proteins exhibit a range of biochemical properties exceeding that encountered with DNA and these are linked to the precise 3D structure of folded polypeptides. The diversity of traits exhibited by proteins, ranging from extreme pI values to membrane association to post-translational modification mean that a universal method to handle and process proteins is not currently available. Another large hurdle is the characterisation of low abundance proteins as in contrast to RNA or DNA proteins cannot be amplified by methods analogous to PCR.

A mainstay of proteomic analysis has been the 2D gel and mass spectrometry (MS) approach. MS has become a primary tool for proteomics as it is capable of sensitive and rapid protein identification combined with quantitation. While it is possible to identify thousands of proteins from microgram sample quantities in a single day the need for increased capability is required. Central to success of the MS approach is the separation methodology primarily used. 2D-gel separations are the traditional approach however liquid phase separations are growing in use. These are primarily based on liquid phase chromatography (LC). At present most LC-MS uses an electrospray ionisation (ESI) interface to produce ions from liquid samples and matrix assisited laser desorption ionisation (MALDI) is most commonly used for the analysis of individual processed samples.

1.13 RNA interference

RNAi has proved to be a useful reverse genetic tool in the context of assigning function to individual genes. Systematic RNAi screening has been used to assign function to 13.9% genes on chromosome I in *C.elegans* (Fraser et al., 2000). In addition it has been employed in *Drosophila* to identify genes involved in phagocytosis (Ramet et al., 2002) and in *Trypanosoma brucei* to establish glycolysis as modulating glycoprotein expression (Morris et al., 2002).

However in mammalian cells use of dsRNA as a reverse genetic tool must be undertaken using short sequence specific dsRNAs. Innate immune responses to microorganisms developed by higher eukaryotes include the recognition of

dsRNAs. dsRNAs represent a replicative intermediate for many viruses not normally present in eukaryotic cells. In mammalian cells this response involves the production of Interferon. Interferon can reduce viral spread by inhibiting viral gene expression and causing apoptosis of infected cells. A key characteristic of RNAi is its sequence specificity. mRNAs homologous in sequence to the dsRNA are specifically degraded.

Work in *Drosophila* has contributed to the current mechanistic understanding of RNAi (Zamore et al., 2000, Elbashir et al., 2001). DsRNAs introduced to *Drosophila* cells are cleaved into 21 or 22-nt dsRNAs with a 2-nt or 3-nt overhang referred to as small interfering RNAs (siRNAs). DICER, an RNase III-like enzyme mediates this cleavage (Bernstein et al., 2001). These siRNAs are incorporated into a multiprotein complex of approximately 500kD known as the RNA-induced silencing complex (RISC). RISC may undergo an ATP dependant activation step that involves unwinding of the double stranded siRNA component to give a single stranded RNA guide that targets RISC to homologous RNAs. Binding of the homologous mRNA to RISC occurs and a ribonuclease component cleaves the target mRNA at the centre of the region complementary to the guide RNA. The cleaved RNA is degraded by cellular exonucleases after release of RISC. Synthetic siRNAs can be incorporated into RISC and induce targeted mRNA degradation (Elbashir et al., 2001). DsRNAs less than 30 bp do not induce an interferon response and as a result siRNAs can effectively inhibit gene expression in mammalian cells.

1.14 Summary

The work described in this thesis investigates the function of HIV Nef. The aims of the work were to clarify the in vivo relevance of described Nef in vitro protein-protein interactions by examining the potential downstream consequences of these interactions in terms of gene expression. Large scale gene expression profiling was used to investigate gene expression changes induced by Nef in CD4 T cells as a consequence of T cell signalling. The demonstration Nef can

induce gene expression changes compatible with T cell activation using this approach led to an attempt to define the molecular mechanism by which this occurs.

Nef is one of the HIV proteins for which there is currently no drug inhibitor. Better drug treatments are required to attenuate the progression of HIV. Investigating how Nef interacts with host cell proteins to induce HIV pathogenicity may permit design of inhibitors. It has recently been demonstrated engineered cyclic D-peptides can inhibit HIV-1 entry by targeting a prominent pocket on the surface of the NH2-terminal coiled coil of the pre-hairpin intermediate (Root et al., 2001). These observations have led to phase I/II clinical evaluation of the Trimeris C peptide, T-20 as an inhibitor of HIV entry. T-20 is the first of a new target class for the treatment of HIV-1 infection. The proof-of-concept for this target has fuelled the search for more drug-like candidate molecules that act in a similar manner. Inhibition of the effect of Nef on viral productivity and on MHC 1 down-regulation would have obvious benefits for the infected individual. In addition delineation of the molecular mechanism of action should yield insight into undiscovered aspects of vesicular trafficking and signalling.

Chapter 2

Materials and Methods

2.1 Source of Chemicals and Enzymes

Chemicals were purchased from Aldrich, BDH, or Sigma and were of Analytical Reagent or Molecular Biology grade. Bacterial media products were from Oxoid, tissue culture materials from Gibco-BRL, agarose was from FMC Bioproducts, pre-mixed acrylamide/bis-acrylamide (37:5:1) was from Amresco, radioisotopes were purchased from Amersham. Oligonucleotides were purchased from Gibco. Enzymes were purchased as follows:

Superscript II reverse transcriptase-Gibco-BRL
Calf Alkaline phosphatase -Boehringer Mannheim
RNase –free DNase I -Boehringer Mannheim
Taq DNA polymerase-Boehringer Mannheim
Restriction enzymes-Boehringer Mannheim
T4 DNA ligase-Boehringer Mannheim

2.2 Solutions

Solutions were prepared in water from an Elga Primostat purification system, and were sterilised by autoclaving. Solutions for RNA work were treated with DEPC for 15 hours at 37^0C and autoclaved.

TFB 1
30mM KOAc pH 5.8
100mM KCl_2
10mM $CaCl_2$
50mM $MnCl_2$

15%v/v glycerol

TFB 2
10mM MOPS pH 6.8
75mM $CaCl_2$
10mM KCl_2
15% v/v glycerol

L Broth
1% w/v bactotryptone
1% yeast extract
85mM NaCl

TE
10mM Tris-Cl pH 8.0
1mM EDTA

5X TBE
500mM Tris-borate
10mM EDTA

SDS running Buffer
100mM Tris-Cl pH 8.3
960mM Glycine
0.5%w/v SDS

10x Formamide Loading Buffer
10mg/ml Bromophenol Blue
10mg/ml Xylene Cyanol
10mM EDTA
80% v/v Formamide

10X denaturing solution

1 M NaOH

10 mM EDTA

2X neutralizing solution (1 M NaH 2 PO 4 [pH 7.0])

27.6 g NaH 2 PO 4 •H 2 O

Add 190 ml of H 2 O. Adjust pH to 7.0 with 10 N NaOH if necessary. Add H 2 O to 200 ml.

20X SSC

175.3 g NaCl

88.2 g Na 3 Citrate•2H 2 O

Add 900 ml of H 2 O. Adjust pH to 7.0 with 1 M HCl if necessary. Add H 2 O to 1 L.

20% SDS

200 g SDS

Add H 2 O to 1 L. Heat to 65°C to dissolve.

Wash Solution 1

2X SSC

1% SDS

Wash Solution 2

0.1X SSC

0.5% SDS

FACS buffer-PBA

PBS

1% BSA

0.1% sodium azide

2.3 Restriction Digests

Digests were performed in Boehringer Mannheim buffers using the optimal buffer for single digests and the best compromise buffer for double digests. Digestion products were analysed by agarose gel electrophoresis. If fragment extraction was required DNA extraction kit from Qiagen was used.

2.4 Electrophoresis

DNA markers

Agarose gel markers XIV and XVII were obtained from Boehringer Mannheim.

Agarose gel electrophoresis

Samples were run in 1X Orange G buffer on 1-2% agarose TBE gels containing 1μg/ml ethidium bromide with current limiting at 200mA (minigels). DNA was visualised on a UV transilluminator (Stratagene model 2040EV), and photographed using a UVP digital camera system. When fragments were being isolated the gel was visualised using low wavelength UV and excised from the gel with a clean razorblade. DNA was isolated using gel purification kit from Qiagen.

SDS Polyacrylamide gel electrophoresis

50ml native and denaturing (7M urea gels) were prepared in 1x TBE using 40% acrylamide: bisacrylamide (19:1). Polymerisation was initiated with the addition of 50μ TEMED and 500μl 10% ammonium persulphate, and the gel was cast

between two glass plates. Gels were run at 80V through the stacking gel and 160V thereafter in SDS PAGE running buffer.

2.5 Cloning

Vector preparation

3μg of vector DNA was linearised by addition of 6μl DNA, 3μl restriction enzyme digest reaction buffer, 3μl restriction enzyme and 18μl sterile distilled H_2O. This was incubated for 3 hours at 37°C and subsequently heat inactivated at 70°C for 2 minutes. After cooling on ice for 60 seconds 2μl of alkaline phosphatase was added together with 4μl 10x reaction buffer and 4μl of H_2O. This reaction was incubated for a further 30 minutes at 37°C before running on TBE agarose gel and DNA purification using Qiaquick (Qiagen) purification reagents.

Ligations

These were carried out using rapid ligation kit (Boeringer Mannheim). 1μl vector DNA was mixed with 3μl insert DNA, 2μl DNA dilution buffer and 4μl H_2O. This was mixed with 10μl ligation buffer and finally 1μl T4 DNA ligase. The reaction was allowed to proceed at room temperature for 15 minutes prior to bacterial transformation.

2.6 Bacterial Transformation

Bacterial strains

DH5α F'*/endA1 hsdR17* ($9r_k^-m_k^+$) *supE44 thi-1 recA1 gyrA* (Nal^r) *relA1 Δ (lacIZYA-argF)U169 deoR (ϕ80dlacΔ(lacZ)M15)]*

XL-1 Blue F::Tn*10proA+B+lacIq Δ(lacZ)M15/recA1 endA1 gyr A96* (Nal^r) *thi hsdR17* ($r_k^-m_k^+$) *supE44 relA1 lac*

Preparation of competent cells

A single colony of DH5α or XL-1 Blue was inoculated into a 50ml culture in LB broth and grown overnight. 10ml of this was used to inoculate 500ml cultures that were grown to obtain an OD_{600} of 0.5. The culture was cooled and the cells harvested after centrifugation (10 minutes at 5000 rpm) in a pre-cooled JA-10 rotor using a Beckman J2-20 centrifuge. The cell pellet was then resuspended in 100ml pre-chilled TFB 1 and incubated on ice for 30 minutes then harvested as before. Cells were resuspended in 20ml TFB 2 and incubated for 15 minutes before 500μl aliquots were frozen at -70^0C.

Transformation with plasmid DNA

Aliquots of frozen competent cells were thawed on ice. 200μl of cells were mixed with 2μl of ligation reaction and incubated on ice for 40 minutes, heat shocked at 42°C for 90 seconds and then returned to ice for 2 minutes. The cells were added to 1ml of LB and shaken at 37°C for 30 minutes. The cells were isolated by centrifugation and spread on pre-warmed selective plates of either LB containing 50μg/ml Ampicillin or Kanamycin. These were incubated at 37 °C overnight.

2.7 DNA isolation

Small and large scale DNA isolation was carried out using Qiagen DNA extraction kits.

2.8 DNA Sequencing

Automated sequencing reactions using an Applied Biosystems 3373 stretch DNA sequencer were performed as recommended.

2.9 Cell stimulation and Drug treatment

For stimulation with anti-CD3 30μl of 10μg/ml OKT3 was added to 96-well round-bottom microtiter plates and incubated at 37°C for 90 minutes. The wells were washed with PBS three times and 2×10^5 cells added to each well in 0.2 ml media. Cells were incubated at 37^0C and harvested at designated time points. For anti-CD28 stimulation of Jurkat 10μg/ml was used following the same procedure. Anti-CD28 antibody (clone CD28.2) was obtained from Pharmingen. For Cyclosporin inhibition experiments cells were treated with 200ng/ml CsA for the duration of induction with Doxycycline. Trypan blue staining was performed on CsA treated and non-treated Jurkat to exclude the possibility of toxicity prior to harvesting cells for RNA preparation. Drug inhibition assays used Cyclosporin obtained from Sigma and DRB obtained from Calbiochem.

2.10 RNA preparation

RNA was prepared using RNeasy extraction kits (Qiagen). Samples were DNase treated by incubation at 37^0 C for 30 minutes with DNase before cleaning using RNeasy spin columns. Samples were stored as ethanol precipitates at -70^0 C.

2.11 cDNA Synthesis

RNA (5μg in 5μl DEPC water) was incubated with gene specific primers (Clontech) at 70^0C for 2 minutes, then at 50^0C for 2 minutes before addition of the reaction mix. This consisted of 5 mM deoxyribonucleotides (dNTPs), 0.1 M DTT (dithiothreitol, Melford Laboratories), Superscript Reverse Transcriptase buffer and finally Superscript Reverse Transcriptase (Gibco-BRL).

2.12 Microarray Hybridisation

Gene specific primers were used to prime first strand cDNA synthesis. ^{32}P-labelled cDNA probes were hybridised overnight to microarray membranes. After washing arrays were exposed to a phosphoimager screen for 24 hours.

2.13 cDNA Microarrays

The microarrays used were Atlas Human 1.2 Array, Atlas Human 1.2 Array II and Atlas Human 1.2 Array III from Clontech. These arrays represented a total of 3528 genes. Controls include bacterial DNA, housekeeping genes and human genomic DNA. Arrays were made using gene specific primers to amplify 200-400-bp cDNA fragments that lack strong secondary structure. cDNA's were selected after sequence analysis to minimise cross hybridisation to other genes on the array. In addition selected cDNAs lack repetitive elements and poly-A sequences. Each individual microarray contained only 1,176 genes to maximise hybridisation sensitivity.

2.14 GenePix Pro 3.0 Data Analysis

Data was gathered from phosphoimager-scanned images using GenePix Pro 3.0 software (Axon Instruments). Intensity values were obtained by first masking over array images. A grid containing a series of circles corresponding to the spots of the array was laid over the image, and the circles adjusted to each spot. The intensity of each pixel within the circle was calculated for each channel, termed "feature". For each raw image the mean, median and standard deviation of the pixel intensities in each feature indicator was computed. To reduce the effect of non-specific flourescence the background intensity was subtracted from the feature intensity before any ratio calculations were performed. A local background technique was used to subtract the background intensity. A different background was computed for each individual feature-indicator and the mean, median and standard deviation of the background pixel intensities were reported. For all ratio calculations that require background subtraction the median background is used. Various ratio quantities are computed by Genepix Pro 3.0 allowing different appreciation of aspects of the raw data. These include ratios of overall derived feature properties, quantities derived from pixel-by-pixel ratios

and quality factors such as the sum of medians, sum of means and log ratio-a base two logarithm of the ratio of medians.

2.15 Atlas Navigator Data Normalisation and Analysis

Before import to Atlas Navigator software the average of the median intensity values for each gene was calculated for at least three replicate experiments. In order to conduct comparisons between different experimental conditions average raw median intensity values were normalised at two levels. To eliminate differences due to varying exposure times I normalised each experiment to itself. By dividing the signal intensity of Gene A in Experiment 1 by the median signal intensity of all genes in experiment 1, the median of all measurements for each array was converted to 1. To eliminate the variation in intensity scale across different genes I normalised by comparing average raw median intensity values of all experiments to average raw median intensity values for non-treated control experiments. Here the signal intensity of gene A in experiment 1 was divided by the signal intensity of gene A in experiment X.

2.16 Cell lines

Cells were maintained in RPMI 1640 media (Gibco-BRL) with 10% tetracycline free fetal calf serum (Clontech) and penicillin/streptomycin (Gibco-BRL). For induction of transgene expression cells were treated with 1 μg/ml doxycycline (Sigma). Cell lines Jurkat E6-1 and J.RT3 3 5.1 were obtained from American Type Tissue Collection (ATCC). p116 ZAP-70 and Syk negative Jurkat were kindly provided by Dr R. Abraham – Duke University. Cell line Jurkat Tat III (Rosen et al., 1986) stably transfected with HIV III B Tat was obtained from the United Nations Programme of HIV/AIDS (UNAIDS) repository provided by Dr C.A. Rosen. All cell lines were tested routinely to confirm the absence of mycoplasma infection. Cells were incubated at 37^0C, 5% CO_2 and100% humidity.

2.17 DNA Transfections

DNA transfections were performed by electroporation of 5-10 million cells using a Biorad electroporator. Cells were resuspended with 30μg DNA in 0.4mls RPMI supplemented with FCS, penicillin and streptomycin and placed in electroporation cuvettes. Cells were electroporated using 950V, 72R 250 capacitance. After electroporation cells were incubated in RPMI supplemented with FCS, penicillin and streptomycin as usual.

2.18 Luciferase assays

The HIV-1 LTR luciferase construct pBlue3'LTR-luc was obtained through the AIDS Research and Reference Reagent Program, Division of AIDS, National Institute of Allergy and Infectious Diseases, NIH from Dr. Reink Jeeninga and Dr. Ben Berkhout (Jeeninga et al., 2000). pLTR-luc, pRL-TK (Promega) and either PI2 or PI2-WT were electroporated into Jurkat III Tat cells. In all experiments transfections were performed in triplicate. Drug treatment with 10 or 20 μM DRB was performed on a single pool of transfected cells. The Luciferase Assay system (Promega) was used to assay for luciferase activity at 36 hours post transfection. Transfection efficiency was normalised using the co-transfected Renilla luciferase activity.

2.19 Northern blots

Poly (A) RNA was prepared from Jurkat transfected with PI2-WT and control plasmids. RNA was electrophoresed through a 1% agarose formaldehyde gel and transferred to nylon membranes. [α-^{32}P] dCTP labelled cDNAs for CDK9 and β-actin were prepared using Rediprime II from Amersham. Primer sequences used to prepare a 268bp CDK9 cDNA fragment are available from Clontech.

2.20 Lipid Raft Extraction

Lipid raft fractions were purified by sucrose density gradient centrifugation. 50x 10^6 cells were washed with cold PBS and lysed with lysis buffer containing 1% Triton X 100. Samples were cleared at 14,000g for 30 minutes before being overlayed with sucrose density gradient. This was composed of 1ml 85% sucrose in sucrose density gradient buffer, then 6mls 30% and finally 3.5mls of 0.5%. These were subjected to centrifugation at 34000g for 16 hours using a Beckman Ti40 rotor before 1ml fractions were harvested sequentially from each sample.

2.21 Immunoprecipitations

Immunoprecipitations were performed after lysis of cells with NP40 lysis buffer on ice for 30 minutes. Lysis buffer contained protease and phosphatase inhibitors. Samples were cleared at 14,000g for 15 minutes and subsequently precleared with either Protein A or Protein G (Sigma) for 1 hour at 4°C. Antibody was added and the sample rotated at 4°C for a further hour. Finally protein A or G was added before rotating for a final hour. Samples were pulse spun and the supernatant removed. Beads were boiled in SDS sample buffer for 5 minutes before loading on SDS PAGE gels.

2.22 Western Blots

For Nef western blots cells were lysed with NP40 lysis buffer and whole cell lysates electrophoresed on 12.5% SDS gels. Western blot was performed with anti-Nef antibody obtained from the UNAIDS repository supplied by Dr M. Harris. Anti-β-Actin antibody (clone A15) was obtained from Sigma.

2.23 CDK9 western blot and In vitro kinase assay

For CDK9 western blot and kinase assays cell lysates were prepared 36 hours post transfection with Nef or control expression plasmids. 1 x 10^7 cells were

pelleted and washed in PBS at 4^0C. Lysis buffer containing NP40 was added and cells left 5 minutes on ice. The lysate was spun and the pellet washed once with Tris buffer. Pellets were then disrupted by passing 10 times through a 26 gauge, 0.375in injection needle and cleared at 14, 000 x g for 40 minutes. After electrophoresis on 12.5% SDS gels western blot was performed with anti-CDK9 antibody (Santa Cruz). For in vitro kinase assays (IVKA) CDK9 was immunoprecipitated using anti-CDK9 antibody and kinase assays were performed as described by Herrmann et al., 1995. Beads were incubated for 30 minutes at room temperature in kinase buffer in the presence and absence of CTD peptide as substrate. Proteins were blotted to nitrocellulose membranes after electrophoresis on tricene gels.

2.24 Primer Sequences for PCR Primers

Vector p-IRES-2-EGFP

Forward Primer GGA AGA TCT TCC ACC ATG GGT GGC AAG TGG

Reverse Primer TCC CCG CGG GGA TCA GCA GTC TTT GTA GTA

Vector PJEF

Forward Primer CGC GGA TCC GCG ACC ATG GGT GGC AAG TGG TCA AAA CGT

Reverse Primer CGCGGA TCC GCG GCA GTC TTT GTA GTA ATA AGG

Vector tet-on-IRES-EGFP

Forward Primer CGC GGA TCC GCG ACC ATG GGT GGC AAG TGG TCA AAA CGT

Reverse Primer CGCGGA TCC GCG GCA GTC TTT GTA GTA ATA AGG

HA-tagged Nef

Forward Primer CGC GGA TCC GCG ACC ATG GGT GGC AAG TGG TCA AAA CGT

Reverse Primer CGC GGA TCC GCG AGC GTA GTC TGG GAC GTC GTA TGG GTA GCA GTC TTT GTA GTA CTC CGG ATG

2.25 PCR Reaction Conditions

50μl Taq reaction

(Primers 0.2 μM each, dNTPs 0.5mM, $MgCl_2$ 2.5mM, 1μl Taq, 5μl 10x reaction buffer). 30 cycles: 95°C denaturing for 30 seconds, 60°C annealing for 30 seconds and 72°C extension for 5 minutes. The annealing conditions varied from 55°C to 68°C depending on each particular reaction set.

2.26 FACS Staining

Preparation of Cells for FACS Analysis

Cells were washed in cold PBS, counted and aliquoted between FACS tubes. They were further rinsed in FACS buffer before staining with appropriate antibodies and fixed with FACS fix solution.

Staining Reagents

Staining reagents were obtained from DAKO in the case of anti-CD4-RPE and W632-RPE. Anti-CD27-RPE antibody was obtained from Pharmingen. Samples were analysed by Becton-Dickenson FACScalibur or FACScan machines and CellQuest software.

2.27 Creation of Tetracycline Inducible cell lines

Tetracycline operator vector DNA was linearised at Bgl II. 16 reactions of 3μg DNA were mixed in a linearisation reaction and gel purified. A 2μg reaction of a hygromycin resistance cassette (Clontech) was linearised at Hind III and gel purified. Both tetracycline vector and hygromycin cassette DNA were ethanol precipitated to give linearised DNA of tetracycline operator and selectable marker in a ratio of 24:1. Jurkat transactivator T cells obtained from (Clontech) had been split the previous day and were electroporated with the linearised DNA. After 24

hours in culture in RPMI containing tetracycline free FBS, penicillin, streptomycin and neomycin, hygromycin was added in a concentration of 200μg per ml. This resulted in widespread death of cells. After 2-3 weeks Hygromycin resistant Jurkat began to grow out. Single cell cloning of these cells was performed. After two weeks of growth in 96 well plates clones had grown sufficiently to be split into two and grown in 24 well plates. After a further week in culture with both neomycin and hygromycin one out of the two wells deriving from a single cell were subjected to induction with doxycycline at a concentration of 1μg/ml. After 24 hours these clones were analysed for EGFP expression by FACS. Clones demonstrating reasonable level of EGFP induction were then observed for evidence of background EGFP expression in the absence of doxycycline treatment.

2.27 2D gel Analysis

For whole cell lysates 24 hours post Nef expression 20 x 10^6 cells were lysed with NP40 lysis buffer. Lysates remained on ice for 30 minutes before centrifugation at 14,000g for 15 minutes. Acetone precipitation of the lysate was carried out and the resulting protein pellet resuspended in IPG rehydration buffer pH 3-10. pH gradient markers (Carbamylyte Calibration Kit, Pharmacia) were added. First dimension gels analysis was performed using 24cm IPGphor IPG strips pH 3-10 (Pharmacia). Gels were rehydrated for 12 hours, and isoelectric focusing was performed at 500V for 1 hour, followed by 1000V for 1 hour and 8000V for 6 hours 30 minutes. After the IEF the IPG strips were equilibrated for 15 minutes in buffer containing DTT and sealed over the second dimension gel using agarose. For the second dimension pre-cast 30cm 12.5% SDS gels were run at 15W until the focused proteins had run into the gel. Subsequently gels were run at 160W for 4 hours.

2.28 Silver Staining of 2D gels

Gels were silver stained using Plus One silver staining kit from Pharmacia.

2.29 2D Gel Analysis

2D gels were scanned using UMAX Vista Scan and grayscale images analysed using the software package Melanie 3.0 (Genebio).

2.30 Gel excision and Mass Spectrometry

Selected protein slices/spots were excised, deposited in 96-well plates, in-gel reduced, alkylated with iodoacetamide and digested with trypsin as described (Schevchenko et al., 1996). The resulting peptides were digested with MALDI-MS and nanoES tandem MS. MALDI mass spectra were acquired automatically on a Bruker RE-FLEX III reflectron time of flight (TOF) mass spectrometer (Bruker Franzen, Bremen, Germany) as previously described (Vorm et al., 1994; Jensen et al., 1997). Peptides were analysed by nanoES tandem MS on a quadrupole time-of-flight mass spectrometer (QSTAR Pulsar, PE Sciex, Toronto, Canada) equipped with a nanoES ion source (MDS-Proteomics, Denmark). The peptide mixtures from in gel digests were purified and concentrated prior to nanoESMS as described (Wilm et al., 1996), except that the remaining supernatant were loaded on columns in parallel from 96-well plates.

Chapter 3

The Nef CD4 T cell Gene Expression Profile

3.1 Introduction

In order to probe a molecular basis for the function of Nef in alteration of T cell signalling I undertook large scale gene expression profiling analysis screening for expression changes in 3528 known genes. I reasoned any effect of Nef on T cell signal transduction paths should manifest itself in differential gene regulation with the potential to affect the viral life cycle. In order to undertake such an analysis it was necessary to develop a system that allowed tight temporal control of Nef expression. HIV is a cytopathic virus. Except in the case of post-integration latency the time from viral entry to virion production and cytopathicity has been estimated to be around 24-48 hours. Therefore it was appropriate to attempt to document gene expression changes at early time points after Nef expression in T cells.

3.2 The tetracycline inducible system

The study of gene function in complex cellular environments requires systems that allow stringent control of the expression of individual genes. The aim of such a system is not only to provide temporal control but regulated control of the level of gene expression. Several systems are available for inducible control of gene expression. These include use of promoters responsive to heavy metal ions (Mayo et al., 1982, Brinster et al., 1982, Searle et al., 1985), heat shock (Nouer et al., 1991), or hormones (Lee et al., 1981, Hynes et al., 1981, Klock et al., 1987, Israel et al., 1989). All of these systems have suffered from leakiness of the inactive state. In addition results are affected by the pleiotropic effect of the

inducing agent (Lee et al., 1988) making them less than ideal candidates for studies of gene expression.

Bujard and Gossen described an inducible system based on the regulatory elements of the Tn*10*-specified tetracycline-resistance operon of *E.coli* (Hillen et al., 1989). Transcription of resistance mediating genes in this system is negatively regulated by the tetracycline repressor (*tet*R). In the presence of tetracycline *tetR* does not bind to its operator sequences in the operon promoter and transcription is facilitated. Bujard and Gossen combined the *tet*R with the C-terminal domain of VP16 from HSV. VP16 is essential for HSV immediate early gene (IEG) transcription. This chimera stimulates minimal promoters bound to tetracycline operator sequences. In the presence of tetracycline the tetracycline transactivator (tTA) is prevented from binding to *tet*O sequences. The tetracycline system has subsequently been modified by a single amino acid change in the tetracycline transactivator such that it will only bind the operator sequences in the presence of tetracycline. This modification is of use in the context of animal experiments preventing complications and costs of prolonged periods of tetracycline treatment. More generally the modification is of benefit as it allows tighter temporal control of gene induction. This is because transcription of the transgene is not dependant on the half-life of disappearance of tetracycline from plasma or tissue culture media.

3.3 Generation of Nef expression constructs

A panel of *nef* expression constructs was created. Tetracycline operator constructs containing *nef* or *nef* mutants were made. These constructs were of three varieties: containing *nef* alone, *nef* bicistronic for *EGFP*, and *nef* C-terminal *EGFP* fusions. Tetracycline operator constructs containing *nef* alone were made by cloning *nef* into the vector pJEF4 obtained from Manfred Gossen (Figure 3a) IRES-EGFP tetracycline operator vectors were made by cloning the tetracycline operator sequences from pJEF4 and inserting them upstream of the MCS in p-IRES-EGFP from Clontech. Wild type (WT) *nef* was cloned from HIV SF2

backbone expression construct (Sanchez-Pescador et al., 1986). Mutant vectors contained *nef* mutated in the SH3 binding domain (P76A), in a motif implicated in

Fig 3a. Schematic representation of *nef* expression constructs. *EGFP* is represented by a green diamond, *IRES* by a filled rectangle and *nef* by an empty rectangle. The *nef* mutant G2A contains an alanine for glycine substitution at position 2. This destroys myristoylation of Nef. In P76A an alanine for proline substitution at position 76 of the SH3 binding domain is present. RR consists of a dileucine substitution for diarginine at positions 109 and 110. This disrupts the Nef PAK kinase association. EDAA contains a dialanine substitution at amino acids 178 and 179 disrupting a motif implicated in CD4 downregulation. In Tetracycline expression vectors these inserts are expressed from the Tet response element (TRE). Otherwise they are expressed under control of the CMV promoter.

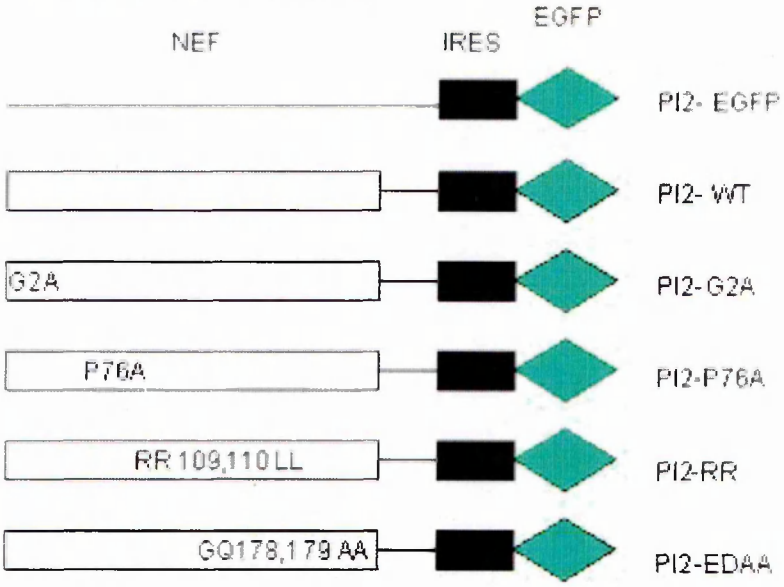

CD4 downregulation (EDAA) and in the di-arginine domain mediating association with PAK kinase (RR). In addition to the tetracycline operator vectors a panel of vectors for conventional expression of *nef* in transient transfection were made. These consisted of *nef* and mutant *nefs* being inserted in the vector pIRES-2-EGFP from Clontech. Inserts were sequenced and expression tested after transient transfection into tetracycline transactivator Jurkat obtained from Clontech. After treatment with doxycycline for 24-48 hours cells were harvested and FACS analysis performed in the case of constructs containing *EGFP*. In

addition the expression of the *nef* insert in each vector was confirmed by western blot.

3.4 Generation of Double Stable tetracycline inducible cell lines

A detailed account of the construction of tetracycline inducible cell lines is provided in materials and methods. DNA constructs were linearised before transfection by electroporation and selection in neomycin and hygromycin. Between 14 and 21 days hygromycin resistant cells were detectable and single cell cloning was commenced. At 14 days clones were split and one half were induced with doxycycline in preparation for screening for EGFP expression by FACS analysis. Clones exhibiting EGFP fluorescence were tested for little or

Fig 3b. Western blot analysis of cell lines inducibly expressing WT-EGFP and control EGFP alone showing induction of Nef at 12, 24 and 48 hours after addition of doxycycline at 1μg/ml (top panel). The membranes are stripped and blotted for β-Actin (bottom panel).

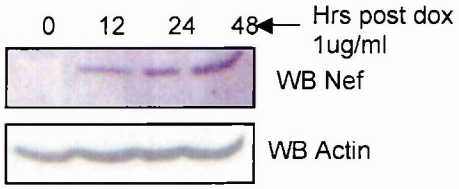

Fig 3c. FACS analysis of EGFP expression pre and post treatment of WT-EGFP and control cell lines with doxycycline illustrating tightly regulated EGFP expression in Nef positive and control cells.

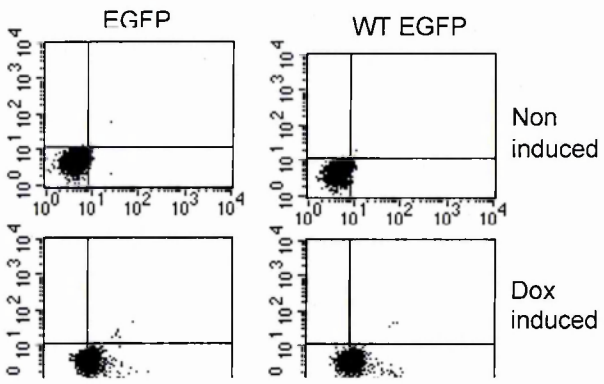

negative background expression. Those that fulfilled these criteria were tested for Nef expression after doxycycline induction by Western blot (Figure 3b). In selected clones Western blot and FACS analysis showed tightly regulated gene expression pre and post treatment with doxycycline (Figure 3c). Growth of the WT-EGFP cell line in doxycycline resulted in a decrease in CD4 and MHC class 1 expression consistent with previous reports (Greenberg et al., 1998) (Fig 3d). A control cell line was generated that expressed EGFP alone after doxycycline induction.

3.5 Loss of expression in the tetracycline inducible system

An unfortunate feature of all of the tetracycline cell lines generated was an irreversible loss of inducibility and loss of expression after more than six weeks in culture. This could have been due to several causes. In the case of Nef tetracycline cell lines as Nef is toxic and causes apoptosis after prolonged expression in T cells any leakiness of the inducible system would result in gradual apoptosis of Nef expressing cells favouring the outgrowth of Jurkat where the insert was silenced. However most of the established clones did not demonstrate background EGFP fluorescence.

Loss of expression is a commonly documented flaw of the tetracycline inducible system. This has been reported to be due to methylation of the promotor in the

Fig 3d. FACS dot plots after dual staining of non-induced and doxycycline induced populations with MHC 1 PE and CD4 TRI. Nef positive cells downregulate MHC 1 and CD4 as expected.

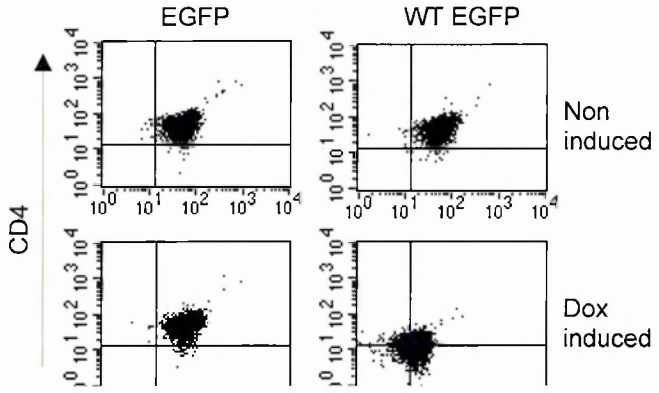

case of a tetracycline inducible BRCA1 cell line (Harkin et al., 1999). In this case the loss of inducibility after withdrawal of doxycycline was reversible after treatment of the Hela cells with the demethylating agent cytidine. Nef tetracycline cells in which Nef expression had become undetectable after induction with doxycycline were tested for hypermethylation of the promoter by treatment with cytidine. No reversal of inhibition was observed. Another known cause of gene silencing is hypoacetylation of histones surrounding promoter elements. This can be reversed by hyperacetylation that may be induced by treatment with butyrate. However treatment of Nef tetracycline cells with butyrate did not result in a reversal of silencing after treatment with doxycycline.

Loss of expression was not dependant on the particular Nef insert or indeed entirely due to Nef as control EGFP tetracycline cells also demonstrated failure of induction after passage in culture. I established by transient transfection of tetracycline transactivator Jurkat from Clontech that between eight and twelve weeks in culture the cells were no longer responsive to doxycycline and the cells therefore had lost expression of the transactivator element. Loss of expression of the rtTA is likely to be a major contributor to the lack of longevity of established tetracycline inducible cell lines in this instance.

3.6 Screening of cDNA microarrays

I screened for differential changes in gene expression occurring over time after induction of Nef in tetracycline inducible cell lines. As an early expressed HIV gene any host cell transcriptional changes exerted by Nef are likely to have relevance for the viral life cycle at earlier time points. Expression profiles at 18, 24, 30 and 36 hours after doxycycline treatment were compared. As Nef is first detectable at 12 hours in the cell lines this is representative of 6, 12, 18 and 24 hours after Nef expression. Total RNA was used to make [^{32}P] cDNA probes. Using Clontech cDNA microarrays 3528 genes were analysed. Raw intensity values were obtained from at least three replicate experiments using GenePix 3.0 (Axon Instruments) software. Atlas Navigator (Clontech/ Sigenetics) software

was used for subsequent normalisation and cluster analysis. Full experimental details describing microarray methods and analysis are found in materials and methods. Nef produces widespread differential gene expression in the T cell that escalates in breadth and intensity over time. In contrast doxycyline treatment of control EGFP expressing cell lines resulted in no significant changes in gene induction (Fig 3e).

3.7 The Nef T cell gene expression profile

An initial analysis focused on upregulated genes as these are the most commonly described targets of signal transduction cascades. We defined significantly upregulated genes as exhibiting a normalised relative intensity ratio of three or above, with a raw intensity value more than 150. A complete list of genes upregulated by Nef over 24 hours is available in the Appendix. K-tuple means clustering (Eisen et al., 1998) was used to display the kinetics of Nef induced gene expression. Using the standard correlation coefficient genes clustered into two nodes of upregulated transcripts (Figure 3f). Cluster group A contains genes whose expression is gradually induced over the time course and whose expression peaks towards later time points. Cluster group B contains genes whose expression achieves a plateau at earlier time points. A relative over representation of transcription factors, RNA processing genes and genes directing post-translational modification is observed in cluster group A. Cluster group B contains intracellular transducers, genes regulating protein turnover and metabolic regulators. Genes on the arrays that were previously demonstrated as induced by Nef included *MIP-1β* and *MIP-1α* (Swingler et al., 1999) and these were upregulated as expected.

Fig 3e. Serial scatter profiles demonstrate gene expression over time after induction of Nef. Raw intensity values are plotted against control values for each gene (see normalisation methods, materials and methods). The green lines indicate the relative expression of the data sets relative to time 0. The upper line marks a two-fold increase, the lower line marks a two-fold decrease and the centre line indicates equivalent expression. The colour scale indicates relative up and downregulation of genes with red representing up and purple downregulation. The intensity of the colour gives a indication as to the significance of the change in gene expression with high intensity correlating with more significant changes.

Relative Intensity ratio

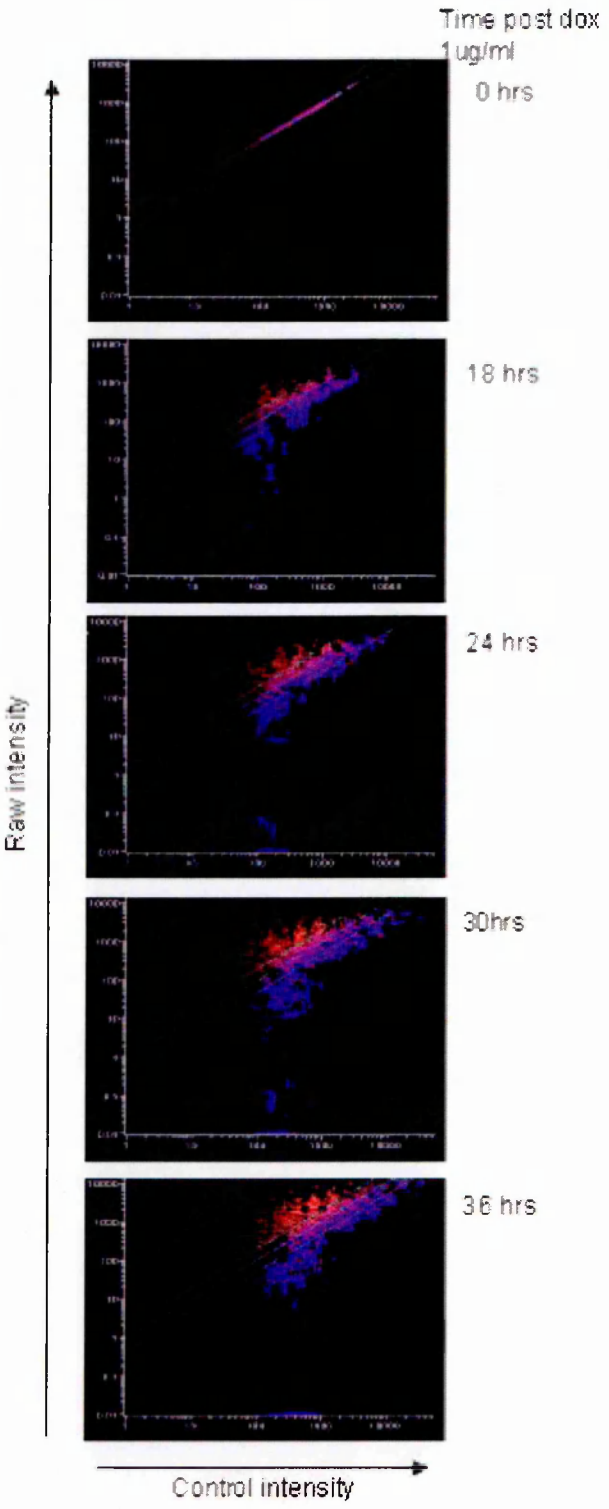

Fig 3f. K-tuple clustering was used to display the expression ratios of Nef induced genes over time. Included in the cluster analysis were genes that are upregulated more than three in normalised relative intensity ratio of signal to control. All measurements are relative to time 0. The colour scale ranges from saturated red for up-regulated genes to saturated blue for down-regulated genes according to the key. A single row of coloured boxes represents each gene and each column a single time point. Significantly induced (raw intensity more than 150) functional groups of co-regulated genes are indicated.

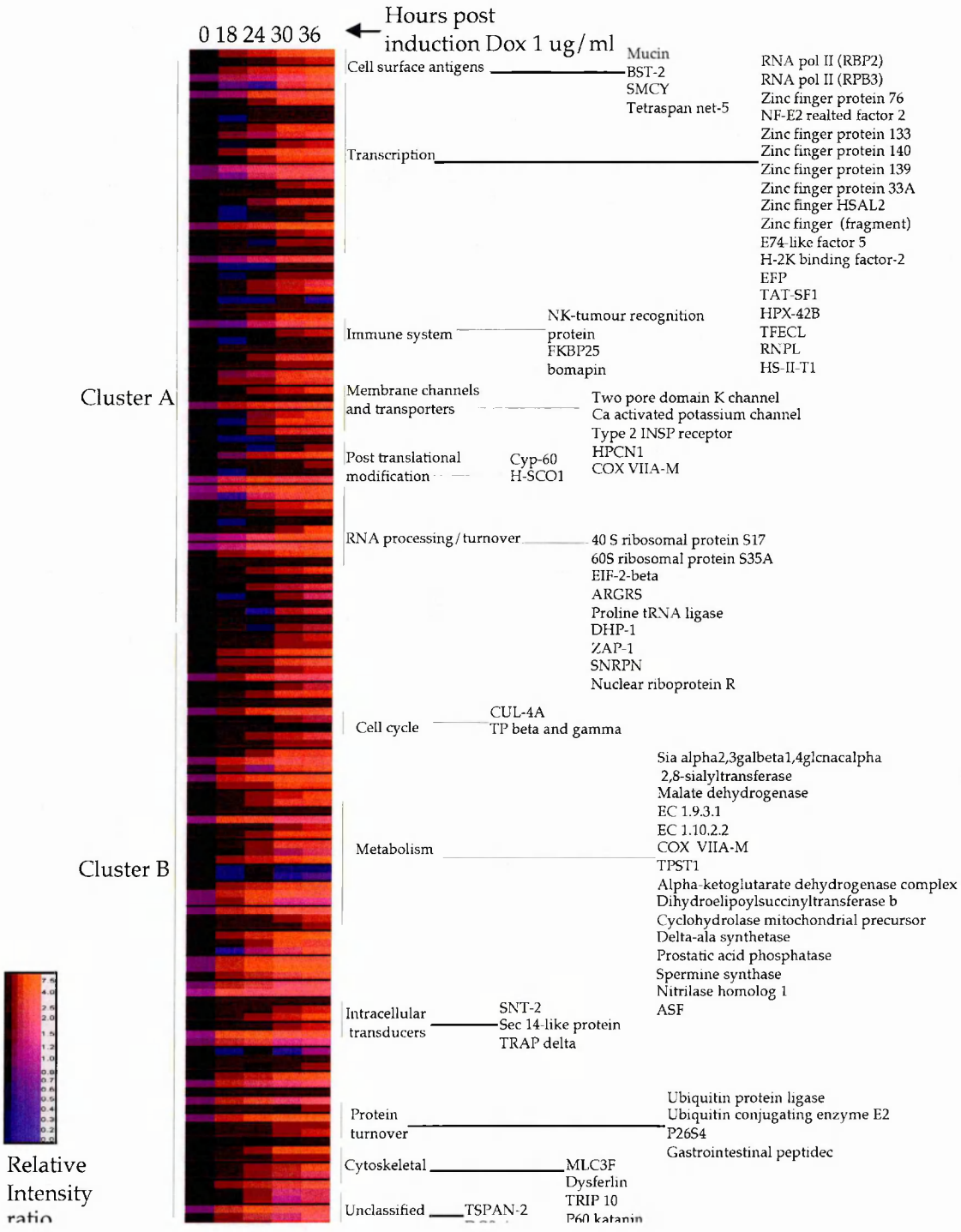

3.8 Nef induces positive regulators of viral replication

A series of genes impacting on the viral life cycle are upregulated by Nef (Table 3.1). Strikingly fifteen transcription factors that activate the HIV-1 LTR are induced. Cellular host proteins bind to a variety of cis acting DNA sequences located within the LTR and tightly regulate HIV-1 proviral gene expression. Multiple regulatory regions are required for LTR transactivation. Mutations in the SP1, TATA, TAR loop and stem secondary structure severly disable the response of LTR reporters to exogenous activators. Nef induces *ETS-1*, which acts co-operatively with NF-κB and NFAT to mediate synergistic activation of the HIV-1 and HIV-2 enhancers (Bassuk et al., 1997). ETS-1 also acts synergistically with USF-1 at the HIV distal enhancer region of the LTR (Sieweke et al., 1998). ATF-2 induces HIV transcription and increased levels of ATF proteins and DNA binding activity are observed in nuclear extracts of T cell lines infected with HIV (Rabbi et al., 1997). GAPB alpha activates the LTR in a Raf1 responsive manner (Flory et al., 1996). IRF-1 and IRF-2 bind to the downstream binding factor site in the HIV promoter to exert a positive effect on viral replication (Van Lint et al., 1997). In addition IRF-2 inhibits virus induced IFN-β transcription by preventing enhanceosome-dependant recruitment of the CBP-Pol II holoenzyme complex (Senger et al., 2000). Several of the HIV LTR transactivators Nef upregulates (*NFATc, c-fos*, *JunD, IRF-1, c-myb, CIITA* and *HIV-EP2*) are inducibly expressed on T cell activation. (Chupvila et al., Bosselut et al., 1992, Dasgupta et al., 1990, Kinoshita et al., 1997, Mercier et al., 1994, Saifuddin et al., 2000).

It was interesting to observe upregulation of several host cell factors required for action of another viral accessory gene product, Tat. One of these, *CDK9*, is the catalytic component of transcription elongation factor b (P-TEFb) that acts in concert with Tat to direct the processivity of HIV transcription (Zhu et al., 1997; Mancebo et al., 1997). *CDK9* mRNA and protein levels are induced following T cell activation and this correlates with kinase activity (Herrmann et al., 1998). In addition to upregulating *CDK9* Nef may prevent its degradation by induction of *heat-shock protein 70 (Hsp70).* Hsp70 serves as a chaperone that stabilises

CDK9 prior to binding by a cyclin partner (O'Keeffe et al., 2000). Hsp70 is known to be induced following HIV infection of CD4 T cell lines and this induction is coincident with the presence of singly and multiply spliced HIV-1 transcripts, declining on the emergence of full-length genomic HIV-1 mRNA (Wainberg et al., 1997). Nef induces several other genes that positively regulate Tat. These include *Tat-SF1* whose over-expression specifically stimulates transcriptional

Table 3.1 Nef upregulated genes associated with HIV

Transcription Factors Positively regulating the HIV-1 LTR		
Encoded Protein	GenBank Accession number	Maximal normalised relative intensity ratio
Pur-alpha	M96684	8.0
NFATc	U08015	5.1
NF-κB p100; p52	X61498	3.3
IRF2	X15949	4.6
IRF1	X14454	4.0
c-myb	M15024	14.4
c-fos	K00650	3.5
Jun-D	X56681	3.2
ETS-1	J04101	4.0
ATF-2	L05515	3.4
CIITA	X74301	4.1
HIV-EP2	M60119	4.6
GABP-alpha	D13316	4.4
TFIID 28KD subunit	X83928	7.9
Tat facilitators required for processivity of transcription		
TAR binding protein	M60801	3.0
RNA pol II (RPB 3)	J05448	3.9
RNA pol II (RPB 2)	X63563	4.8
RNA pol II (RPB 6)	Z27113	3.1
CDK9	L25676	10.7
TAT-SF1	U76992	3.3
c-abl	M14752	7.3
Formation of full length transcripts		
U1 SNRNP A protein	X06347	5.0
Nuclear pore transporter		
NUP-98	U41815	15.6
Increased in HIV PBMC		
70Kd HSP 1	M11717	4.8
Heat shock related 70kd protein 2	L26336	10.1
IL6 receptor beta subunit	M57230	6.7
Paracrine effectors		
IL4 precursor	M13982	4.8
MIP-1 alpha	M23452	9.9

MIP-1 beta	J04130	3.2
TGF beta	X02812	3.4
Incorporation in virions		
ezrin	X51521	4.1

activity of Tat in vivo (Kim et al., 1999); *TAR binding protein (TRBP)* which acts in synergy with Tat to activate the LTR (Gatignol et al., 1996) and *Pur* α, a single strand DNA binding protein that binds TAR RNA and activates HIV transcription (Chepenik et al., 1998). In addition Nef upregulates *c-abl tyrosine kinase* that phosphorylates the carboxy terminal domain (CTD) of RNA polymerase II activating the HIV promoter in the absence of Tat (Baskaran et al., 1999). Upregulation of *U1 SNRNP* is observed. U1 SNRNP maintains inactivity of the 5' LTR poly (A) site required for the formation of mature HIV transcripts by interaction with the major splice donor site (Ashe et al., 1997).

Nef induces several paracrine effectors over 24 hours (Table 3.1). Apart from *MIP-1*α and *MIP-1*β two have been described as influencing the HIV life cycle. TGF-β is increased in the supernatants of HIV infected peripheral blood mononuclear cell (PBMC) cultures (Kekow et al., 1990) and is capable of stimulating transcription from the LTR by activating NF-κB (Li et al., 1998). IL4 stimulates the expression of all HIV isolates via a transcriptional activation mechanism (Valentin et al., 1998). Altogether the expression profile hints Nef acts to further the viral life cycle by directing the accessibility of multiple CD4 T cell factors via an intrinsic activation trigger.

3.9 Nef downregulates various T cell genes

Nef differentially regulates expression of multiple genes in T cells. Less is known about the effect of signal transduction pathways on the downregulation of T cell transcripts. Atlas navigator software gives normalised raw intensity values of between 0 and 1 for downregulated genes. I defined downregulated genes as exhibiting a normalised relative expression value of less than or equal to 0.3. By these criteria 131 genes were downregulated. Of note Nef downregulates both

Fig 3g. Nef downregulates 131 genes less than 0.3 in normalised relative intensity ratio over 24 hours. This ordered list taken from array HG 1.2 III is representative of all three arrays. The most downregulated genes are represented as saturated blue according to the key. Each row represents a single gene and each column time points after induction of Nef from *nef* tet T cell lines.

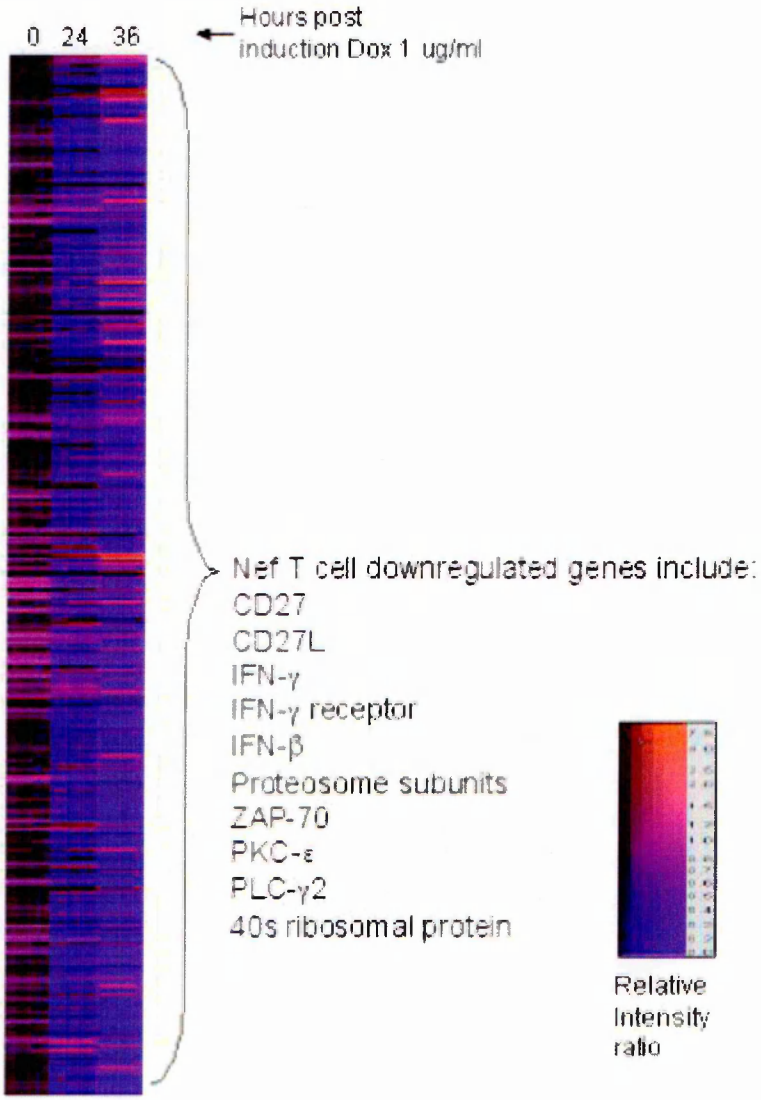

CD27 and CD27 ligand which are conventionally induced on T cell activation and which are believed to play a role in T cell proliferation. Interferon gamma and interferon gamma receptor are downregulated that may mediate evasion from the immune response. In addition interferon beta shows downregulation in the presence of Nef. Proteosome components involved in antigen presentation are downregulated as is another immune mediator macrophage stimulating protein. Interestingly several positive effectors were downregulated including the kinases ZAP-70 and PKC-ε, the phospholipase PLC-γ2 and the 40S Ribosomal protein (Figure 3g). A complete list of genes downregulated by Nef over 24 hours is available in the Appendix.

3.10 Immediate early genes induced by Nef

As any Nef mediated alteration of the host CD4 T cell transcriptional environment is likely to have relevance for viral replication very early in the life cycle I attempted to define immediate early gene (IEG) expression induced by Nef. Changes to the cellular environment result in expression of a characteristic set of genes known as immediate early genes (IEGs). These rapidly activated genes have been have been observed to be identical whether induced after activation through multiple growth factors. Distinct signalling pathways triggered from the same receptor lead to upregulation of the same pattern of immediate early genes (Fambrough et al. 1999). These genes include c-fos and c-Jun, two components of the transcription factor AP-1 involved in activating gene expression from a variety of genes involved in growth and differentiation (Foletta et al. 1998; Shaulian and Karin 2001). Other IEGs include HSP70 which aids in protein folding and heat shock responses, CPBP a transcription factor that enhances transcription from TATA-less promoters, MKP-1 a phosphatase that dephosphorylates MAP kinases; and TTP which binds certain mRNAs and promotes their degradation.

A hurdle in performing this analysis involved definition of the time point after Nef induction in the Nef tetracycline cells that represents a period where IEG

induction might occur. EGFP expression is observed at 18 hours after doxycycline treatment at the earliest. Nef tetracycline cells were harvested for RNA generation after 19 hours treatment with doxycycline. Microarray analysis was performed as described previously. Due to the difficulties in definition of the time period of true IEG induction in this system the results must be interpreted with caution.

Induction of several genes classically described as IEGs was observed. In addition several genes were induced that are not upregulated at later time points in the Nef expression profile. The functional logic that links these IEGs is not known.

3.11 The Nef expression profile as an indicator of specific functions

The potential for individual genes differentially regulated by Nef to exert effects on viral replication was examined. Nef mediated induction of *CDK9* mRNA was observed in the cDNA microarray analysis. CDK9 is a key component of the positive elongation factor complex (P-TEFb) that acts in concert with Tat to facilitate processive transcription by phosphorylating the C-terminal domain (CTD) of RNA polymerase II. Nuclear extracts depleted of CDK9 lose ability to stimulate processive transcription (Mancebo et al., 1997; Zhu et al., 1997). In addition the purine nucleoside analogue 5, 6-dichloro-1-β-D-ribofuranosylbenzimidazole (DRB) that specifically inhibits CDK9 can effectively terminate Tat transcriptional activity (Marciniak and Sharp, 1991, Zhou et al., 2000). *CDK9* mRNA and CDK9 catalytic activity is induced in activated primary T lymphocytes (Yang et al., 1997; Hermann et al., 1998). Nef expression in Jurkat was found to induce CDK9 protein (Fig 3i) and kinase activity (Fig 3j) in addition to mRNA (Fig 3h). The effect of Nef mediated CDK9 upregulation on the efficiency of HIV-1 transcription directed by Tat was investigated. Jurkat stably transfected with Tat were transiently transfected with either an HIV-1 LTR luciferase reporter or HIV-1 LTR luciferase and Nef. HIV-1 LTR activity in the presence of Nef and Tat was hyperinduced in comparison with activity observed

Fig 3h. Northern blot shows CDK9 mRNA induction after transfection of Jurkat with PI2 or PI2-WT(WT) vectors.

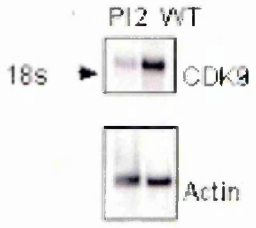

Fig 3i. Western blot of nuclear lysates shows induction of CDK9 after transfection with PI2 or WT.

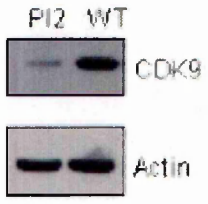

Fig 3j. CDK9 in vitro kinase assay of Jurkat transfected with PI2 or WT using CTD peptide as substrate. The presence or absence of CTD substrate is indicated above each lane. Hypophosphorylated (CTD_A) and hyperphosphorylated (CTD_O) forms of CTD peptide are indicated.

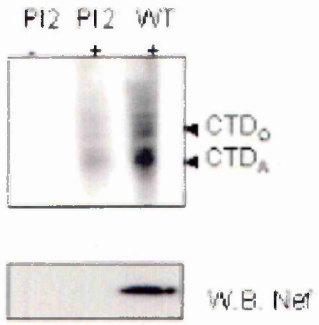

Fig 3k. Jurkat cells stably transfected with tat (JT Tat III) were co-transfected with an HIV-1 LTR luciferase reporter together with pRL-TK as an internal control and either PI2 or WT. Cells were left untreated or treated with 10 or 20 μM DRB for six hours prior to analysis of luciferase activity. Results are representative of three experiments.

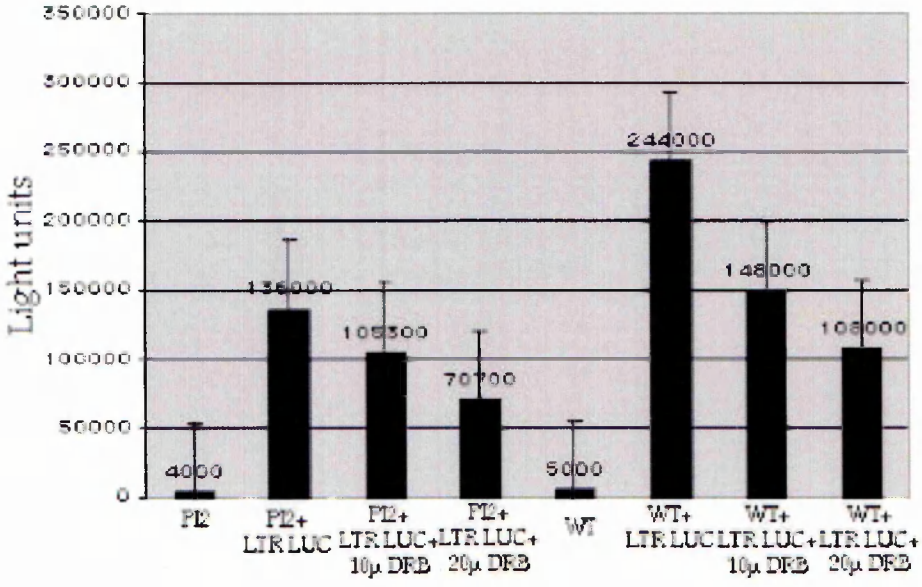

in the presence of Tat alone (Fig 3k). To establish the contribution of Nef mediated induction of CDK9 to this effect co-transfected cells were treated with 10 or 20 μM DRB which resulted in a dose dependent reduction in LTR luciferase activity. Induction of CDK9 may be a significant aspect of the mechanism by which Nef enhances viral production.

3.12 Discussion

As the earliest expressed gene of HIV the ability of Nef to influence host cell gene expression is tantalising as it has implications for HIV replicative fate. Several of the genes Nef induces have previously been identified as influencing events in the viral life cycle. In addition 26 of the genes induced more than three fold in normalised relative expression ratio have been described as being upregulated after T cell activation. It is possible different variants of Nef may differ in their ability to induce or repress expression of host cell factors influencing HIV replication. In this way Nef might exert some control of level of HIV disease progression. The ability of Nef to induce a transcriptional program in T cells indicates that the described in vitro interactions with key T cell signalling proteins may lead to a functional outcome in vivo. As there is currently no drug inhibitor of Nef action delineation of the protein-protein interaction that leads to T cell gene expression changes will be important if this function of Nef is to be targeted therapeutically.

Chapter 4

Characterisation of the Nef CD4 T Cell Transcriptional Programme

4.1 Introduction

Within the Nef expression profile upregulation of 23 genes that are also induced on T cell activation was observed. These included *ETS-1, CDC2, CDK9, ezrin, Jun-D, c-abl, CDK4, c-fos, c-myb, NF-kB p100; p52, GAPB-alpha, NFATc, PUR alpha, MIP 1-beta, Heat shock related 70kd protein 2, 70kd HSP 1, TGF beta, MIP 1-alpha, IL4 precursor, HIV-EP2, CIITA, NUP-98, beta'-COP, RNA pol II-(*RP3), (RPB2) and *(RPB6), TAFII-28, TAT SF1, U1 SNRNP A* and *TAR binding protein.* Previous assessments of activation of T cells by Nef have utilised readouts obtained from NF-κB, NFAT, AP1 and IL2 reporter constructs, measurements of calcium flux, changes in tyrosine phosphorylation or in vitro kinase assays assessing catalytic activity of key T cell signaling molecules. While giving insight to the effect of Nef on T cell activation paths in specific experimental contexts, they do not provide a unifying picture as to extent or specificity of Nef T cell activation. Indeed some studies have inferred a inhibitory effect of Nef on T cell signaling (Bandres and Ratner, 1994, Collette et al., 1996, Greenway et al., 1996, Iafrate et al., 1997). Large scale gene expression profiling enables comparison of the Nef profile to reference activation states. I attempted to compare the expression profiles obtained after Nef expression in CD4 T cells with that occurring after either anti-CD3 or anti-CD28 activation.

4.2 Comparison of the Nef gene expression profile with that of reference T cell activation states

I activated Jurkat with plate bound anti-CD3 and performed cDNA microarray analysis at 12 and 24 hours. These profiles were compared to those obtained after Nef induction at 24 and 36 hours in the tetracycline inducible cell lines (representative of 12 and 24 hours from when Nef is detectable). Ligation of CD3 induces a transcriptional program of similar magnitude to that of Nef (Figure 4a).

While T cell activation by TCR triggering and Nef expression induce a number of shared genes that promote the virus life cycle some potentially important differences were noted. Ten transcripts absent from the anti-CD3 activation profile are upregulated by Nef (Table 4.1). Three of these genes *TAT-SF1*, *IRF-2* and *U1 SNRNP* are positive regulators of the viral life cycle. IRF-2 prevents virus

Remarkably the activation of Jurkat via this route revealed 97% identity ($p<0.01$) in upregulated transcripts with those of Nef (Figure 4b). In contrast activation of Jurkat via plate bound anti-CD28 results in induction of 145 genes over 24 hours with 80% identity in induced genes (Fig 4b). A full list of CD28 induced genes is provided in the Appendix. The entire Nef expression profile including downregulated and equivalently regulated genes demonstrates a high degree of similarity with that of anti-CD3 triggering as demonstrated in Figure 4c.

While T cell activation by TCR triggering and Nef expression induce a number of shared genes that promote the virus life cycle some potentially important differences were noted. Ten transcripts absent from the anti-CD3 activation profile are upregulated by Nef (Table 4.1). Three of these genes *TAT-SF1*, *IRF-2* and *U1 SNRNP* are positive regulators of the viral life cycle. IRF-2 prevents virus

induced IFN-β gene transcription (Senger et al., 2000). Anti-CD3 activation resulted in upregulation of 8 transcripts absent from the Nef profile (Table 3.1). These include the transcription factor *YY1* that represses HIV-1 LTR activity (Coull et al., 2000) and cytokine *IL16* that inhibits HIV growth in cell culture (Center et al., 2000). I examined whether the differences observed in mRNA level correlated with expression changes in protein for several of these genes. It

Figure 4a. The Nef expression profile compared with that of anti-CD3 activation. Scatter plots show equivalent induction of differential gene expression between Nef activated and anti-CD3 activated T cells. The colour key indicates upregulated genes as sauturated red and downregulated genes as saturated blue.

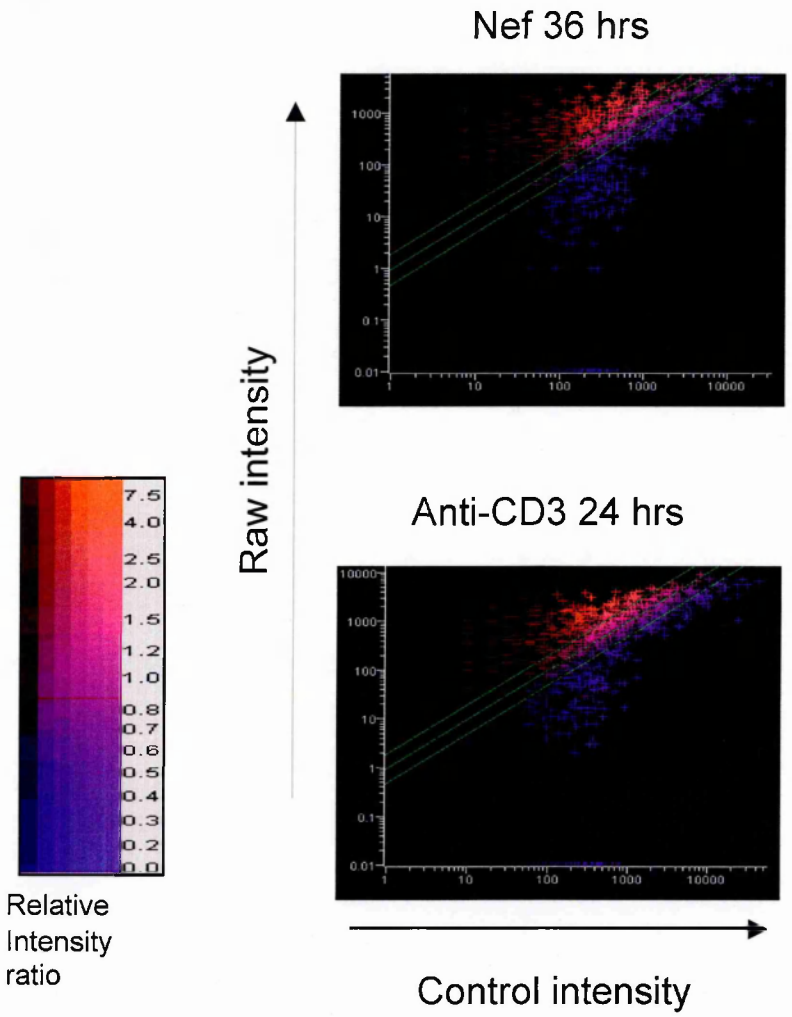

Figure 4b. Ordered list representation of genes upregulated more than 3 in normalised relative intensity value from array HG 1.III. This is representative of all three arrays used. Upregulated genes show a similar expression pattern both in kinetics and magnitude of induction after Nef expression or anti-CD3 stimulation. In contrast anti-CD28 stimulation shows less similarity. The colour key indicates upregulated genes as saturated red. Each row represents a single gene and each column time points after induction of Nef, or after stimulation with anti-CD3 or anti-CD28.

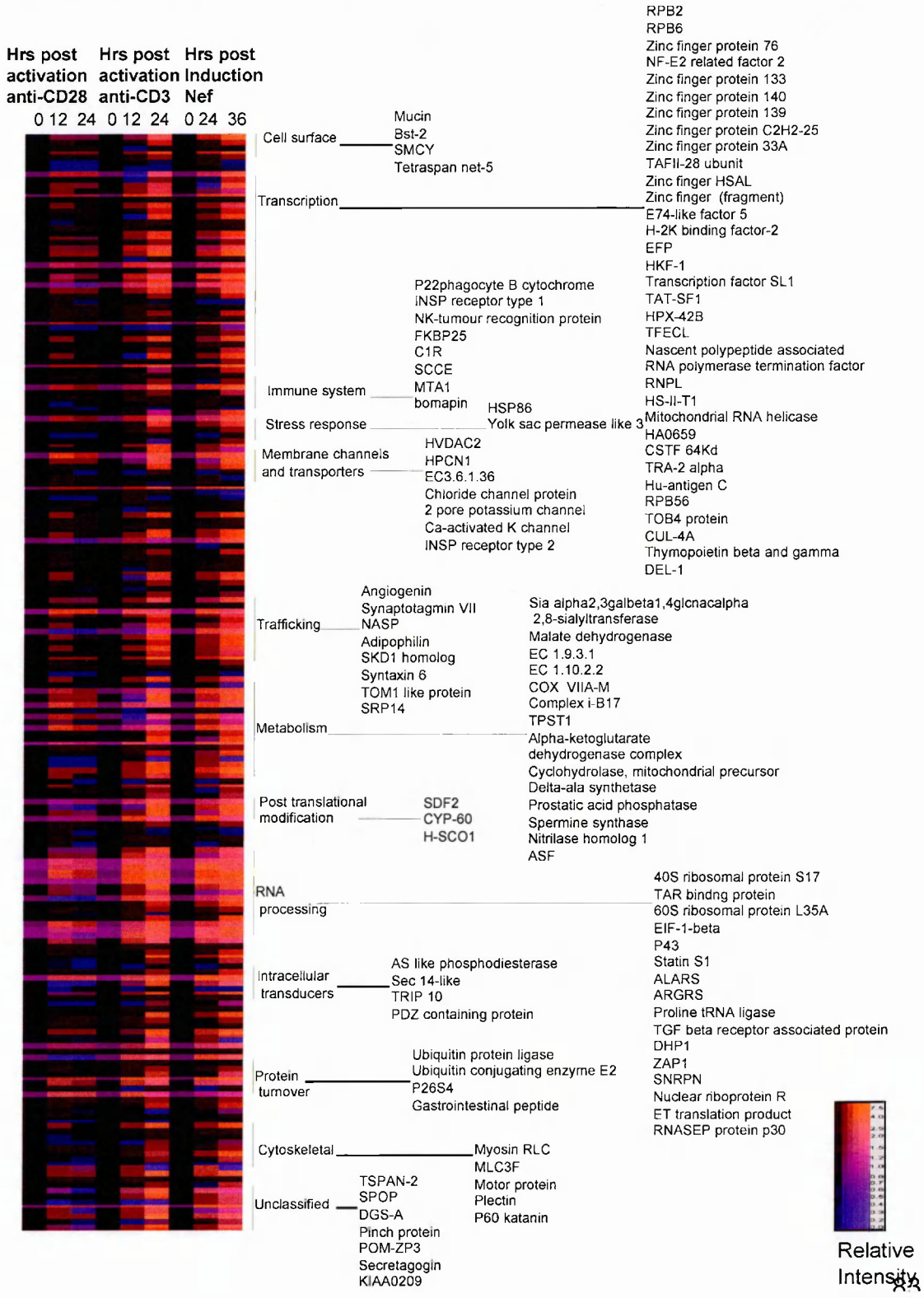

Figure 4c. The kinetics and magnitude of the Nef and anti-CD3 expression profiles are similar for up and downregulated genes.

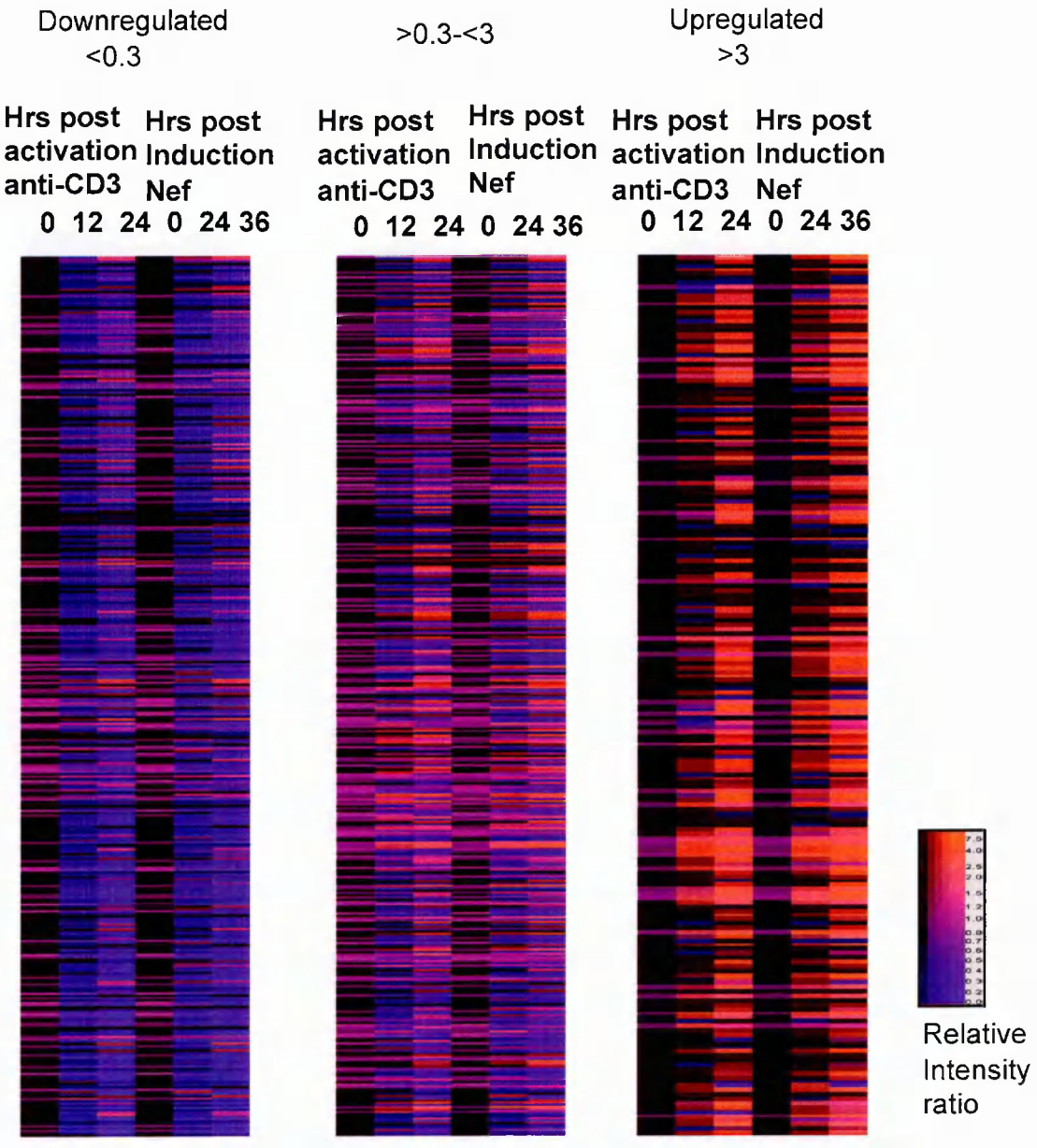

Table 4.1 Differences between the Nef and anti-CD3 expression profiles and how these are preserved after exogenous stimulation

Encoded Protein	GenBank Accession number	Maximal normalised relative intensity ratio
Genes upregulated by Nef but not anti-CD3		
IRF-2	**X15949**	**4.6**
Tat SF1	**U76992**	**3.4**
U1 SNRNP A	**X06347**	**5.0**
β'-COP	X70476	3.9
DP1	L23959	4.0
Pinch protein	U09284	9.0
PLC-β 3	Z16411	4.0
Genes upregulated by anti-CD3 but not Nef		
IL16	**M90391**	**17.1**
YY1	**M76541**	**5.8**
CD27	**M26842**	**5.9**
NF-X1	U15306	3.3
MTA1 like 1	AB016591	6.2
ALARS	D32050	4.0
Mitochondrial Lon protease homolog precursor	X74215	21.3
hTRF2	AF002999	3.1

Normalised intensity ratios for HIV associated genes after CD3/CD28 stimulation

Encoded Protein	GenBank Accession number	Maximal normalised relative intensity ratio (CD3/CD28)	Maximal normalised relative intensity ratio (Nef and CD3/CD28)
IRF-2	**X15949**	**2.3**	**8.4**
Tat SF1	**U76992**	**1.4**	**6.3**
U1 SNRNP A	**X06347**	**2.8**	**7.4**
IL16	**M90391**	**17.4**	**1.1**
YY1	**M76541**	**5.2**	**2.3**
CD27	**M26842**	**6.3**	**2.9**

was possible to demonstrate a difference in protein expression for the transcripion factor IRF-2 (Figure 4dii). CD27 is exclusively induced by CD3 crosslinking of Jurkat but not by Nef. This was demonstrated by FACS analysis of anti-CD3 activated T cells transfected with a control EGFP expression vector in comparison with Jurkat transfected with pIRES2-WT-EGFP (Figure 4di). These differences hint the mode of Nef T cell activation may be highly specific and geared towards a heightened replicative state for the virus over and above a conventional activation stimulus.

Fig 4d. Differences between Nef and anti-CD3 expression profiles indicate that Nef may activate T cells in a manner specifically geared to promote viral replication. These changes in mRNA levels may not be indicative of changes in protein expression.

(i) CD27 surface expression on Nef transfected and anti-CD3 activated Jurkat. Expression of WT Nef does not correlate with a change in CD27 expression on the cell surface in contrast to anti-CD3 stimulation which results in marked induction of cell surface anti-CD27.

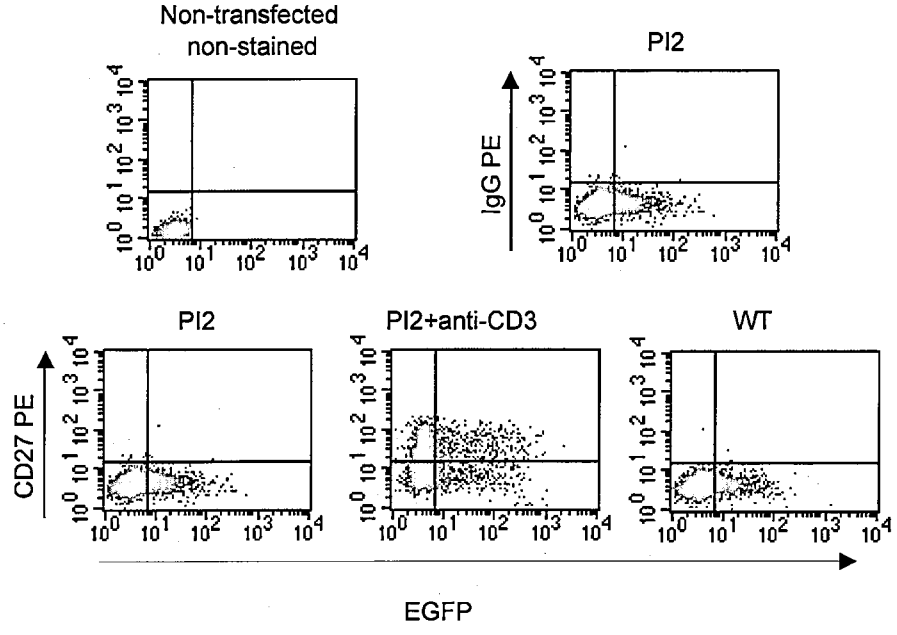

(ii) Comparison between IRF-2 expression levels in Nef transfected And anti-CD3 activated Jurkat. Western blot of IRF-2 expression in nuclear lysates of Nef expressing Jurkat and anti-CD3 activated Jurkat.

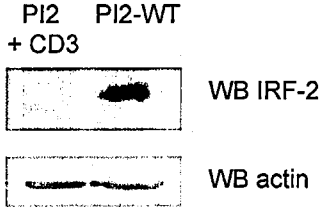

4.3 Effect of Exogenous activation on the Nef expression profile

I examined how this single signal T cell activation triggered by Nef might present an advantage to viral replication following subsequent exogenous activation. This single signal activation by CD3 triggering is weak and may represent more of a priming role. Alternatively it may facilitate induction of anergy and postintegration latency by representing a first single trigger that renders the host T cell resistant to further stimuli. The expression profile of Jurkat activated through CD3 and CD28 was compared to that of Nef expressing Jurkat activated via this route. Genes induced after CD3/CD28 activation represent a combination of the transcripts induced after activation via either route singly. The presence of Nef results in hyperinduction of several T cell inducible genes including *IL2* and *NFATc*. In addition the differences observed between the anti-CD3 and Nef profiles are preserved (Table 4.1). CD3/CD28 stimulation results in upregulation of *interferon αβ receptor* that does not occur in the presence of Nef. *IL3 precursor* is induced exclusively in the presence of Nef. Genes induced after combined CD3/CD28 stimulation of Nef expressing cells are listed in the Appendix.

4.4 Nef acts above the level of calcineurin

It follows from the close identity between Nef and anti-CD3 expression profiles that formation of the Nef transcriptome should occur via the same signalling and transcriptional constraints as govern anti-CD3 T cell activation. To establish to what extent the NFAT/NF-κB family of transcription factors participates in formation of the Nef profile Nef tetracycline cell lines were treated with Cyclosporin A (CsA) during the period of induction with doxycycline. The concentration of CsA used was within the range maintained in the blood of liver transplant recipients receiving CsA. Trypan blue staining revealed no evidence of toxicity at this dose of CsA. The expression profiles obtained at 36 hours post induction (representative of 24 hours post Nef expression) were compared. CsA

treatment led to a marked suppression of the Nef expression profile (Figure 4e and Figure 4f). In the presence of CsA only 49% of Nef induced genes were upregulated. CsA inhibits induction of CIITA (Charreau et al., 2000) and this was inhibited in our analysis. CsA does not affect T cell activation upregulation of CDK4 (Modiano et al., 1994) and this was induced as expected. No new genes were upregulated following CsA treatment of Nef expressing cells. Full documentation of the effect of CsA on Nef induced genes is provided in the Appendix. The in vitro growth advantage of Nef positive HIV virus can be inhibited by cyclosporin (Aiken, C. 1998). It was interesting to note CsA inhibited the Nef mediated induction of several factors that could enhance viral productivity. These included *CDK9, Tat-SF1, NFATc, NF-κB, IRF-2, c-abl, ATF-2, CIITA* and *GAPB-alpha.* The 49% gene repression occuring in the presence of CsA indicates a substantial portion of Nef T cell signalling is transmitted via the NFAT/NF-κB family and that Nef orchestrates formation of the expression profile above calcineurin in the T cell signalling path.

Figure 4e. The Nef expression profile is suppressed by CsA. Nef tet cell lines were treated with cyclosporin at 200ng/ml and were induced with doxycycline. The scatter plots demonstate a general repression in gene induction occurring at 36 hours after CsA treatment. The colour key indicates upregulated genes are represented as saturated red and downregulated genes as saturated blue.

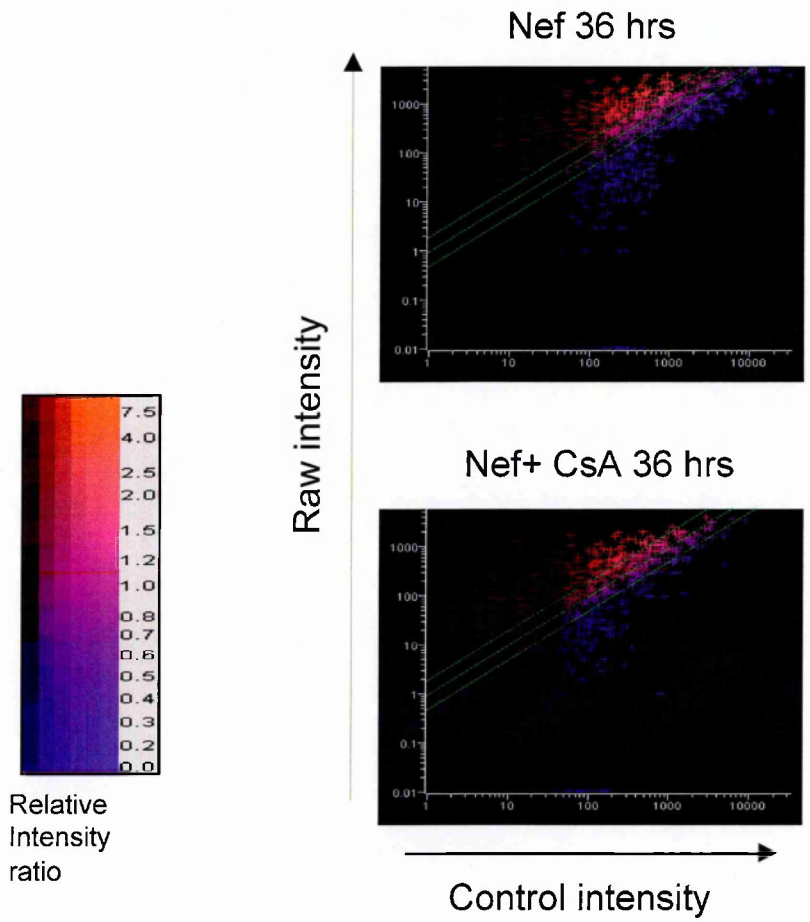

Fig 4f. Nef tet cell lines were treated with cyclosporin at 200ng/ml and were induced with doxycycline. The ordered list indicates genes unaffected in induction or partially and completely inhibited in induction in the presence of CsA. Genes were defined as unaffected by CsA if their expression ratio differs by less than 30% from the ratio obtained in untreated cells. Genes whose expression ratio is reduced by more than 70% are defined as fully repressed and genes whose expression ratio is decreased by less than 30% but more than 70% are defined as partially repressed. The colour key indicates upregulated genes as saturated red and downregualted genes as saturated blue.

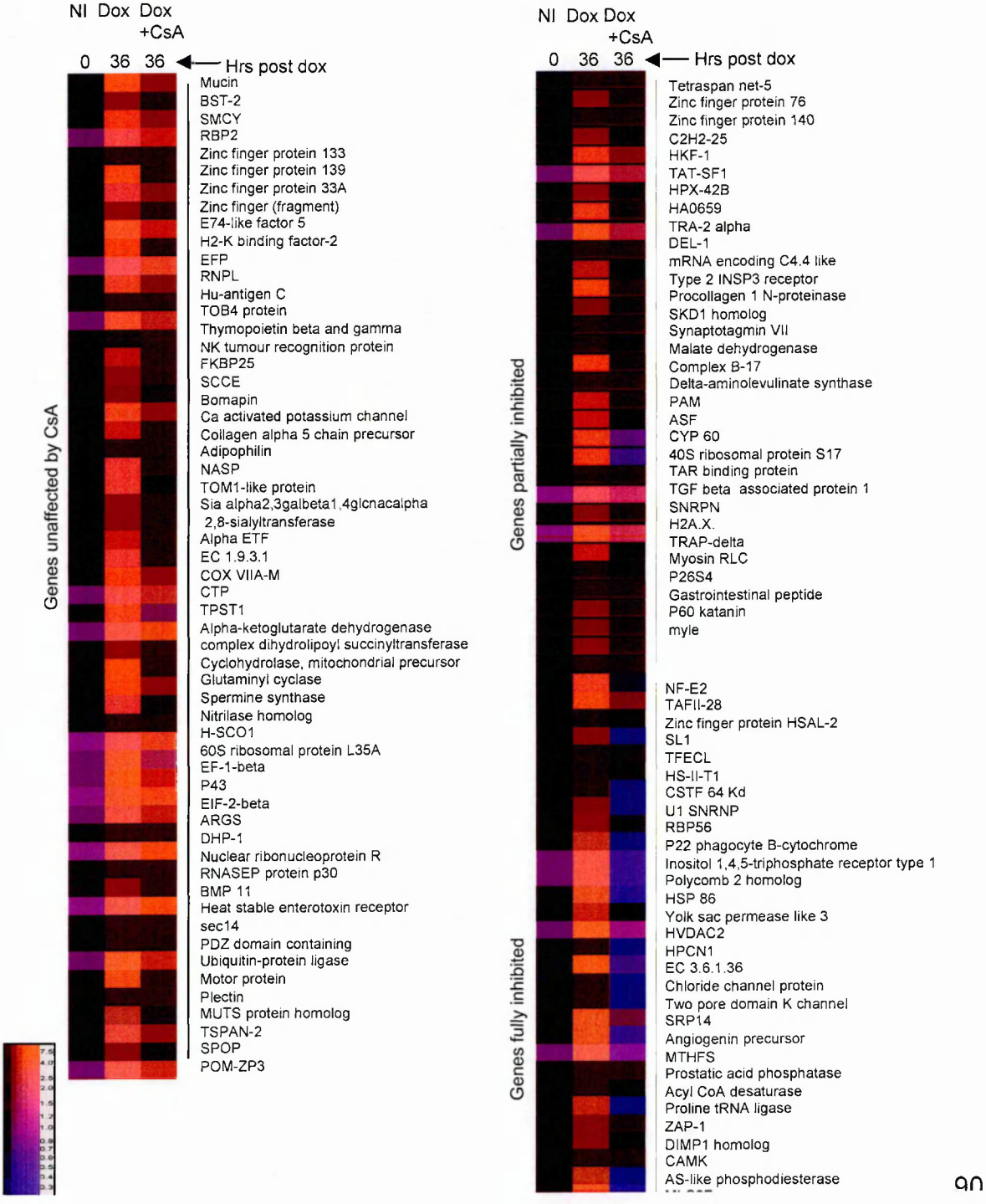

4.5 Use of genetic T cell signalling mutants to locate position of Nef action

We elected to use the hallmark Nef expression profile to investigate the role of key T cell signalling molecules in its induction. Nef can interact with a number of these and in addition is associated with accumulation of others in lipid rafts. The most proximal T cell signalling Nef binding protein described is TCRζ. In order to define the exact position where Nef might act we compared gene profiles obtained when Nef was expressed in cell lines lacking functional TCRζ (J RT3-T3.5 Ohashi et al., 1985) and genetically deficient in ZAP-70 (p116). Nef tet inducible J RT3-T3.5 and p116 cell lines were constructed by co-transfection of tet transactivator and operator plasmids containing *nef*. Stable cell lines were selected on the basis of high inducible expression with minimal background leak (Figure 4g). Induction of Nef expression in both J RT3-T3.5 and p116 resulted in an attenuation of Nef's transcriptional response which was most marked in cell line J RT3-T3.5 (Figure 4h and Figure 4i). We analysed the transcripts upregulated more than 3 fold in each cell line. Absence of TCRζ resulted in a loss of 52% of Nef induced genes while in the absence of ZAP-70 44% of Nef induced genes were not upregulated. (The Appendix contains gene lists of those Nef induced genes prevented from induction in the absence of TCRζ and ZAP-70). An 89% overlap was observed between genes repressed in the absence of TCRζ and those repressed in the absence of ZAP-70. The Nef TCRζ interaction may contribute to Nef virulence enhancement as several genes associated with increased viral productivity are not induced in its absence including *c-myb, NFATc, IRF2, CDK9, TAT SF1, TRBP, U1 SNRNP* and *c-abl.* Therefore formation of the complete Nef transcriptional program requires TCRζ and ZAP-70. In addition it is initiated at the highest level in the T cell signalling path.

Fig 4g. Nef tet inducible cell lines were created in p116 and RT3-T3.5 Jurkat cell lines by co-transfecting each cell line with plasmids containing the tet transactivator element, the tet operator sequence and *nef* bicistronic with EGFP and a hygromycin resistance casette. Western blots of Nef expression after treatment of these cell lines with doycycline for 12 and 36 hours is shown. Cell line p116 is genetically deficient in ZAP-70 and RT3-T3.5 contains functionally deficient TCRζ.

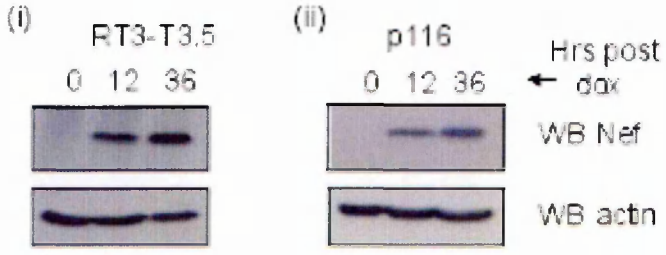

Fig 4h. Scatter plots demonstrate differences in gene induction after *nef* is expressed in RT3-T3.5 or p116. Supression of differential gene regulation is observed after Nef is expressed in RT3-T3.5 or p116. The colour key indicates upregulated genes as saturated red and downregulated genes as saturated blue.

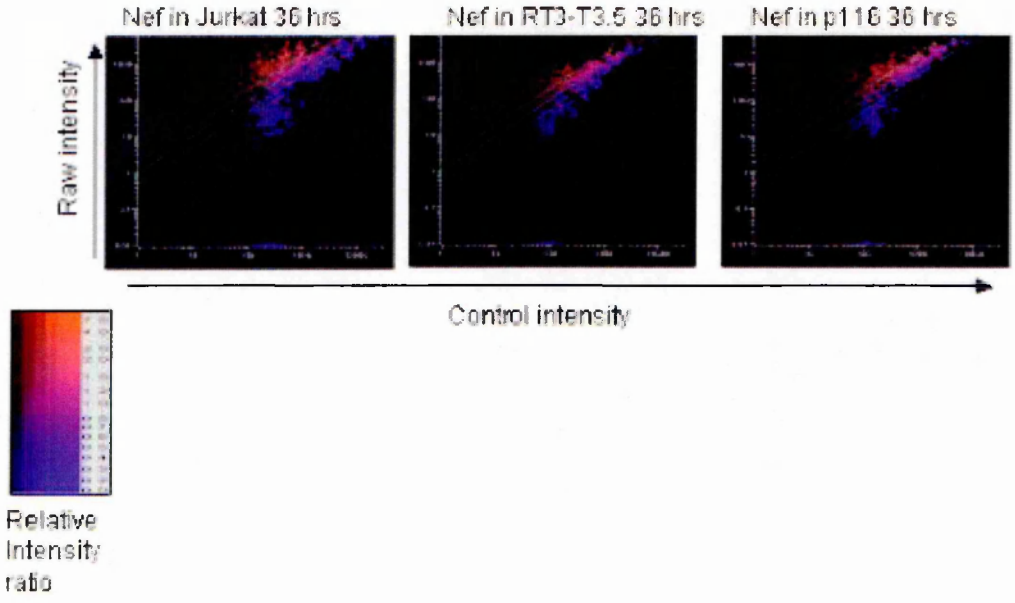

Figure 4i. Ordered lists showing genes inhibited in induction in the absence of functional TCRζ or ZAP-70 and genes unaffected after Nef expression. Gene inhibition is defined by normalised relative expression ratio reduced by more than 30% of the value obtained after Nef expression in Jurkat at 36 hours. This data is obtained from array HG 1.2 III but is representative of data obtained from all three arrays studied. A full list of genes inhibited in induction in each condition is supplied in the appendix. The colour key indicates upregulated genes as saturated red.

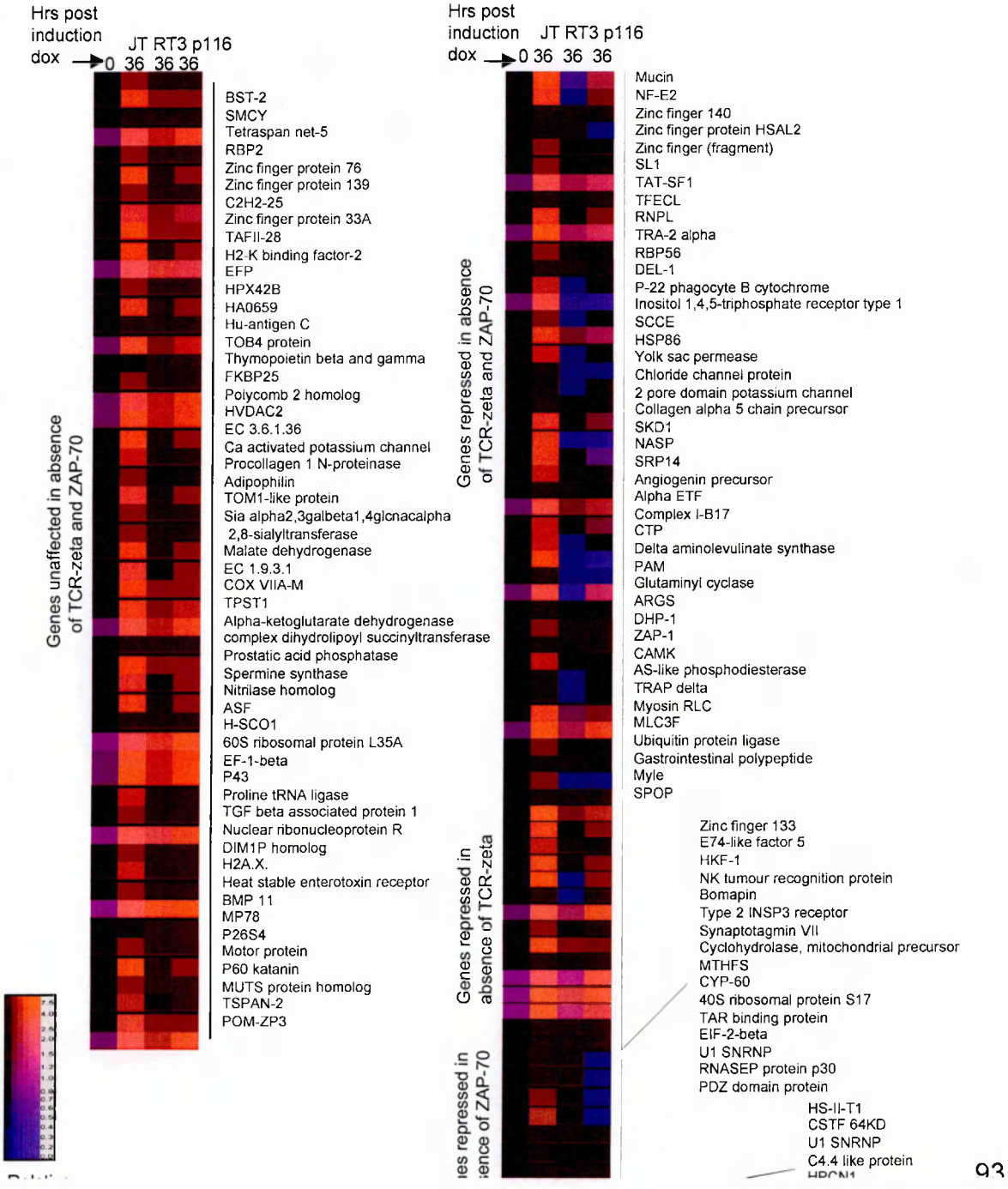

4.6 Contribution of the SH3 binding domain to transcriptional programme

The domain of Nef that has most commonly been implicated in binding to host T cell signalling moieties is the SH3 binding domain. To explore the contribution of this domain to the Nef gene expression profile a tetracycline inducible cell line using the mutant Nef construct P76A was created. Western blot and FACS analysis of gene induction of this mutant in Jurkat is demonstrated (Figure 4j). Many single cell clones must be screened before identification of a clone exhibiting reasonable gene induction with minimal background leak. Most clones screened show no evidence of EGFP expression (Figure 4.11). Cells were induced and RNA prepared for cDNA microarray analysis. Examination of the P76A expression profile demonstrated 59% of WT Nef induced genes were not detected (Figure 4k and Figure 4l). This is the most marked attenuation of the expression profile of all the conditions tested. However the failure to repress 100% of the induced genes indicates other domains apart from the SH3 binding domain must be involved in generating expression changes. HIV related genes induced by WT Nef but failing to be expressed by P76A are listed in red in Table 4.2. Among them are several factors that positively regulate viral replication.

Figure 4j. A P76A Nef tet inducible cell line was generated and expression tested by western blot after induction with doxycycline. Many clones are screened to identify a clone with reasonable Nef expression and minimal background leak. The bottom panel shows FACS analysis of EGFP expression after doxycycline treatment in two single cell clones. Most clones screened demonstrate no EGFP expression as shown for clone 113.056 in the middle panel. Successful EGFP induction was observed for clone 11.073.

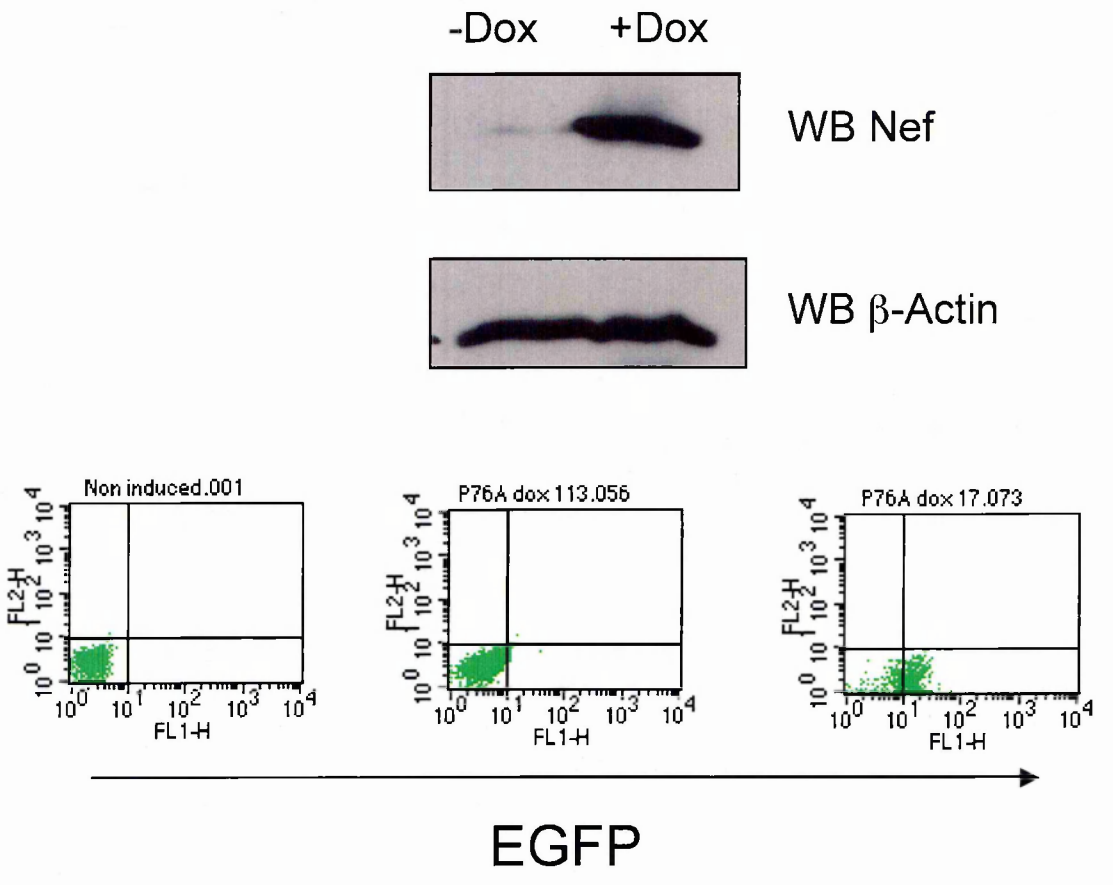

Figure 4k. Scatter plots demonstrating removal of the Nef SH3 binding domain suppresses a large amount of differential gene expression occuring after expression of WT Nef in T cells. Raw intensity values are plotted against control values for each gene. The green lines indicate the relative expression of the data sets relativeto time 0. The upper line marks a two-fold increase, the lower line marks a two-fold decrease and the centre line indicates equivalent expression. The colour scale indicates relative up and downregulation of genes with red representing up and purple downregulation.

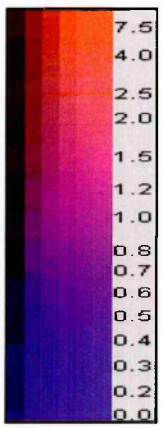

Relative Intensity ratio

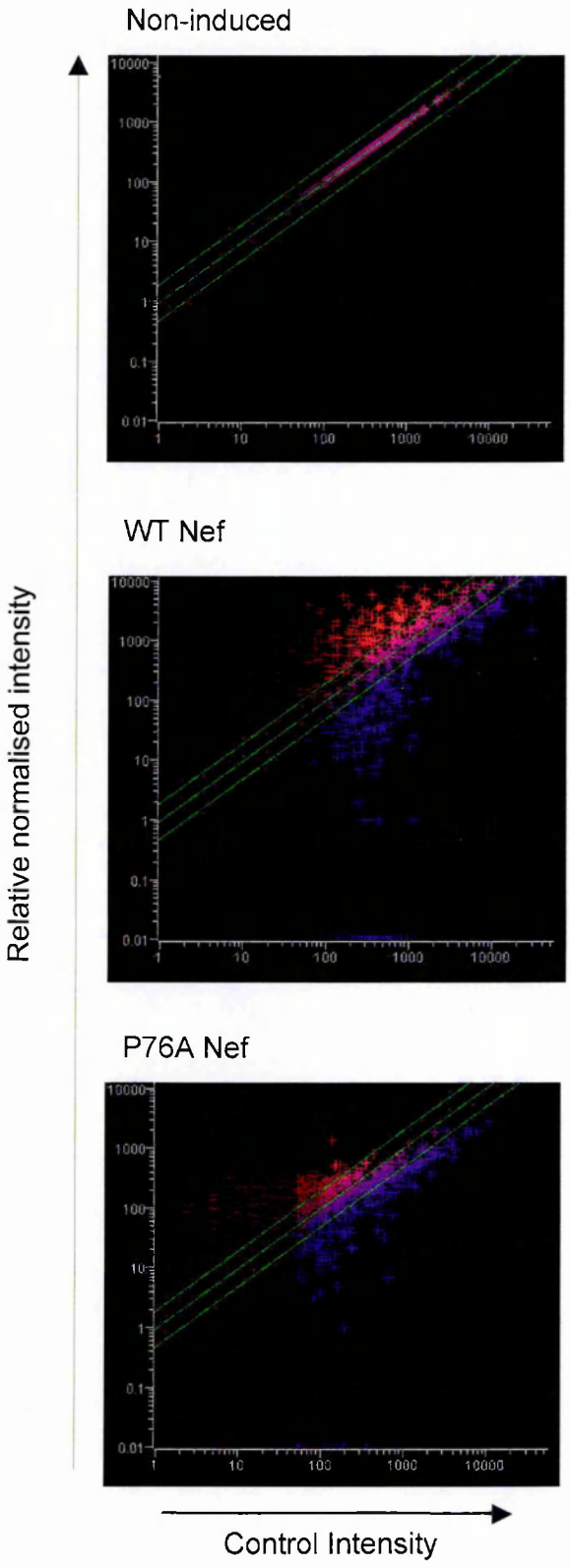

Figure 4l. Ordered list representation of WT Nef induced genes in comparison with P76A induced genes. The colour key indicates upregulated genes as saturated red. In total removing the Nef SH3 binding domain removes 59% Nef induced genes. P76A Nef exclusively induces some genes not upregulated by WT Nef. This ordered list is generated from data obtained from array HG 1.2 III. It is representative of results obtained from all three arrays.

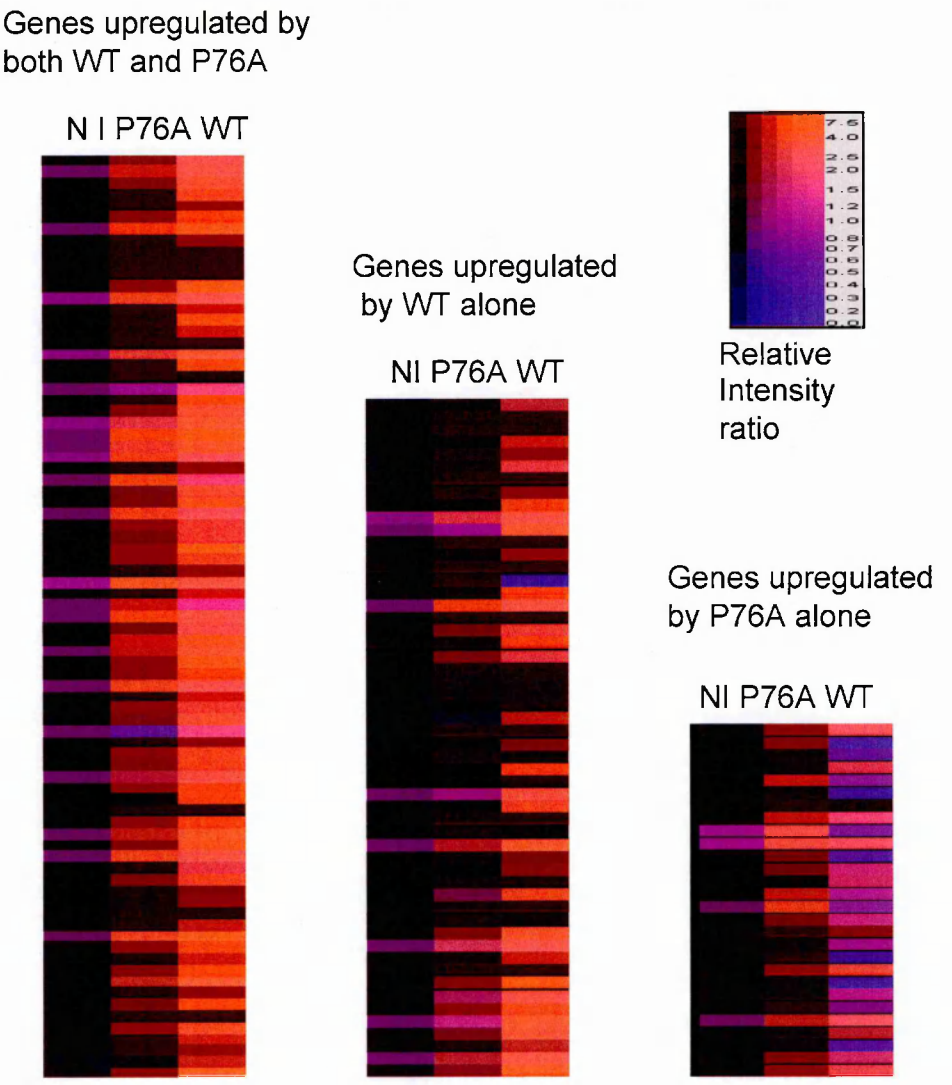

4.7 Summary

It has been possible to compare reference activation states to the Nef expression profile and demonstrate a close identity to a reference T cell activation state. The strength of using Jurkat T cells as a model system derives from the fact that this cell line has been used to delineate many aspects of T cell signalling. In addition several genetically null and functionally deficient mutants are available that enable a dissection of a mechanism for Nef signalling. Evidence obtained from the different conditions examined demonstrates Nef acts at the highest level in the T cell signalling path. In addition the SH3 binding domain of Nef is involved in generation of the gene expression profile.

Chapter 5

Proteomic Analysis of Nef in T Cells

5.1 Introduction

The Nef gene expression profile suggests Nef may exert a specific effect on T cell transcriptional activity. In addition it indicates that Nef activates T cell signalling cascades at a point proximal to TCRζ-associated ZAP-70. As discussed previously it is unlikely that Nef acts via a single protein-protein interaction to induce these effects but likely as part of a multi-component complex. In support of this there is no described structural basis by which a motif in Nef could facilitate phosphorylation of tyrosine residues in the cytoplasmic tail of TCRζ without participation of a third party.

T cell activation requires sustained T cell receptor interaction with MHC-peptide complexes in the immunological synapse formed between the T cell and antigen presenting cell (APC). A synaptic basis for immune cell interaction was suggested in 1984 after the identification of T cells, APCs, lymphocyte cell adhesion molecules and the TCR (Norcross, 1984). Subsequently many T cell-APC interactions have fulfilled parameters equating with neurological synapse behaviour. These include the fact T cells and APCs remain discrete cells during the interaction (Unanue, 1984) and the fact adhesion molecules link the two cell types together (Springer, 1990). In addition vectorial secretion is a property of immune cell interaction (Paula and Seder, 1994 and the TCR:MHCp interaction delivers a stop signal to ensure positional stability (Dustin et al., 1997).

The immunological synapse is composed of SMACs (supramolecular activation clusters (Dustin et al., 1998). The central or cSMAC is composed of a central cluster of TCR:MHCp interactions surrounded by a ring of LFA-1:ICAM-1 integrin mediated interactions (peripheral or pSMAC) (Monks et al., 1998). The Golgi and

microtubule organising centre are positioned within a micrometer of the cSMAC and radiating microtubules contact the pSMAC (Kupfer et al., 1994). Mature synapse formation takes minutes but may be stable for hours (Grakoui, 1999).

SMACs contain several signalling components. These include Src and Syk family kinases, PKCθ and Cdc42-GTP (Bromley et al., 2001). The immunological synapse also contains adaptor proteins such as SLP-76, Fyb and Nck that are linked directly or indirectly to proteins such as WASP, Ena/VASP family members that are involved in actin polymerisation (Krause et al., 2000; Monks et al., 1998).

Interaction between the T cell receptor (TCR) and peptide loaded major histocompatibility complex (MHC) molecules on the surface of the APC induces the formation of clusters at the contact site that are enriched in filamentous actin (F-actin) (Grakoui et al., 1999; Penninger and Crabtree, 1999). The accumulation of F-actin at the T cell APC interface is thought to stabilise a connection between T cells and APCs that is continuous and required for optimal T cell activation. Inhibition of F-actin polymerization by cytochalasin blocks synapse formation and T cell activation (Wulfing and Davis, 1998).

The earliest step in formation of the immunological synapse can be correlated with topologically based receptor segregation based on the size of different receptor ligand pairs (Springer 1990). Evidence for this has been obtained by using CD48 artificially lengthened to contain several additional domains. Here CD2:CD48 pairs inhibited efficient TCR activation by the APC (Wild et al., 1999). The driving force for this segregation might be the thermodynamic advantage of aligning membrane surfaces with nm precision that serves to enhance interactions (Dustin et al., 1997).

How the SMAC becomes organised is not clear. Several hypotheses have arisen. There is some evidence to suggest that direct actin-myosin based transport toward the synapse is active during synapse formation (Wulfing and Davis., 1998). An alternative suggestion is based on the coupling between thermally driven membrane fluctuations and the kinetics and mechanisms of the different types of receptor-ligand interactions (Qi et al., 2001). This model has been named the synapse assembly model. When the membrane oscillations

harmonize with kinetics of receptor-ligand interactions patterns like the immunological synapse can be generated by computer simulation. This model predicts that some self-MHCps may synergise with agonist MHCp to lower the threshold for mature synapse formation (Lee et al., 2002/3). Recently experimental evidence in support of this prediction has been derived (Wulfing et al., 2002).

Nef can localise to lipid rafts in T cells (Wang et al., 2000, Schrager et al., 1999). It is possible Nef forms a signalosome within rafts to facilitate signalling. Lipid rafts appear to play essential roles in signalling initiated through TCRs (Xavier et al., 1998), BCRs (Cheng et al., 2001) and several Fc-receptors (Field et al., 1995). These receptors are in their resting state devoid of any associated protein tyrosine kinases. Then upon cross linking their aggregates merge with membrane rafts and immune-receptor based tyrosine activation motifs (ITAMS) present in the cytoplasmic tails of their signalling chains become exposed to Src kinases in rafts (Harder, 2001). Several other components of the early phase of signalling such as PIP_2 and LAT also constitutively reside in rafts. TCRs may be pre-associated with membrane rafts and their crosslinking may reorganise this assembly to allow for optimal CD3 exposure to Src family kinases. Support for this comes from several lines of evidence.

Constitutive association of the pre-TCR with lipid rafts is sufficient for eliciting signals required for pre-thymocyte survival (Foti et al., 2002). Partial raft dispersal by cholesterol depletion inhibits early TCR-triggered events such as tyrosine phosphorylation of TCRζ and calcium flux (Stulnig et al., 1998/ Membrane rafts are also partially disrupted in T cells exposed to corticosteroid correlating with defective TCR signalling (Van Laethem et al., 2001). T cells from acid shingomyelase knockout mice which are deficient in membrane rafts due to decreased cholesterol content have defects in TCR induced tyrosine phosphorylation and T cell proliferation (Nix et al., 2000). Wild-type Lck and LAT molecules capable of targeting to rafts but not their membrane associated raft non-targeted mutants are able to reconstitute TCR signalling defects in appropriate mutant T cell lines (Kabouridis et al., 1997). In addition artificial

targeting of other cytoplasmic molecules such as SHP-1 (Veri et al., 2001), CD45 (He et al., 2002) or PLCγ (Melkonian et al., 1999) to membrane rafts results in marked functional effects on TCR induced signalling. Finally mutation of the TCR connecting peptide that interferes with increased ζ chain raft association in response to partial agonist antigen affects Erk activation and thymocyte positive selection (Werlen et al., 2000). Similar signalling defects are observed in T cells of CD3δ knockout mice where the TCR/CD3 complex is deficient in membrane raft association (Delgado et al., 2000).

The manner by which rafts coordinate T cell signalling is poorly understood. Major subsets of CD4 and CD8 are located in rafts (Parolini et al., 1996) as is Fyn (Stuemer et al., 2001). It is not clear whether sequestration in membrane rafts helps keep Src family kinases in an active or inactive state. CD45 is a major positive regulator of these kinases however it is sequestered away from rafts. In contrast a fraction of the negative regulator Csk is a raft component. Activation induced association of TCRs with membrane rafts seems to be dependant on an extracellular proteoglycan agrin, previously known to aggregate receptors at the neuromuscular junction. A T cell specific form of agrin has been shown can aggregate lipid rafts and enhance T cell activation induced by either CD3 crosslinking or by peptide antigen (Khan et al., 2001). It is possible agrin functions like antibodies to GPI-anchored proteins present in rafts although the ligand has not so far been demonstrated. Membrane rafts also play an important role in the process of co-stimulation. CD28 mediated co-stimulation is accompanied by a major raft redistribution from intracellular reservoirs to the cell surface (Viola et al., 1999). This appears to be regulated by a cytoskeletal dependant mechanism that is poorly understood.

TCR interactions with membrane rafts have been correlated with actin cytoskeletal rearrangements on T cell activation. Lipid raft polarisation in the immunological synapse depends on various signalling proteins including Vav-1, Rac and WASP (Villalba et al., 2001). Another molecular complex playing roles in these raft membrane rearrangements include Slp-76, Nck, Fyn, PAK and PKCθ. The activated TCR complex crosslinks to the actin cytoskeleton through the

tyrosine phosphorylated ζchain and this interaction is enhanced when aggregated TCRs associate in lipid rafts (Kosugi et al., 1999). Association of lipid rafts with cytoskeleton may be mediated through some of the proteins residing in rafts such as the PAG/Cbp connected to F-actin through EPB50 and ezrin/radixin/moesin (Torgersen et al., 2001) or the adhesion protein CD44. The phospholipid PIP_2 is also involved in recruitment of the WASP protein to be aggregated to membrane rafts where it functions in actin nucleation through associated Arp2/3 complex (Rozelle etal., 2000). Accumulation of F-actin under patches of aggregated rafts correlates with presence of tyrosine phosphorylated proteins (Harder et al., 1999). It is not known whether reorganisation of actin cytoskeleton is required for raft clustering or whether raft clustering promotes polymerisation of the actin cytoskeleton. Interestingly Nef has been shown to facilitate actin polymerisation in 293 cells with resultant induction of lamellipodia in a Vav/Cdc42 dependant interaction (Fackler et al., 1999).

Previous attempts to define a signalling module by which Nef acts have utilised information gleaned from structural studies and from in vitro pull down assays. Nef is promiscuous in binding in vitro and thus many described interactions may have little relevance in vivo. The yeast-2-hybrid system was previously used to probe Nef protein-protein interactions. This system can probe millions of interactions and is therefore suitable for large scale screening of protein-protein interactions however in general this in vivo system cannot readily detect interactions with multiple components or interactions occurring under particular environmental conditions eg. (Ca^+ concentration and co-factors such as low molecular weight metabolite and post-translational modifications ie. phosphorylation, glycosylation, acrylation and alkylation). As activation of a signalling cascade by Nef is likely to involve an interaction dependant on changes in phosphorylation the yeast-2-hybrid is unlikely to identify such a complex.

Proteomics using 2D gel analysis followed by mass spectrometry was undertaken to attempt to define a signalling complex by which Nef might relay specific information to the T cell nucleus. Figure 5a illustrates the steps involved.

Figure 5a Flow diagram illustrating steps involved in proteomic analysis investigating Nef mediated signalling in T cells.

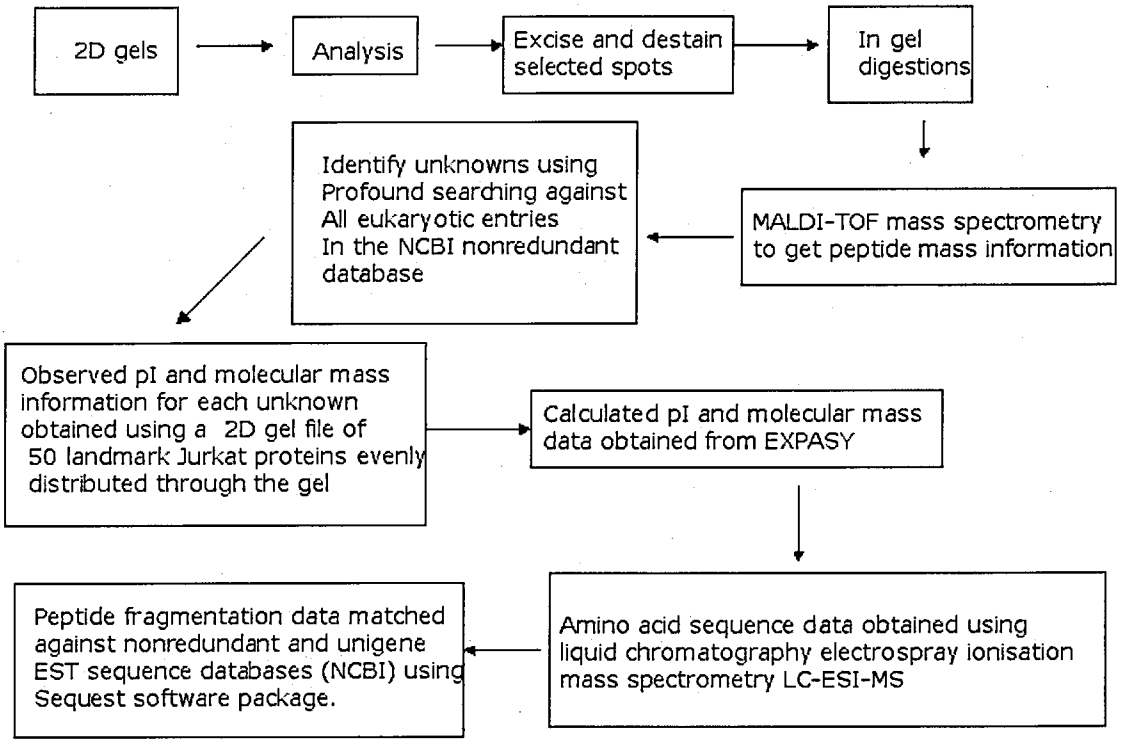

Protein samples were run on 2D gels using pH 3-10 linear IPG strips from Amersham and subsequently electrophoresed on 12.5% precast SDS gels. Gels were analysed using a software (Melanie 3.0) normalising and aligning gel images after silver staining. Automated spot picking resulted in generation of a number of gel fragments that were digested (Figure 5b) and analysed by mass spectrometry or peptide microsequencing. While this approach appears reasonable in attempting to delineate a complete functional Nef signalling module it is worth noting 2D gel analysis is currently seriously limited with regard to detection of very basic or acidic proteins, those with very large or small molecular weights and in detection of proteins present in very low abundance. In addition it is notoriously difficult to separate proteins embedded in cell membranes using this methodology.

Figure 5b. Method for in gel digestion of protein samples prior to mass spectrometry.

Manual digest (general, from holger)
Dry gel pieces in speedvac (1-2 hrs)
Wash: 3 times Add 50 µl of 20 mM NH_4HCO_3 in water – Shake for 20 min at room temperature- Remove supernatant
Reduction with DTT: Add 10 mM DTT in 20 mM NH_4HCO_3 in water (volume should cover gel piece) – shake for 45 min at room temperature – Remove supernatant
Alkylation with Iodoacetamide: Add 50 mM Iodoacetamide in 20 mM NH_4HCO_3 in water (volume should cover gel piece) – shake for 20 min at room temperature in dark – Remove supernatant
Wash: 3 times Add 50 µl of 20 mM NH_4HCO_3 in 50% acetonitrile – Shake for 20 min at room temperature – Remove supernatant Add 50 µl of 100% acetonitrile - Shake for 20 min at room temperature – Remove supernatant **Dry gel pieces** in speedvac (1h) Note: gel pieces turn white
Trypsin (sequence grade): Add 10 µl (volume may be increased based on size of gel piece) of 10 ng/µl trypsin solution in 20 mM NH_4HCO_3 in water - After 5 min, remove excess trypsin solution and add 10 µl of 20 mM NH_4HCO_3 in water – Incubate over night at 37° C (12-15 hrs). Note: modified trypsin may be used to minimize autolysis products. Prepare trypsin digest solution from original stock solution just before use **Extraction of peptides:** 3 times with 50 µl of 5% formic acid in 50% acetonitrile – 20 min shake – Collect and pool supernatants in new vials (discard gel pieces) **Dry peptide extracts** in speedvac
Reconstitution: Dissolve in 0.1% TFA (MALDI) or 0.1% FA (ESI) in H_2O (6-10 µl) by vortex for 3 s – shake for 20 min – sonicate for 2 min

5.2 Nef interacting proteins in lipid rafts

In order to perform an analysis of Nef interacting proteins in rafts it was necessary to immunoprecipitate Nef without disrupting any potential interaction. C-terminal HA tagged Nef was created by including the haemaglutinin (HA) sequence in a PCR primer and cloning WT-HA Nef into pIRES-2-EGFP expression vector. Jurkat were then transfected with this construct or a control empty vector. Lipid raft fractions were isolated by sucrose density gradient centrifugation. The presence of the raft marker GM1 and absence of the phosphatase CD45 was confirmed by western blotting of serial 1ml fractions harvested from the rafts samples (Figure 5c). Nef was immunoprecipitated from the raft fractions using an anti-HA antibody. The resulting immunoprecipitate was run on 2D gels pH gradient 3-10. Immunoprecipitates obtained with WT Nef

were compared to those obtained with the SH3 binding mutant P76A Nef. WT HA-tagged Nef co-immunoprecipitates specifically with several proteins in this context (Figure 5d). The identity of these is being investigated at present.

Figure 5c. Lipid rafts were purified by sucrose density gradient centrifugation. Western blot confirms fractions 2 and 3 contain rafts as GM1 is present and CD45 excluded.

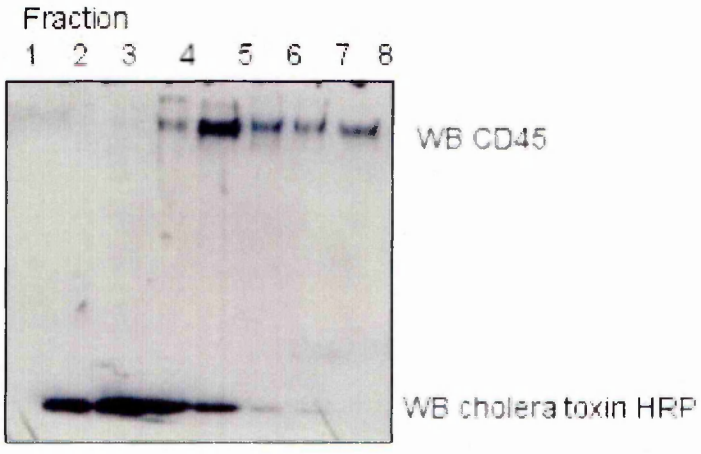

Figure 5d. 2D gel analysis of WT Nef and P76A Nef immunoprecipitated from raft fractions.

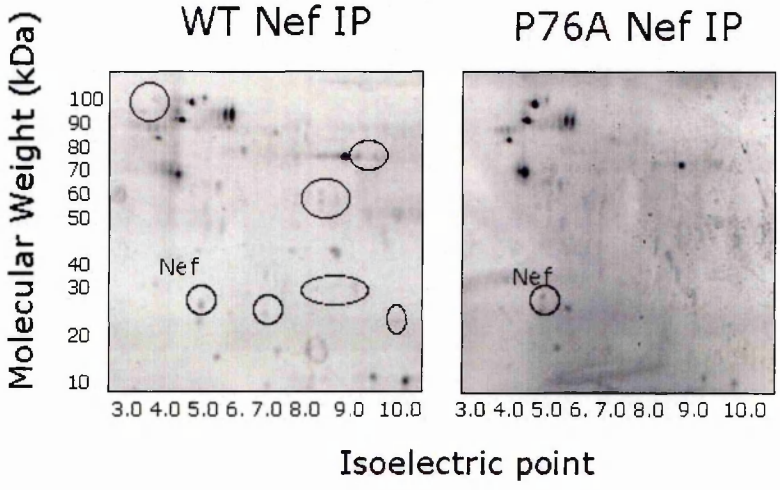

5.3 Raft proteome in the presence and absence of HIV Nef

Activation of T lymphocytes is initiated by interaction of clonally distributed antigen receptors with peptide-MHC ligands on the surface of antigen presenting cells. Signalling resulting from these recognition events is initiated in seconds and persists for hours. Surrounding the TCR and peptide MHC are multiple co-receptors and counter-receptors that influence the signalling event. The molecular basis of signal initiation and integration via co-receptors is not understood. Recently the mechanism of signal initiation after TCR stimulation has begun to be explored in the context of cell biology. Membrane sub-domains known as DIGs, GEMs or lipid rafts are lipid fractions insoluble in low concentrations of non-ionic detergents at 4°C. A significant fraction of acylated and glycosyl-phosphadoidylinositol linked proteins are concentrated in lipid rafts. Upon TCR engagement translocation of non-lipid modified signal transduction molecules are drawn towards the raft fraction. Difficulties in standardisation between experiments have occurred and controversy exists how much TCR is translocated to the lipid raft fraction after antigen receptor engagement. Some have claimed that only a significant fraction of the phosphorylated ζ chain but not α/β dimer is present. Translocation of various signalling components represents an ideal way of compartmentalisation of signalling modules and bringing them into proximity with their substrates.

Analysis of the role of lipid rafts in generation and propagation of signals is unclear. It has been shown stimulation through the TCR increases raft expression, One group has shown that co-stimulation via CD28 results in raft aggregation that might lead to more efficient signalling by bringing more signalling components into proximity. Lipid raft reorganisation is not sufficient for co-stimulation simply aggregating rafts by applying cholera toxin does not facilitate signalling. Rafts also provide a link between the TCR and the cytoskeleton (Penninger et al., 1999). Association of the TCRζ with the cytoskeleton after receptor engagement is dependant on lipid raft integrity.

The protein complement of CD4 T cell lipid rafts in the presence and absence of Nef was explored. Current mass spectrometry methods for elucidating membrane proteins involve either gel based methods or "shotgun" methods in

which complex protein mixtures are proteolytically digested before separation and analysis by LC/MS approaches. The limitation of the gel based approach for membrane proteins remains solubility. Many hydrophobic proteins are not solubilised in the non-detergent isoelectric focusing sample buffer. In addition solubilised proteins are prone to precipitation at their isoelectric point. Limited dynamic range of detection is also an issue because membrane proteins are typically lower in abundance when compared with soluble proteins. However subcellular fractionation and directed biochemical enrichments can overcome many of these issues. In addition improved solubilization of membrane fractions can be achieved by treatment with organic solvents or non-ionic or zwitterionic detergents before gel analysis. In this analysis lipid rafts were obtained after sucrose density gradient centifugation. Samples then underwent dialysis to remove sucrose. During this procedure it was noted a high proportion of protein was lost. 400μg protein was loaded for each 2D gel run. Differences were noted between Nef expressing and nonexpressing raft fractions (Figure 5e). New proteins were recruited to rafts in the presence of Nef and their identity is currently being established by mass spectrometry.

Figure 5e. Changes in lipid raft protein content in control and Nef expressing Jurkat CD4 T cells. Lipid rafts were run on pH 3-10 linear IPG strips and 12.5% precast SDS gels. Figures 5c (i), (ii), (iii) and (iv) represent gels obtained with control samples and Figures 5c (v), (vi), (vii) and (viii) are gels obtained after Nef expression.

(i)

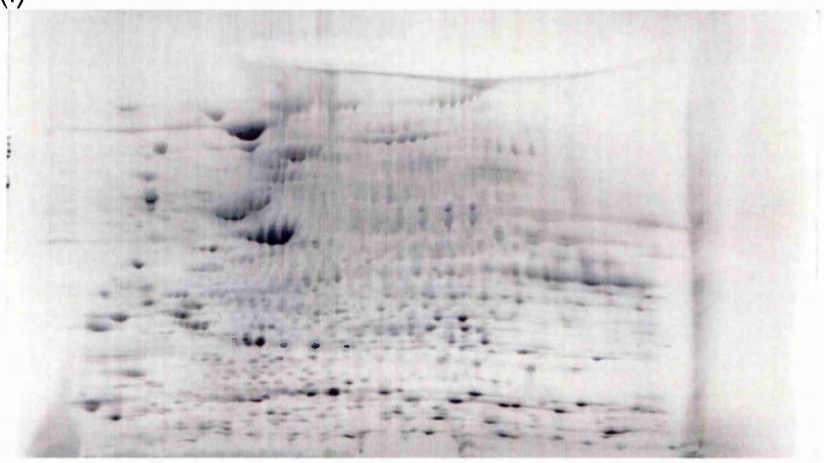

(ii)

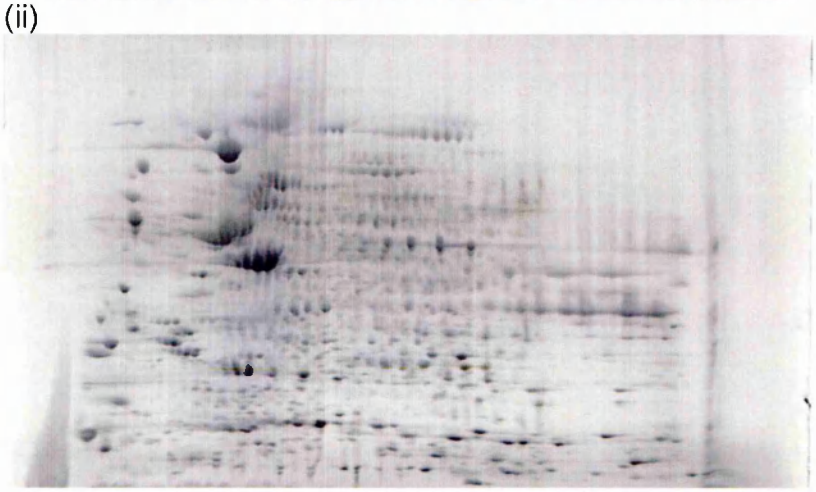

(iii)

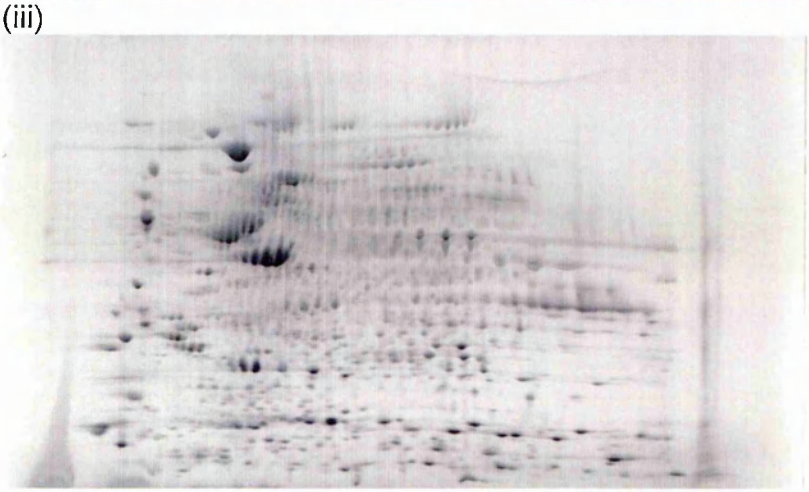

(iv)

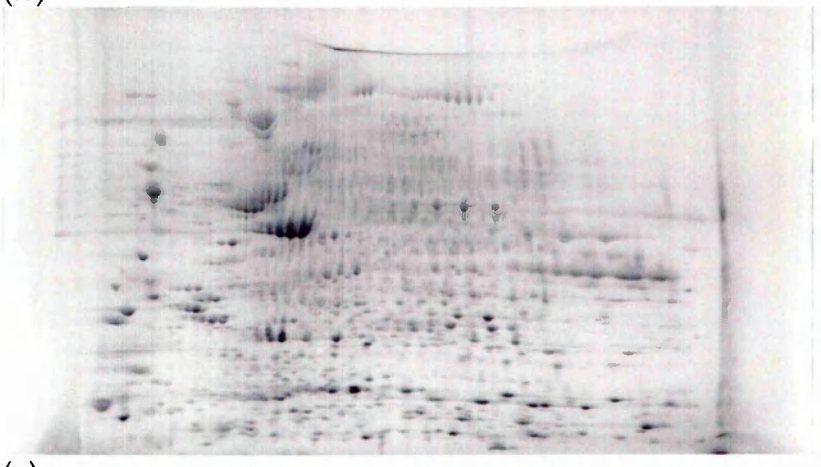

(v)

(vi)

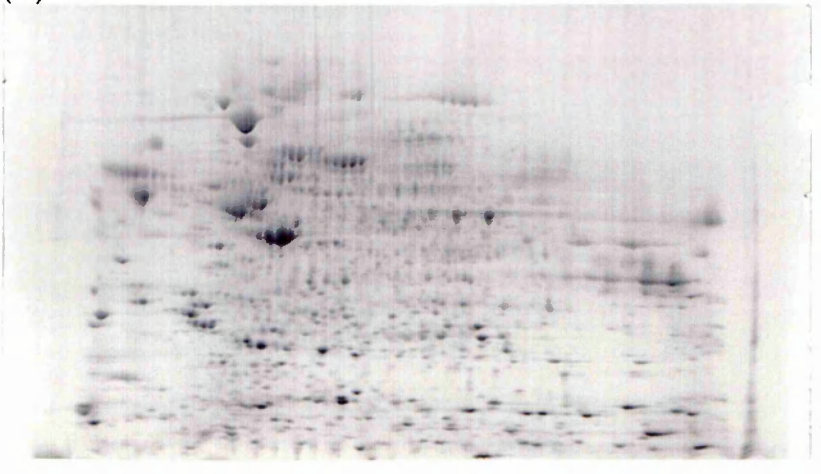

(vii)

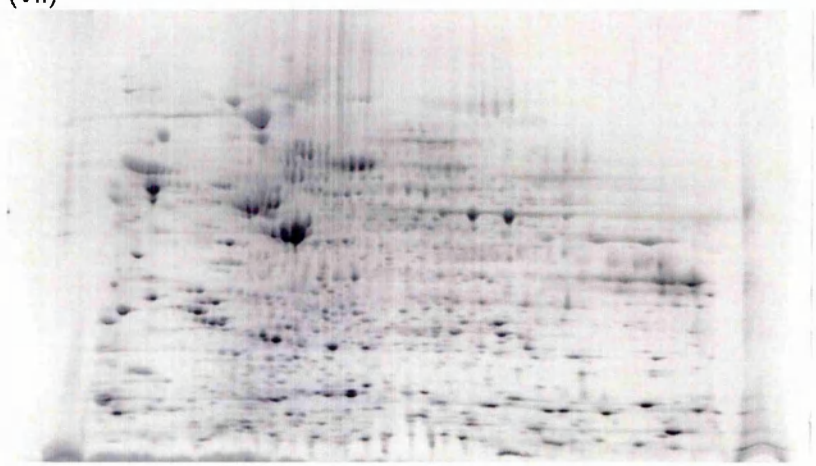

(viii)

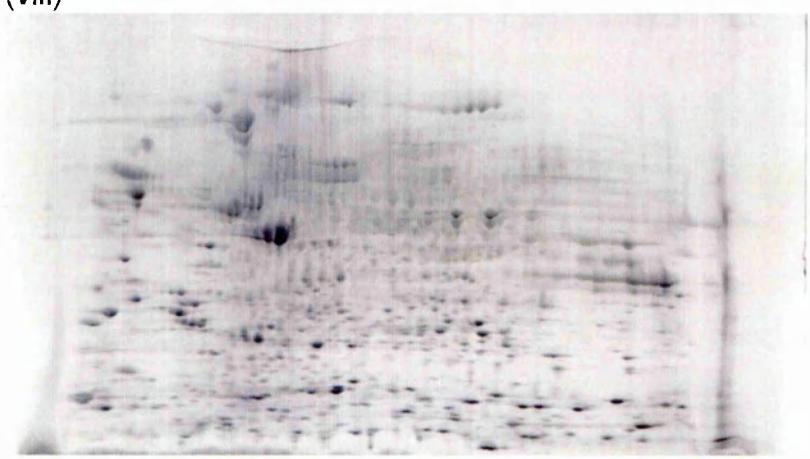

5.4 Use of siRNA to establish which Nef interacting proteins functionally contribute to Nef T cell activation

Use of siRNA to inhibit protein expression enables functional characterisation of individual genes in specific contexts. The mechanism of siRNA action in facilitating degradation of cognate mRNA is illustrated in Figure 5f.

Figure 5f. Schematic representing the known stages of degradation of mRNA after endogenous dsRNA formation in mammalian cells. The diagram shows how synthetic siRNAs introduced by transfection or produced from a vector feed into the RISC complex.

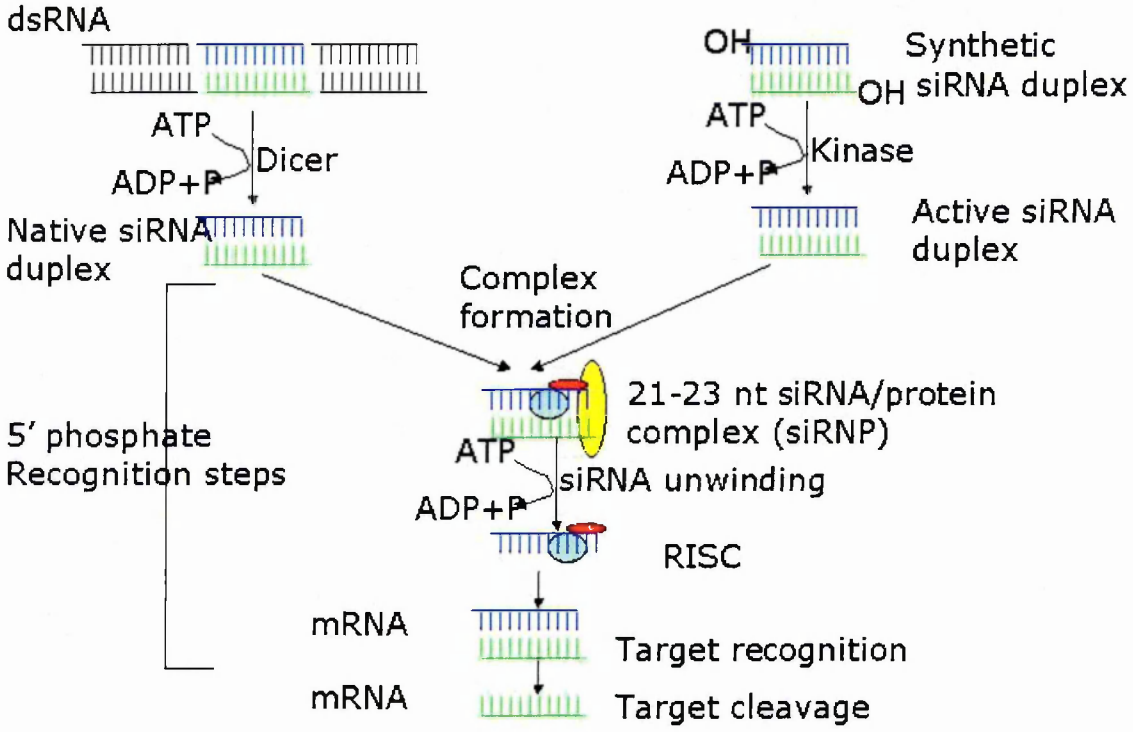

In order to identify which Nef interactors identified by mass spectrometry contribute to Nef mediated T cell signalling a screening system was constructed using siRNA expression vectors. As several proteins are likely to be involved using gene expression profiling as a readout is time consuming and expensive. Nef has previously been demonstrated to induce actin polymerisation in T cells via an interaction with Vav and Cdc42 (Fackler et al., 1999) (Figure 5g).

Figure 5g. Confocal image of Nef transfected cells stained for filamentous actin using phalloidin oregan green.

The assay for functional contribution of proteins identified by mass spectrometry measures actin polymerisation as a read-out. Co-transfection of Jurkat with Nef and a siRNA vector corresponding to the gene of interest and documentation of actin polymerisation observed by confocal microscopy is being used to assess which proteins functionally contribute to Nef mediated T cell activation.

5.5 Design of siRNA expression vectors

siRNA expression vectors were designed. The U6 RNA polymerase III promoter was used. This promoter has been shown to successfully direct expression of 21 nt siRNAs in mammalian cells. U6 promoter directs expression of snRNAs physiologically and transcripts are processed to contain terminal TT. This TT signal is recognised by the RISC complex that facilitates degradation of cognate mRNA. Oligonucleotides corresponding to sequence from EGFP were annealed by heating at 100^0C for 5 minutes and then cooling on the bench. These were ligated to ApaI/ EcoRI cloning sites in pBS-U6. An additional vector was designed to act as an siRNA reporter vector and to direct expression of *nef* simultaneously. The bi-directional rtTA Tet vector pBI from Clontech was used. IRES-EGFP was subcloned from pIRES-2-EGFP at PstI/ NotI in MCS 1. The U6 was shuttled from pBS-U6 at XhoI after a XhoI linker was placed at Pst I. The second MCS was used to express *nef.*

The functional contribution to Nef mediated signalling of proteins identified by mass spectrometry is being assessed. First the proteins are being knocked down in Jurkat by transfection of siRNA expression vectors. The ability of these vectors to inhibit proteins expression is being determined using western blot, confocal analysis or FACS analysis. In the case of western blot this is less than ideal for Jurkat as invariably a maximal transfection efficiency of 30-40% only is obtained after transient transfection. Therefore it is hard to quantitate the effect of a particular vector as shown in Figure 5f. Here a siRNA vector directed against LAT has been transfected in Jurkat and protein level of LAT assessed by western blot after 48 hours. The changes are unconvincing. Confocal enables direct assessment of transfected cells by analysis of EGFP and staining for the protein of interest.

Figure 5f. Western blot of LAT expression in Jurkat after transfection of a control and anti-LAT siRNA vector.

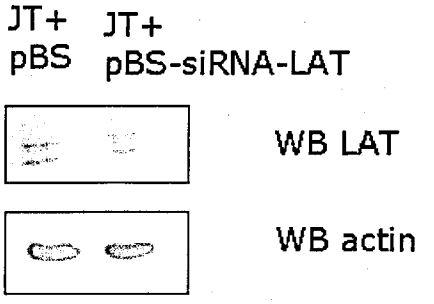

5.6 The Nef Proteome in T cells

Microarray analysis suggests Nef generates a transcriptional programme in T cells that mimics the gene expression profile obtained after Jurkat CD4 T cells are cross-linked with anti-CD3. These findings point to role of Nef in regulating some of the earliest stages of the viral life cycle. This is intriguing given the recent evidence that *nef* transcripts are produced prior to integration of the virus

into the genome of resting T cells, resulting in accumulation of Nef protein that primes viral synthesis upon T cell activation (Wu and Marsh., 2001). Transcriptional changes do not necessarily reflect changes in protein synthesis. Indeed it has been noted that changes in level of mRNA species often correlates poorly with changes in respective protein expression.

A proteomic analysis of Jurkat CD4 T cells was performed after expression of Nef in these cells. At 24 hours post Nef expression 50 x 10^6 cells were lysed with NP40 lysis buffer. Results of 2D gel analysis of control and Nef positive lysates

Figure 5.c 2D gel analysis of Jurkat whole cell lysates in the absence (i, ii, iii, iv) and presence of Nef (v, vi, vii, viii). 500μg protein was used for each gel. 24 cm linear IPG strips were used together with pre-cast 12.5% SDS gels. Gels were silver stained prior to Melanie analysis.

(i)

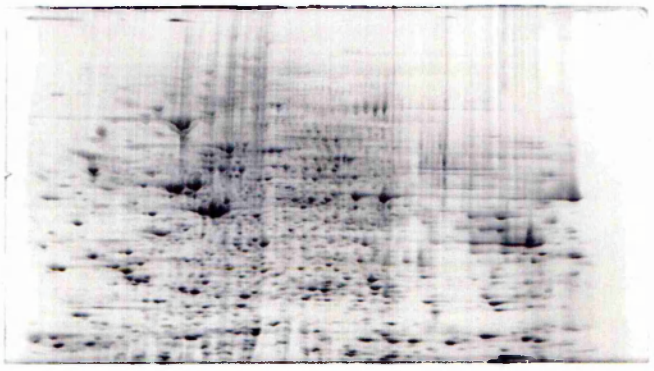

(ii)

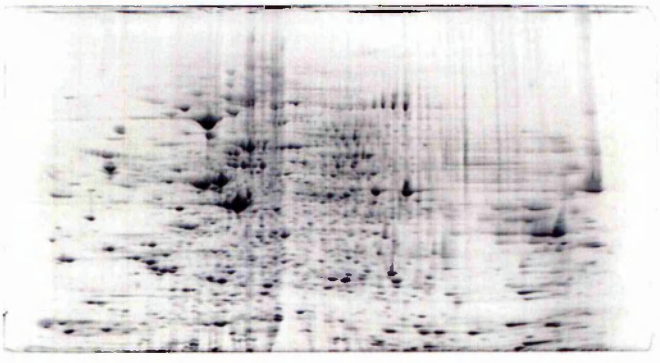

(iii)

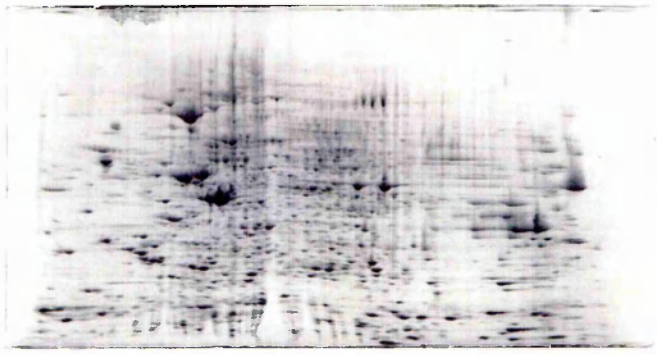

(iv)

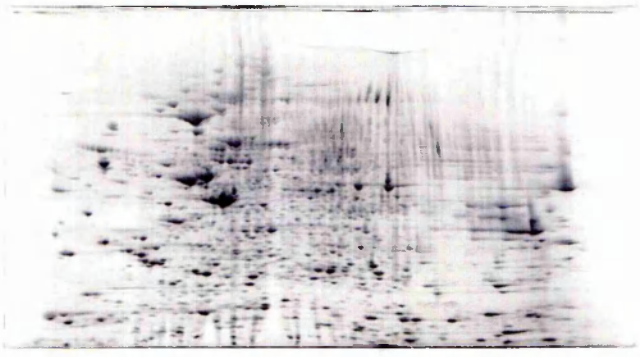

(v)

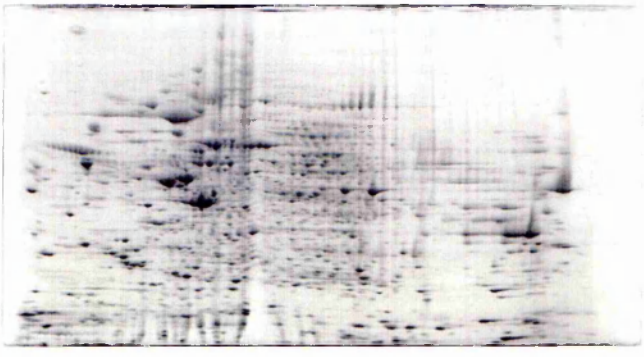

(vi)

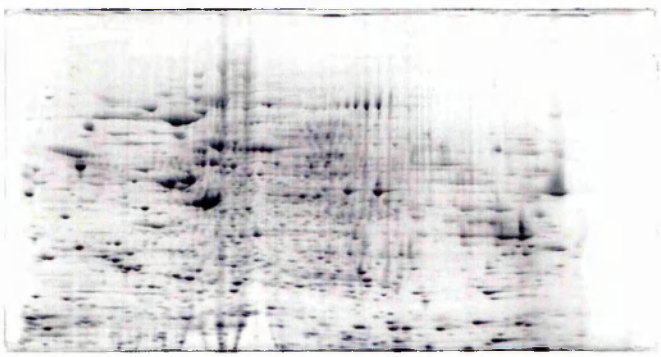

(vii)

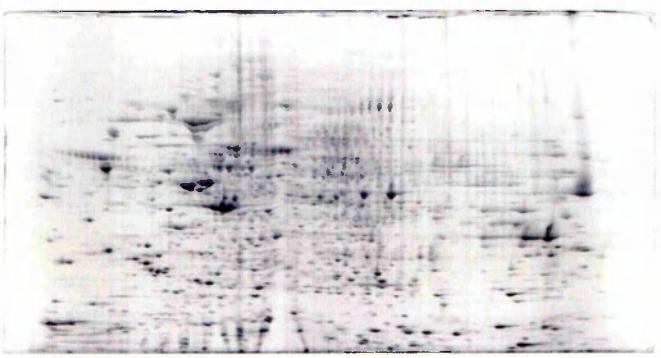

(viii)

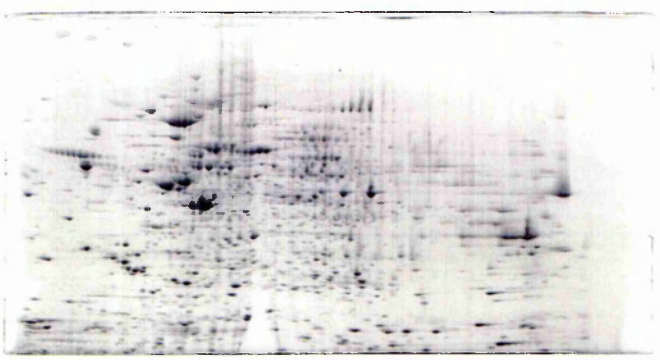

are shown in figure 5c. The experiment was imperfect for several reasons. Firstly it was not possible to utilise the tetracycline inducible system in this instance. To

perform each experiment large quantities of cells were required to generate enough protein for each 2D gel. Due to leakiness and loss of expression in the tet system it is difficult to generate the quantites of Nef expressing cells required in a short time period. However the purpose of carrying out a proteomic analysis was not simply one of annotating a possible Nef effect but to generate leads that could be followed and individually substantiated. Expression data invariably falls short in this regard as often changes in gene expression are not indicative of changes in gene function. Samples used were Jurkat transiently transfected with Nef expression vectors. In each instance 35-40% transfection efficiency was achieved with either Nef or control vectors. Analysis of results therefore must take into account the fact changes in protein levels might reflect changes occuring directly in Nef expessing cells or in bystander cells as a secondary phenomenon.

Another shortfall of this experiment was the methodology utiltised for 2D gel analysis. The ideal method for use in this experiment would be to use differential in gel electrophoresis. Proteins from one sample are tagged with a single fluorescent compound, while those from another sample are tagged with a different fluorescent dye. The two samples are then mixed together and the individual proteins are separated on a single 2D gel. This enables clear analysis of differentially regulated proteins. In addition 2D gels analysis is currently seriously limited with regard to detection of very basic or acidic proteins, those with very large or small molecular weights and in detection of proteins present in very low abundance. In addition it is notoriously difficult to separate proteins embedded in cell membranes.

The 2D gel results indicate that Nef generates gene expression changes in T cells that result in induction of a specific Nef T cell proteome. The identity of these proteins is being elucidated using mass spectrometry. The nature of the proteins differentially expressed in whole cell lysates by Nef and post-translational modifications produced may give clues as its role in viral pathogenesis

5.7 Summary

With 30,000 to 40,000 genes potentially expressed in the human genome cells face the task of assembling these gene products into functional complexes and localising them to appropriate sites. Estimates of the number of proteins encoded by the human genome have varied between 200,000 and 2 million. One of the strategies employed to tackle this problem is to spatially restrict proteins to their site of function. In particular the targeting of proteins to membranes has proved to be an effective means of obtaining fidelity and organisation of protein-protein interaction modules. Nef is found expressed throughout the T cell but is concentrated in several subcellular compartments in particular the plasma and nuclear membrane. It is likely to function differently in each. In order to elucidate a mechanism by which Nef mediates T cell signalling Nef and interacting partners were extracted from lipid rafts in the T cell plasma membrane. T cell signalling is initiated from lipid rafts after recognition of antigen on the surface of antigen presenting cells. This revealed association of Nef with several interacting partners in an SH3 domain dependant manner under the experimental conditions specified. Nef also changes the composition of lipid rafts. The identity of interactors and differentially distributed raft proteins detected by 2D gel analysis is being established using mass spectrometry and peptide microsequencing.

Chapter 6

Conclusions and Discussion

6.1 Nef transcriptional program

A central goal of the gene expression study was the identification of physiologically relevant targets of the Nef transduction pathway. In this way many of the genes induced by Nef provide pointers for unravelling individual virulence mechanisms. HIV-1 proviral gene expression is tightly regulated by binding of host cell proteins to a variety of cis acting DNA sequences located within the LTR. Nef induced expression of fifteen transcription factors capable of positively regulating the viral LTR. Seven of these are inducibly expressed on T cell activation. T cell inducible transcription factors demonstrate a threshold level of activity that is concentration dependant (Fiering et al., 1990). The subversion of the T cell activation path to induce these genes is likely to represent an important mechanism facilitating increased virion production. Expression profiling allows formation of new hypotheses regarding the function of Nef. Induction of Tat interacting proteins suggests a role for Nef in the indirect regulation of the activity of other HIV accessory genes. Tat is expressed at relatively low levels in HIV infected cells and requires the presence of additional factors to effectively direct processive transcription. Upregulation of CDK9 is important as failure of transcriptional elongation occurs in its absence (Mancebo et al., 1997; Zhu et al., 1997). It is conceivable that among the other genes differentially regulated by Nef there may be some that have as yet un-described effects on the viral life cycle.

6.2 Specificity of The Nef gene expression profile

In the present study a characterisation of Nef mediated T cell signalling has been undertaken in terms of the resulting transcriptional response. Comparison of the

Nef expression profile with that obtained after T cell activation through CD3 has revealed strong identity but also a small number of important differences. The mode of Nef T cell activation may allow a replicative advantage to the virus over and above a conventional activation stimulus. It was notable that within upregulated transcripts particular to either the Nef or anti-CD3 activation profile there was a relative over-representation of genes that influence HIV replication. This begs the question of how a viral gene might achieve specificity in signalling. In order to produce gene expression changes akin to those observed after anti-CD3 triggering it is likely similar signal transduction cascades will be activated. How specific signal transduction pathways relay information to the nucleus and dictate specific gene expression is unclear. The idea that signal transduction processes convey detailed amounts of information has recently been debated with respect to receptor tyrosine kinases (RTK).

Upon binding to their cognate ligand receptor tyrosine kinases undergo dimerisation and autophosphorylation on specific tyrosine residues. These phosphotyrosines and their adjacent sequences recruit neighbouring molecules via SH2 domains causing their subsequent activation. The specific activation of one type of RTK therefore leads to the generation of a signalling cascade. It has been suggested each pathway would serve a distinct function but recent gene profiling studies have provided evidence against this.

Fambrough et al have documented gene expression profiles obtained after ligation of Platelet Derived Growth Factor (PDGF) RTK. The profiles showed that downstream pathways were redundant in terms of what genes they activate. NIH 3T3 cells were transfected with constructs encoding the hybrid receptors with an intracellular domain from the PDGFRβ and extracellular domain from the M-CSF receptor. The chimeras contained mutations in the SH2 binding sites in the PDGFRβ receptor. Simultaneous mutations in 5 SH2 binding sites had very little quantitative effect on immediate early gene induction in response to the heterologous ligand M-CSF. In addition mutations in any single one of these binding sites resulted in broad overlap in immediate early gene induction after M-CSF stimulation. Each site has been shown to bind PI-3K, Ras-GAP, SHP-2, and

PLCγ respectively. Thus the expression data suggest that signalling pathways may be functionally redundant and leave open the question of how specificity is achieved. Two caveats of this study are that saturating levels of ligand and overexpressed receptor were used in the experimental system under examination. These caveats can be avoided in animal models where ligands and receptors are expressed at physiological levels in correct temporal and tissue contexts. Studies in engineered mice have demonstrated that the SH2 docking sites in PDGFR cytoplasmic tail are not functionally redundant. Knockins of PDGFRβ containing a mutation in the PI-3K docking site show a defect in interstitial fluid homeostasis and double mutants in PI-3K and PLCγ SH2 binding sites show a defect in vascular fitness.

Other model genetic systems employed to address this question include *Drosophila* and *C.elegans*. *Drosophila* studies support the evidence obtained in mice that distinct molecules bound to distinct RTKs have specific functions. An example is a study of effects of mutations in drosophila DSHC (a homolog of mammalian SHC adaptor). *Dshc* mutants are defective in signalling from Torso and EGF RTKs but not from sevenless RTK demonstrating it functions within a receptor complex (Luschnig et al., 2000). Genetic analysis implied DSHC acts in parallel with other signalling proteins thought to be activated by Torso, however DSHC plays the central role; the redundancy with other signalling molecules here is partial. Therefore in vivo signalling pathways emerging from Torso RTK are not equivalent. A homozygous null *dshc/dshc* mutation is capable of negating the effects of a dominant constitutive Torso allele [Tor^{4021}] (Luschnig et al., 2000). If DSHC were truly redundant with other effectors of Torso RTK this result would not be obtained. In this experiment it was possible the activated Torso allele elevates signalling to an artificially high level. Nevertheless the study is supportive of a distinct role for individual RTKs.

Investigation of Ras-MAP kinase pathway in C.elegans has revealed mechanisms by which specificity is achieved in specification of cell types in distinct developmental pathways. In part appropriate responses are obtained by tissue specific expression of distinct transcription factors which are targets of

common downstream targets of the Ras-MAP kinase path. So when the Ras-MAP kinase path is the effector the cell type provides the necessary specificity. Here the Ras-MAP kinase path was activated by triggering the LET-23 EGF receptor. This receptor has 8 YxxL motifs in its cytoplasmic tail. Four of these sites can activate through the Ras-MAP kinase path via the SH2-SH3 adaptor protein SEM-5 (Lesa and Sternberg 1997).

In the gene profiling results presented little signalling moiety redundancy is demonstrated as in each of the four conditions described between 40-59% of the induced genes were removed. In addition the specific differences in induced genes between the Nef activated and anti-CD3 activated expression profiles suggest the mechanism by which Nef relays signals to the nucleus is capable of achieving a high degree of specificity.

6.3 Overlap between the various conditions

Treatment of Nef expressing cells with the calcineurin inhibitor CsA prevents upregulation of 49% of Nef induced transcripts. Comparison of the hallmark Nef profile with that produced in TCRζ and ZAP-70 deficient T cells reveals a key requirement for these in formation of the full Nef transcriptional response and place Nef as acting high in the T cell signalling path. Considerable overlap occurs between repressed genes after treatment with CsA or expression of Nef in TCRζ and ZAP-70 negative Jurkat. Of the 44% genes repressed in the Nef ZAP-70 expression profile, 89% of these remain non induced in the Nef TCRζ profile. Expression of Nef in TCRζ negative T cells generates 56% overlap between genes repressed after CsA treatment. This overlap is greater in ZAP-70 negative cells at 61%. In T cells exposure of an SH3 binding domain in the CD3 cytoplasmic tail after antigen receptor triggering facilitates Nck binding. Subsequently Src family tyrosine kinases are activated and phosphorylation of ITAM motifs in TCRζ cytoplasmic tail results in recruitment of ZAP-70. Our results provide genetic evidence for a requirement for TCRζ and ZAP-70 in generation of the Nef transcriptome. Elucidating how Nef usurps the activation

path above the level of TCRζ may provide information about the initial events occurring after antigen receptor triggering.

A potential limitation in interpretation of the observations of wide overlap between gene expression sets among the various conditions described is that complementation of the missing signalling molecules studied was not performed. It is possible that the mutant cell lines have undergone other adaptive changes and that the levels of Nef protein in each cell line under test were not identical. In addition the study was limited in usefulness as only 3528 genes were tested. However the evidence from gene profiling would suggest that multiple signalling components are involved in triggering an activation response.

6.4 Mechanism of T cell signalling triggered by Nef

The molecular interaction by which Nef generates gene expression changes is being determined. A proteomic analysis has revealed Nef expression is associated with an alteration of the protein complement of lipid rafts in T cells. Initial analysis has revealed Nef mediated assocation of signalling proteins and proteins implicated in actin polymerisation with rafts. In addition Nef appears associate with several proteins in lipid rafts the identity of which are currently being determined. Putative in vivo interactions are being confimed by co-immunoprecipitation, co-localisation and by knockdown of the identified protein using siRNAs. A series of siRNA expression vectors have been constructed to enable identification of transfected cells with a fluorescent reporter. Bi-directional vectors expressing *nef* and the respective siRNA oligonucleotide targeted to a gene of interest are transfected into Jurkat. Ability of Nef to induce actin polymerisation in the presence and absence of each siRNA will be assessed. This will provide a functional readout for the contribution of each Nef interactor in Nef mediated T cell signalling.

Nef possesses no intrinsic enzymatic ability and there is no known structural basis for its ability to associate with certain signalling proteins such as TCRζ and PAK kinase. It is likely Nef acts as an adaptor in the T cell signalling path. An

unusual feature of Nef structure is the presence of several flexible regions that is not common for a cytoplasmic protein. This could explain so many of the diverse reported interactions of Nef as the flexible regions can provide an extensive accessible surface. It is possible Nef may act as an alternative signalling scaffold enforcing proximity between divergent signalling modules that would not normally interact in T cells. The gene expression profile generated by Nef does not exactly match that of anti-CD3 triggering. The induction of genes positively regulating the viral life cycle exclusively by Nef is suggestive of a degree of specificity in the activation trigger. The exact means by which Nef subverts T cell signalling is being investigated. We are determining whether Nef acts as alternative signalling scaffold or simply replaces an exogenous activation signal. It has been postulated adaptors might facilitate signalling by acting as "meta-enzymes". They might bind, orient, align and allosterically regulate kinases. Alternatively they may simply spatially regulate and facilitate signal transmission through enforced proximity. Evidence supportive of a role for scaffolds in enforced proximity has recently been gathered in yeast using the scaffold protein Ste5. This scaffold is critical for mating pheromone responses in budding yeast. When Ste5 is present, pheromone causes Fus3 to be activated and mating occurs. When Ste5 is absent, there is no Fus3 activation and no mating response. Ste5 binds all three members of the Ste11-Ste7-Fus3 MAP kinase cascade, thereby allowing them to be activated by their upstream regulators. Evidence for alternative signalling scaffolds acting to promote adaptor function has come from a study by Park et al., 2003. Here a new signalling pathway was created by uniting two defective scaffolds. The experiment relied on the fact that four distinct MAK kinase cascades in *S.cerevisiae* use the same MAPKKK, Ste11, and yet each cascade receives signals from distinct upstream inputs and relays them to specific downstream effectors, with little interfering cross-talk. Park et al linked a Ste5 protein that could receive signals from Ste4, but relay them only as far as Ste11, to a Pbs2 protein defective for receiving osmotic signals from the upstream Sho1 protein. Expression of this defective scaffold caused mating pheromone to trigger typical hyperosmolar responses rather then mating responses.

The modules in which Nef acts are being compared to that occurring after T cell activation. We are immunoprecipitating various constituents of the Nef signalling module in the presence and absence of Nef and pre and post T cell activation. It will be established whether Nef acts as alternative connector of various signalling proteins producing a novel signalling path. By combining simple modular binding interactions in a combinatorial fashion scaffolds could generate high molecular complexity and impose specificity without requiring the evolution of signalling proteins themselves.

6.5 Role of the Nef expression profile in the viral life cycle

The Nef expression profile provides a molecular explanation for the observations of anti-CD3 hyper-reactivity of Nef transgenic thymocytes (Hanna et al., 1998) and Nef transfected T cells (Schrager and Marsh, 1999; Wang et al., 2000). This form of priming results in hyperinduction of T cell inducible genes after full exogenous activation and is likely to present a platform for heightened viral production. This study focused on the target genes of one Nef variant from HIV-1, SF2. SF2 is an example of a T tropic isolate of HIV commonly present in late stage disease. The mode of T cell activation and the expression profile generated by such a variant may be heightened compared to those from more indolent or M tropic counterparts. Cataloging the transcriptional signature of Nef variants from understanding of the contribution of this accessory gene in dictating viral post-integration fate.

Bibliography

Aboul-ela F, Karn J, Varani G. 1995. The structure of the human immunodeficiency virus type-1 TAR RNA reveals principles of RNA recognition by Tat protein. J. Mol. Biol. 253:313–32

Addo MM, Yu XG, Rathod A, Cohen D, Eldridge RL, Strick D, Johnston MN, Corcoran C, Wurcel AG, Fitzpatrick CA, Feeney ME, Rodriguez WR, Basgoz N, Draenert R, Stone DR, Brander C, Goulder PJ, Rosenberg ES, Altfeld M, Walker BD. 2003. Comprehensive epitope analysis of human immunodeficiency virus type 1 (HIV-1)-specific T-cell responses directed against the entire expressed HIV-1 genome demonstrate broadly directed responses, but no correlation to viral load. J Virol. 77, 2081-92.

Aiken C. (1998). Mechanistic independence of Nef and cyclophilin A enhancement of human immunodeficiency virus type 1 infectivity. Virology 248, 1, 139-47.

Aiken C, Konner J, Landau NR, Lenburg ME, Trono D. (1994). Nef induces CD4 endocytosis: requirement for a critical dileucine motif in the membrane-proximal CD4 cytoplasmic domain. Cell 76, 853-64.

Aiken C, Trono D. (1995). Nef stimulates human immunodeficiency virus type 1 proviral DNA synthesis. J Virol. 69, 5048-56.

Alonso A, Cujec TP, Peterlin BM. 1994. Effects of human chromosome 12 on interactions between Tat and TAR of human immunodeficiency virus type 1J. Virol. 68:6505–13

Ahrendt, S.A. et al.1999. Rapid p53 sequence analysis in primary lung cancer

using an oligonucleotide probe array. Proc. Natl Acad. Sci. USA 96, 7382–7387.

Ashe MP, Pearson LH, Proudfoot NJ. (1997). The HIV-1 5' LTR poly (A) site is inactivated by U1 snRNP interaction with the downstream major splice donor site. EMBO J. 16, 5752-63.

Bandres JC, Ratner L. (1994). Human immunodeficiency virus type 1 Nef protein down-regulates transcription factors NF-kappa B and AP-1 in human T cells in vitro after T-cell receptor stimulation. J Virol. 68, 3243-9.

Barre-Sinoussi F, Chermann JC, Rey F, Nugeyre MT, Chamaret S, Gruest J, Dauguet C, Axler-Blin C, Vezinet-Brun F, Rouzioux C, Rozenbaum W, Montagnier L. 1983. Isolation of a T-lymphotropic retrovirus from a patient at risk for acquired immune deficiency syndrome (AIDS).Science. 220, 868-71.

Baskaran R, Escobar SR, Wang JY. (1999). Nuclear c-Abl is a COOH-terminal repeated domain (CTD)-tyrosine (CTD)-tyrosine kinase-specific for the mammalian RNA polymerase II: possible role in transcription elongation. Cell Growth Differ. 10, 387-96.

Bassuk AG, Anandappa RT, Leiden JM. (1997). Physical interactions between Ets and NF-kappaB/NFAT proteins play an important role in their cooperative activation of the human immunodeficiency virus enhancer in T cells. J Virol. 5, 3563-73.

Baur AS, Sawai ET, Dazin P, Fantl WJ, Cheng-Mayer C, Peterlin BM. (1994). HIV-1 Nef leads to inhibition or activation of T cells depending on its intracellular localization. Immunity 5, 373-84.

Baur AS, Sass G, Laffert B, Willbold D, Cheng-Mayer C, Peterlin BM. (1997). The N-terminus of Nef from HIV-1/SIV associates with a protein complex containing Lck and a serine kinase. Immunity 6, 283-91.

Bayer P, Kraft M, Ejchart A, Westendorp M, Frank R, Rosch P. 1995. Structural studies of HIV-1 Tat protein.J. Mol. Biol. 247:529–35

Berkowitz RD, Ohagen A, Hoglund S, Goff SP. 1995. Retroviral nucleocapsid domains mediate the specific recognition of genomic viral RNAs by chimeric Gag polyproteins during RNA packaging in vivo. J. Virol. 69:6445–56

Bleul CC, Farzan M, Choe H, Parolin C, Clark-Lewis I, et al. 1996. The lymphocyte chemoattractant SDF-1 is a ligand for LESTR/fusin and blocks HIV-1 entry. Nature 382:829–33

Bleul CC, Wu L, Hoxie JA, Springer TA, Mackay CR. 1997. The HIV coreceptors CXCR4 and CCR5 are differentially expressed and regulated on human T lymphocytes. Proc Natl Acad Sci U S A. 94, 1925-30.

Bogerd HP, Fridell RA, Madore S, Cullen BR. 1995. Identification of a novel cellular cofactor for the Rev/Rex class of retroviral regulatory proteins.Cell 82:485–94

Bosselut R, Lim F, Romond PC, Frampton J, Brady J, Ghysdael J. (1992). Myb protein binds to multiple sites in the human T cell lymphotropic virus type 1 long terminal repeat and transactivates LTR-mediated expression. Virology 186, 764-9.

Bour S, Schubert U, Strebel K. 1995. The envelope glycoprotein of human immunodeficiency virus type 2 enhances viral particle release: a Vpu-like factor? J. Virol. 69:1510–20

Briggs SD, Sharkey M, Stevenson M, Smithgall TE. (1997). SH3-mediated Hck tyrosine kinase activation and fibroblast transformation by the Nef protein of HIV-1. J Biol Chem. 272, 17899-902.

Broussard SR, Staprans SI, White R, Whitehead EM, Feinberg MB, Allan JS. Simian immunodeficiency virus replicates to high levels in naturally infected African green monkeys without inducing immunologic or neurologic disease. J Virol. 75, 2262-75.

Bukrinskaya AG, Ghorpade A, Heinzinger NK, Smithgall TE, Lewis RE, Steverson M. 1996. Phosphorylation-dependent human immunodeficiency virus type 1 infection and nuclear targeting of viral DNA.Proc. Natl. Acad. Sci. USA 93:367–71

Cai M, Zheng R, Caffrey M, Craigie R, Clore GM, Gronenborn AM. 1997. Solution structure of the N-terminal zinc binding domain of HIV-1 integrase. Nat. Struct. Biol. 4:567–77

Cameron CE, Ghosh M, Le Grice SF, Benkovic SJ. 1997. Mutations in HIV reverse transcriptase which alter RNase H activity and decrease strand transfer efficiency are suppressed by HIV nucleocapsid protein. Proc. Natl. Acad. Sci. USA 94:6700–5

Camaur D, Trono D. 1996. Characterization of human immunodeficiency virus type 1 Vif particle incorporation. J. Virol. 70:6106–11

Carteau S, Batson SC, Poljak L, Mous-cadet J-F, deRocquigny H, et al. 1997. Human immunodeficiency virus type 1 nucleocapsid protein specifically stimulates Mg2+-dependent DNA integration in vitro. J. Virol. 71:6225–29

Cassan M, Delaunay N, Vaquero C, Rousset JP. 1994. Translational frameshifting at the gag-pol junction of human immunodeficiency virus type 1 is not increased in infected T-lymphoid cells. J. Virol. 68:1501–8

Center DM, Kornfeld H, Ryan TC, Cruikshank WW. (2000). Interleukin 16: implications for CD4 functions and HIV-1 progression. Immunol Today 21, 273-80.

Chan DC, Chutkowski CT, Kim PS. 1998. Evidence that a prominent cavity in the coiled coil of HIV type 1 gp41 is an attractive drug target. Proc Natl Acad Sci USA. 95,15613-15617.

Chan DC, Fass D, Berger JM, Kim PS. 1997. Core structure of gp41 from the HIV envelope glycoprotein. Cell 89:263–73

Charreau B, Coupel S, Boulday G, Soulillou JP. (2000). Cyclosporin inhibits class II major histocompatibility antigen presentation by xenogeneic endothelial cells to human T lymphocytes by altering expression of the class II transcriptional activator gene. Transplantation 70, 354-61.

Checroune F, Yao XJ, Gottlinger HG, Bergeron D, Cohen EA. 1995. Incorporation of Vpr into human immunodeficiency virus type 1: role of conserved regions within the P6 domain of Pr55gag.J. AIDS Hum. Retrovirol. 10:1–7

Chepenik LG, Tretiakova AP, Krachmarov CP, Johnson EM, Khalili K. (1998). The single-stranded DNA binding protein, Pur-alpha, binds HIV-1 TAR RNA and activates HIV-1 transcription. Gene 210, 37-44.

Choe H, Farzan M, Sun Y, Sullivan N, Rollins B, et al. 1996. The beta-chemokine receptors CCR3 and CCR5 facilitate infection by primary HIV-1 isolatesCell 85:1135–48

Chowers MY, Pandori MW, Spina CA, Richman DD, Guatelli JC. (1995). The growth advantage conferred by HIV-1 nef is determined at the level of viral DNA formation and is independent of CD4 downregulation. Virology 1, 451-7.

Chuvpilo S, Zimmer M, Kerstan A, Glockner J, Avots A, Escher C, Fischer C, Inashkina I, Jankevics E,Berberich-Siebelt F, Schmitt E, Serfling E. (1999). Alternative polyadenylation events contribute to the induction of NF-ATc in effector T cells. Immunity 10, 261-9.

Clapham PR. 1997. Trends Cell Biol. 7:264–68

Clapham PR, Weiss RA. 1997. Immunodeficiency viruses. Spoilt for choice of co-receptors Nature 388:230–31

Clever JL, Parslow TG. 1997. Mutant human immunodeficiency virus type 1 genomes with defects in RNA dimerization or encapsidation. J Virol. 71, 3407-14.

Cocchi F, DeVico AL, Garzino-Demo A, Cara A, Gallo RC, Lusso P. 1996. The V3 domain of the HIV-1 gp120 envelope glycoprotein is critical for chemokine-mediated blockade of infection. Nat. Med. 2:1244–47

Colantuoni, C., Henry, G., Zeger, S. & Pevsner, J. 2002. Local mean normalization of microarray element signal intensities across an array surface: quality control and correction of spatially systematic artifacts. Biotechniques 32, 1316–1320.

Collette Y, Dutartre H, Benziane A, Ramos-Morales, Benarous R, Harris M, Olive D. (1996). Physical and functional interaction of Nef with Lck. HIV-1 Nef-induced T-cell signaling defects. J Biol Chem. 271, 6333-41.

Collins KL, Chen BK, Kalams SA, Walker BD, Baltimore D. (1998). HIV-1 Nef protein protects infected primary cells against killing by cytotoxic T lymphocytes. Nature 39, 397-401.

Condra JH, Schleif WA, Blahy OM, Gabryelski LJ, Graham DJ, et al. 1995. In vivo emergence of HIV-1 variants resistant to multiple protease inhibitors. Nature 374:569–71

Connor RI, Sheridan KE, Ceradini D, Choe S, Landau NR. 1997. Change in coreceptor use coreceptor use correlates with disease progression in HIV-1--infected individuals. J Exp Med. 185, 621-8.

Coull JJ, Romerio F, Sun JM, Volker JL, Galvin KM, Davie JR, Shi Y, Hansen U, Margolis DM. (2000). The human factors YY1 and LSF repress the human immunodeficiency virus type 1 long terminal repeat via recruitment of histone deacetylase 1. J Virol. 74, 6790-9.

Cujec TP, Cho H, Maldonado E, Meyer J, Reinberg D, Peterlin BM. 1997. The HIV transactivator TAT binds to the CDK-activating kinase and activates the phosphorylation of the carboxy-terminal domain of RNA polymerase II.Mol. Cell. Biol. 17:1817–23

Dalgleish AG, Beverley PC, Clapham PR, Crawford DH, Greaves MF, Weiss RA.1984. The CD4 (T4) antigen is an essential component of the receptor for the AIDS retrovirus. Nature. 312, 763-7.

Daniel MD, Letvin NL, King NW, Kannagi M, Sehgal PK, Hunt RD, Kanki PJ, Essex M, Desrosiers RC. 1985. Isolation of T-cell tropic HTLV-III-like retrovirus from macaques. Science. 228, 1201-4.

Dasgupta P, Saikumar P, Reddy CD, Reddy EP. (1990). Myb protein binds to human immunodeficiency virus 1 long terminal repeat (LTR) sequences and transactivates LTR-mediated transcription. Proc Natl Acad Sci U S A 87, 20, 8090-4.

Deacon, N.J., Tsykin, A., Solomon, A., Smith, K., Ludford-Menting,M., Hooker,D.J., McPhee, D.A., Greenway, A.L., Ellett, A., Chatfield, C., Lawson, V.A., Crowe, S.,Maerz,A., Sonza, S., Learmont, J.,Sullivan, J.S.,Cunningham, A., Dwyer, D.,Dowton, D.,Mills, J. (1995). Genomic structure of an attenuated quasispecies of HIV-1 from a blood transfusion donor and recipients.Science 270, 988-991.

Delwart EL, Mosialos G, Gilmore T. 1990.Retroviral envelope glycoproteins contain a leucine zipper-like repeat. AIDS Res Hum Retroviruses. 6, 703-706.

Deng H, Liu R, Ellmeier W, Choe S, Unutmaz D, Burkhart M, Di Marzio P, Marmon S, Sutton RE, Hill CM, Davis CB, Peiper SC, Schall TJ, Littman DR, Landau NR. 1996. Identification of a major co-receptor for primary isolates of HIV-1. Nature. 381, 661-6.

Di Noia J, Neuberger MS. 2002. Altering the pathway of immunoglobulin hypermutation by inhibiting uracil-DNA glycosylase. Nature 419, 43-8.

Dorfman T, Gottlinger HG. 1996. The human immunodeficiency virus type 1 capsid p2 domain confers sensitivity to the cyclophilin-binding drug SDZ NIM 811.J. Virol. 70:5751–57

Douek DC, Brenchley JM, Betts MR, Ambrozak DR, Hill BJ, Okamoto Y, Casazza JP, Kuruppu J, Kunstman K, Wolinsky S, Grossman Z, Dybul M, Oxenius A, Price DA, Connors M, Koup RA. 2002. HIV preferentially infects HIV-specific CD4+ T cells. Nature. 417, 95-8.

Dragic T, Litwin V, Allaway GP, Martin SR, Huang Y, Nagashima KA, Cayanan C, Maddon PJ, Koup RA, Moore JP, Paxton WA. 1996. HIV-1 entry into CD4+ cells is mediated by the chemokine receptor CC-CKR-5.Nature. 381, 667-73.

Dunn BM, Gustchina A, Wlodawer A, Kay J. 1994. Subsite preferences of retroviral proteinases. Methods Enzymol. 241:254–78

Dyda F, Hickman AB, Jenkins TM, En-gelman A, Craigie R, Davies DR. 1994. Crystal structure of the catalytic domain of HIV-1 integrase: similarity to other polynucleotidyl transferases. Science 266:1981–86

Ebbets-Reed D, Scarlata S, Carter CA. 1996. The major homology region of the HIV-1 gag precursor influences membrane affinity. Biochemistry 35:14268–75

Eijkelenboom AP, Lutzke RA, Boelens R, Plasterk RH, Kaptein R, Hard K. 1995. The DNA-binding domain of HIV-1 integrase has an SH3-like fold. Nat. Struct. Biol. 2:807–10

Eisen MB, Spellman PT, Brown PO, Botstein D. (1998). Cluster analysis and display of genome-wide expression patterns. Proc Natl Acad Sci U S A 95, 14863-8.

Emerman M. 1996. HIV-1, Vpr and the cell cycle.Curr. Biol. 6:1096–1103

Esnouf R, Ren J, Ross C, Jones Y, Stammers D, Stuart D. 1995. Mechanism of inhibition of HIV-1 reverse transcriptase by non-nucleoside inhibitors. Nat. Struct. Biol. 2:303–8

Fackler OT, Lu X, Frost JA, Geyer M, Jiang B, Luo W, Abo A, Alberts AS, Peterlin BM. (2000). p21-activated kinase 1 plays a critical role in cellular activation by Nef. Mol Cell Biol. 20, 2619-27.

Fackler OT, Luo W, Geyer M, Alberts AS, Peterlin BM. (1999). Activation of Vav by Nef induces cytoskeletal rearrangements and downstream effector functions. Mol Cell 3, 729-39.

Fambrough D, McClure K, Kazlauskas A, Lander ES. (1999). Diverse signaling pathways activated by growth factor receptors induce broadly overlapping, rather than independent, sets of genes. Cell 97, 727-41.

Farnet CM, Bushman FD. 1997. HIV-1 cDNA integration: requirement of HMG I(Y) protein for function of preintegration complexes in vitro. Cell 88:483–92

Feng Y, Broder CC, Kennedy PE, Berger HEVA1 entry cofactor: functional cDNA cloning of a seven-transmembrane, G protein-coupled receptor. Science. 272, 872-7.

Fernandez-Miguel G, Alarcon B, Iglesias A, Bluethmann H, Alvarez-Mon M, Sanz E, de la Hera A. 1999. Multivalent structure of an alphabetaT cell receptor. Proc Natl Acad Sci U S A. 96, 1547-52.

Fischer U, Huber J, Boelens WC, Mattaj W, Luhrmann R. 1995. The HIV-1 Rev activation domain is a nuclear export signal that accesses an export pathway used by specific cellular RNAs. Cell 82:475–83.

Flory E, Hoffmeyer A, Smola U, Rapp UR, Bruder JT. (1996). Raf-1 kinase targets GA-binding protein in transcriptional regulation of the human immunodeficiency virus type 1 promoter. J Virol. 70, 2260-8.

Fouchier RAM, Meyer BE, Simon JHM, Fischer U, Malim MH. 1997. HIV-1 infection of non-dividing cells: evidence that the amino-terminal basic region of the viral matrix protein is important for Gag processing but not for post-entry nuclear importEMBO J. 16:4531–39

Fouchier RA, Simon JH, Jaffe AB, Malim MH. 1996. Human immunodeficiency virus type 1 Vif does not influence expression or virion incorporation of gag-, pol-, and env-encoded proteins. J. Virol. 70:8263–69

Freed EO, Englund G, Maldarelli F, Martin MA. 1997. Phosphorylation of residue 131 of HIV-1 matrix is not required for macrophage infection. Cell 88:171–73

Freed EO, Englund G, Martin MA. 1995. Role of the basic domain of human immunodeficiency virus type 1 matrix in macrophage infection. J. Virol. 69:3949–54.

Fritz CC, Zapp ML, Green MR. 1995. A human nucleoporin-like protein that specifically interacts with HIV Rev. Nature 376:530–33.

Fujita K, Omura S, Silver J. 1997. Rapid degradation of CD4 in cells expressing human immunodeficiency virus type 1 Env and Vpu is blocked by proteasome inhibitors.J. Gen. Virol. 78:619–25

Furuta RA, Wild CT, Weng Y, Weiss CD. 1998. Capture of an early fusion-active conformation of HIV-1 gp41. Nat Struct Biol. 5, 276-279.

Gallay P, Swingler S, Song JP, Bushman F, Trono D. 1995. HIV nuclear import is governed by the phosphotyrosine-mediated binding of matrix to the core domain of integrase. Cell 83:569–76

Gamble TR, Vajdos FF, Yoo S, Worthy-lake DK, Houseweart M, et al. 1996.

Crystal structure of human cyclophilin A bound to the amino-terminal domain of HIV-1 capsid. Cell 87:1285–94

Garcia-Martinez LF, Mavankal G, Neveu JM, Lane WS, Ivanov D, Gaynor RB. 1997. Purification of a Tat-associated kinase reveals a TFIIH complex that modulates HIV-1 transcription. EMBO J. 16:2836–50

Gao F, Yue L, White AT, Pappas PG, Barchue J, Hanson AP, Greene BM, Sharp PM, Shaw GM, Hahn BH. 1992. Human infection by genetically diverse SIVSM-related HIV-2 in west Africa. Nature. 358, 495-9.

Gao F, Bailes E, Robertson DL, Chen Y, Rodenburg CM, Michael SF, Cummins LB, Arthur LO, Peeters M, Shaw GM, Sharp PM, Hahn BH. 1999. Origin of HIV-1 in the chimpanzee Pan troglodytes troglodytes. Nature. 397, 436-41.

Gatignol A, Duarte M, Daviet L, Chang YN, Jeang KT. (1996). Sequential steps in Tat trans-activation of HIV-1 mediated through cellular DNA, RNA, and protein binding factors. Gene Expr. 5, 217-28.

Gil D, Schamel WW, Montoya M, Sanchez-Madrid F, Alarcon B. 2002. Recruitment of Nck by CD3 epsilon reveals a ligand-induced conformational change essential for T cell receptor signaling and synapse formation. Cell. 109, 901-12.

Gossen M, Freundlieb S, Bender G, Muller G, Hillen W, Bujard H. (1995). Transcriptional activation by tetracyclines in mammalian cells. Science 26, 1766-9.

Greenberg ME, Iafrate AJ, Skowronski J. (1998). The SH3 domain-binding surface and an acidic motif in HIV-1 Nef regulate trafficking of class I MHC complexes. EMBO J. 17, 2777-89.

Greenway A, Azad A, Mills J, McPhee D. (1996). Human immunodeficiency virus type 1 Nef binds directly to Lck and mitogen-activated protein kinase, inhibiting kinase activity. J Virol. 70, 6701-8.

Grzesiek S, Bax A, Hu JS, Kaufman J, Palmer I, Stahl SJ, Tjandra N, Wingfield PT. 1997. Refined solution structure and backbone dynamics of HIV-1 Nef.Protein Sci. 6:1248–63

Gulizia RJ, Collman RG, Levy JA, Trono D, Mosier DE. (1997). Deletion of nef slows but does not prevent CD4-positive T-cell depletion in human immunodeficiency virus type 1-infected human-PBL-SCID mice. J Virol. 71, 4161-4.

Halgren RG, Fielden MR, Fong CJ, Zacharewski TR. 2001. Assessment of clone identity and sequence fidelity for 1189 IMAGE cDNA clones. Nucleic Acids Res. 29, 582-8.

Hanna Z, Kay DG, Rebai N, Guimond A, Jothy S, Jolicoeur P. (1998). Nef harbours a major determinant of pathogenicity for an AIDS-like disease induced by HIV-1 in transgenic mice. Cell 95,163-175.

D. Paul Harkin, James M. Bean, David Miklos, Young-Han Song, Vivi B. Truong, Christoph Englert, Fred C. Christians, Leif W. Ellisen, Shyamala Maheswaran, Jonathan D. Oliner, and Daniel A. Haber.1999. Induction of *GADD45* and JNK/SAPK-Dependent Apoptosis following Inducible Expression of *BRCA1* Cell 97, 575.

Harris RS, Petersen-Mahrt SK, Neuberger MS. 2002. RNA Editing Enzyme APOBEC1 and Some of Its Homologs Can Act as DNA Mutators. Mol Cell. 10, 1247-53.

Hernandez LD, Hoffman LR, Wolfsberg TG, White JM. 1996. Virus-cell and cell-cell fusion. Annu. Rev. Cell Dev. Biol. 12:627–61

Herrmann CH, Carroll RG, Wei P, Jones KA, Rice AP. (1998). Tat-associated kinase, TAK, activity is regulated by distinct mechanisms in peripheral blood lymphocytes and promonocytic cell lines. J Virol. 72, 9881-8.

Hill CP, Worthylake D, Bancroft DP, Christensen AM, Sundquist WI. 1996. Crystal structures of the trimeric human immunodeficiency virus type 1 matrix protein: implications for membrane association and assembly. Proc. Natl. Acad. Sci. USA 93:3099–104

Hodge DR, Dunn KJ, Pei GK, Chakrabarty MK, Heidecker G, Lautenberger JA, Samuel KP. (1998). Binding of c-Raf1 kinase to a conserved acidic sequence within the carboxyl-terminal region of the HIV-1 Nef protein. J Biol Chem. 19, 273 15727-33.

Hope TJ. 1997. Viral RNA export. Chem. Biol. 4:335–44

Howe AY, Jung JU, Desrosiers RC. (1998). Zeta chain of the T-cell receptor interacts with nef of simian immunodeficiency virus and human immunodeficiency virus type 2. (1998). J Virol. 72, 9827-34.

Hsiou Y, Ding J, Das K, Clark AD Jr, Hughes SH, Arnold E. 1996. Structure of unliganded HIV-1 reverse transcriptase at 2.7 A resolution: implications of conformational changes for polymerization and inhibition mechanisms. Structure 4:853–60

Huang M, Orenstein JM, Martin MA, Freed EO. 1995. p6 Gag is required for particle production from full-length human immunodeficiency virus type 1

molecular clones expressing protease. J. Virol. 69:6810–18

Huang Y, Khorchid A, Wang J, Parniak MA, Darlix JL, et al. 1997. Effect of mutations in the nucleocapsid protein (NCp7) upon Pr160(gag-pol) and tRNA(Lys) incorporation into human immunodeficiency virus type 1. J. Virol. 71:4378–84

Iafrate AJ, Bronson S, Skowronski J.(1997). Separable functions of Nef disrupt two aspects of T cell receptor machinery: CD4 expression and CD3 signaling. EMBO J. 16, 673-84.

Iyer, V.R. et al. 1999. The transcriptional program in the response of human fibroblasts to serum. Science 283, 83–87.

Jacobo-Molina A, Ding JP, Nanni RG, Clark AD Jr, Lu XD, et al. 1993. Crystal structure of human immunodeficiency virus type 1 reverse transcriptase complexed with double-stranded DNA at 3.0 A resolution shows bent DNA. Proc. Natl. Acad. Sci. USA 90:6320–24

Jeeninga RE, Hoogenkamp M, Armand-Ugon M, de Baar M, Verhoef K, Berkhout B. (2000). Functional differences between the long terminal repeat transcriptional promoters of human immunodeficiency virus type 1 subtypes A through G.J Virol. 74, 3740-51.

Jiang S, Lin K, Lu M. 1998. A conformation-specific monoclonal antibody reacting with fusion-active gp41 from the human immunodeficiency virus type 1 envelope glycoprotein. J Virol 72, 10213-10217.

Jiang S, Lin K, Strick N, Neurath AR. 1993. HIV-1 inhibition by a peptide. Nature 365, 113.

Jones KA, Peterlin BM. 1994. Control of RNA initiation and elongation at the HIV-1 promoter.Annu. Rev. Biochem. 63:717–43

Kane LP, Lin J, Weiss A. 2000. Signal transduction by the TCR for antigen. Curr Opin Immunol. 12, 242-9. Review.

Katz RA, Skalka AM. 1994. The retroviral enzymes. Annu. Rev. Biochem. 63:133–73

Kaplan AH, Manchester M, Swanstrom R. 1994. Conditional human immunodeficiency virus type 1 protease mutants show no role for the viral protease early in virus replication. J. Virol. 68:6782–86

Karsten, S.L., Van Deerlin, V.M., Sabatti, C., Gill, L.H. & Geschwind, D.H.2002. An evaluation of tyramide signal amplification and archived fixed and frozen tissue in microarray gene expression analysis. Nucleic Acids Res. 30, E4 (2002).

Kaur A, Grant RM, Means RE, McClure H, Feinberg M, Johnson RP. 1998. Diverse host responses and outcomes following simian immunodeficiency virus SIVmac239 infection in sooty mangabeys and rhesus macaques. J Virol. 72, 9597-611.

Kekow J, Wachsman W, McCutchan JA, Cronin M, Carson DA, Lotz M. (1990). Transforming growth factor beta and noncytopathic mechanisms of immunodeficiency in human immunodeficiency virus infection. Proc Natl Acad Sci U S A 87, 8321-5.

Kerkau T, Bacik I, Bennink JR, Yewdell JW, Hunig T, et al. 1997. The human immunodeficiency virus type 1 (HIV-1) Vpu protein interferes with an early step in the biosynthesis of major histocompatibility complex (MHC) class I molecules. J. Exp. Med. 185:1295–305

Kestler HW, Ringler DJ, Mori K, Panicali DL, Seghal PK, Daniel MD, Desrosiers RC. (1991). Importance of the nef gene for maintainance of high viral loads and for development of AIDS. Cell 65, 651-662.

Kilby JM. 1999. Therapeutic potential of blocking HIV entry into cells: focus on membrane fusion inhibitors. Expert Opin Investig Drugs. 8,1157-1170.

Kilby JM, Hopkins S, Venetta TM, et al. 1998. Potent suppression of HIV-1 replication in humans by T-20, a peptide inhibitor of gp41-mediated virus entry. Nat Med. 4, 1302-1307.

Kim JB, Yamaguchi Y, Wada T, Handa H, Sharp PA. (1999). Tat-SF1 protein associates with RAP30 and human SPT5 proteins. Mol Cell Biol. 19, 5960-8.

Kinoshita S, Su L, Amano M, Timmerman LA, Kaneshima H, Nolan GP. (1997). The T cell activation factor NF-ATc positively regulates HIV-1 replication and gene expression in T cells. Immunity 6, 235-44.

Kjems J, Sharp PA. 1993. The basic domain of Rev from human immunodeficiency virus type 1 specifically blocks the entry of U4/U6.U5 small nuclear ribonucleoprotein in spliceosome assembly. J. Virol. 67, 4769-76.

Klatzmann D, Champagne E, Chamaret S, Gruest J, Guetard D, Hercend T, Gluckman JC, Montagnier L. 1984. T-lymphocyte T4 molecule behaves as the receptor for human retrovirus LAV. Nature. 312, 767-8.

Klotman ME, Kim S, Buchbinder A, DeRossi A, Baltimore D, Wong-Staal F. (1991). Kinetics of expression of multiply spliced RNA in early human immunodeficiency virus type 1 infection of lymphocytes and monocytes. Proc Natl Acad Sci U S A 88, 5011-5.

Kohlstaedt LA, Wang J, Friedman JM, Rice PA, Steitz TA. 1992. Crystal structure at 3.5 A resolution of HIV-1 reverse transcriptase complexed with an inhibitor. Science 256:1783–90

Kondo E, Gottlinger HG. 1996. A conserved LXXLF sequence is the major determinant in p6gag required for the incorporation of human immunodeficiency virus type 1 Vpr.J. Virol. 70:159–64

Korber B, Gaschen B, Yusim K, Thakallapally R, Kesmir C, Detours V. 2001. Evolutionary and immunological implications of contemporary HIV-1 variation. Br Med Bull. 58, 19-42.

Korber B, Muldoon M, Theiler J, Gao F, Gupta R, Lapedes A, Hahn BH, Wolinsky S, Bhattacharya T. 2000. Timing the ancestor of the HIV-1 pandemic strains. Science. 288, 1789-96.

Krawczyk C, Bachmaier K, Sasaki T, Jones GR, Snapper BS, Bouchard D, Kozieradzki I, Ohashi SP, Alt WF, Penninger MJ. (2000). Cbl-b is a negative regulator of receptor clustering and raft aggregation in T cells. Immunity 13, 463-73.

Kwong PD, Wyatt R, Robinson J, Sweet RW, Sodroski J, Hendrickson WA. 1998. Structure of an HIV gp120 envelope glycoprotein in complex with the CD4 receptor and a neutralizing human antibody. Nature 393, 648-59.

Lama J, Mangasarian A, Trono D. (1999). Cell-surface expression of CD4 reduces HIV-1 infectivity by blocking Env incorporation in a Nef- and Vpu-inhibitable manner. Curr Biol. 9, 622-3.

Lamb RA, Pinto LH. 1997. Do Vpu and Vpr of human immunodeficiency virus

type 1 and NB of influenza B virus have ion channel activities in the viral life cycles? Virology 229:1–11

Laughrea M, Jette L, Mak J, Kleiman L, Liang C, Wainberg MA. 1997. Mutations in the kissing-loop hairpin of human immunodeficiency virus type 1 reduce viral infectivity as well as genomic RNA packaging and dimerization.J. Virol. 71:3397–406

Lesa GM, Sternberg PW. 1997. Positive and negative tissue-specific signaling by a nematode epidermal growth factor receptor. Mol Biol Cell. 5, 779-93.

Levy JA, Hoffman AD, Kramer SM, Landis JA, Shimabukuro JM, Oshiro LS. 1984. Isolation of lymphocytopathic retroviruses from San Francisco patients with AIDS. Science. 225, 840-2.

Li JM, Shen X, Hu PP, Wang XF. (1998). Transforming growth factor beta stimulates the human immunodeficiency virus 1 enhancer and requires NF-kappaB activity. Mol Cell Biol. 18, 110-21.

Lindblad-Toh, K. et al. Loss-of-heterozygosity analysis of small-cell lung carcinomas using single-nucleotide polymorphism arrays. 2000. Nature Biotechnol. 18, 1001–1005.

Lindblad-Toh, K. et al. 2000. Large-scale discovery and genotyping of single-nucleotide polymorphisms in the mouse. Nature Genet. 24, 381–386.

Liu HM, Wu XY, Newman M, Shaw GM, Hahn BH, Kappes JC. 1995. The Vif protein of human and simian immunodeficiency viruses is packaged into virions and associates with viral core structures. J. Virol. 69:7630–38

Lo, A.W. et al. 2001. A novel chromatin immunoprecipitation and array (CIA) analysis identifies a 460-kb CENP-A-binding neocentromere DNA. Genome Res.

11, 448–457.

Lock, C. et al. 2002. Gene-microarray analysis of multiple sclerosis lesions yields new targets validated in autoimmune encephalomyelitis. Nature Med. 8, 500–508.

Lu YL, Bennett RP, Wills JW, Gorelick R, Ratner L. 1995. A leucine triplet repeat sequence (LXX)4 in p6gag is important for Vpr incorporation into human immunodeficiency virus type 1 particles. J. Virol. 69:6873–79

Lodi PJ, Ernst JA, Kuszewski J, Hickman AB, Engelman A, et al. 1995. Solution structure of the DNA binding domain of HIV-1 integrase.Biochemistry 34:9826–33

Lock C, Hermans G, Pedotti R, Brendolan A, Schadt E, Garren H, Langer-Gould A, Strober S, Cannella B, Allard J, Klonowski P, Austin A, Lad N, Kaminski N, Galli SJ, Oksenberg JR, Raine CS, Heller R, Steinman L. 2002. Gene-microarray analysis of multiple sclerosis lesions yields new targets validated in autoimmune encephalomyelitis. Nat Med. 8, 500-8.

Loetscher P, Uguccioni M, Bordoli L, Baggiolini M, Moser B, Chizzolini C, Dayer JM. 1998. CCR5 is characteristic of Th1 lymphocytes. Nature. 391, 344-5.

Lu XB, Heimer J, Rekosh D, Hammarskjold ML. 1990. U1 small nuclear RNA plays a direct role in the formation of a rev-regulated human immunodeficiency virus env mRNA that remains unspliced. Proc. Natl. Acad. Sci. USA 87:7598–602

Luban J.1996. Absconding with the chaperone: essential cyclophilin-Gag interaction in HIV-1 virions.Cell 87:1157–59

Luo W, Peterlin BM, (1997). Activation of the T-cell receptor signaling pathway by nef from an aggressive strain of simian immunodeficiency virus. J Virol. 71, 9531-9537.

Luban J, Bossolt KL, Franke EK, Kalpana GV, Goff S. 1993. Human immunodeficiency virus type 1 Gag protein binds to cyclophilins A and B.Cell. 73, 1067-78.

Luschnig S, Krauss J, Bohmann K, Desjeux I, Nusslein-Volhard C. 2000. The Drosophila SHC adaptor protein is required for signaling by a subset of receptor tyrosine kinases. Mol Cell. 5, 231-41.

Luukkonen BG, Fenyo EM, Schwartz S. 1995. Overexpression of human immunodeficiency virus type 1 protease increases intracellular cleavage of Gag and reduces virus infectivity. Virology 206:854–65

Mammano F, Ohagen A, Hoglund S, Gottlinger HG. 1994. Role of the major homology region of human immunodeficiency virus type 1 in virion morphogenesis. J. Virol. 68:4927–36

Mancebo HS, Lee G, Flygare J, Tomassini J, Luu P, Zhu Y, Peng J, Blau C, Hazuda D, Price D, Flores O. (1997). P-TEFb kinase is required for HIV Tat transcriptional activation in vivo and in vitro. Genes Dev. 11, 2633-44.

Mansky LM. 1996. The mutation rate of human immunodeficiency virus type 1 is influenced by the vpr gene. Virology 222:391–400

Marciniak RA, Sharp PA. (1991). HIV-1 Tat protein promotes formation of more-processive elongation complexes. EMBO J. 10, 4189-96.

McPhee F, Good AC, Kuntz ID, Craik CS. 1996. Mutational anatomy of an HIV-1 protease variant conferring cross-resistance to protease inhibitors in clinical

trials. Compensatory modulations of binding and activity. Proc. Natl. Acad. Sci. USA 93:11466–81

Mercier G, Galien R, Emanoil-Ravier R. (1994). Differential effects of ras and jun family members on complex retrovirus promoter activities. Res Virol. 145, 361-7.

Meyer BE, Malim MH. 1994. The HIV-1 Rev trans-activator shuttles between the nucleus and the cytoplasm. Genes Dev.8:1538–47.

Miki, R. et al. 2001. Delineating developmental and metabolic pathways in vivo by expression profiling using the RIKEN set of 18,816 full-length enriched mouse cDNA arrays. Proc. Natl Acad. Sci. USA 98, 2199–2204.

Miller MD, Bor YC, Bushman F. 1995. Target-sequence preferences of HIV-1 integration complexes in vitro. Curr. Biol. 5:1047–56

Miller MD, Bushman FD. 1995. HIV integration. Ini1 for integration? Curr. Biol. 5:368–70

Miller MD, Farnet CM, Bushman FD. 1997. Human immunodeficiency virus type 1 preintegration complexes: studies of organization and composition.J. Virol. 71:5382–90

Miller MD, Wang B, Bushman FD. 1995. Human immunodeficiency virus type 1 preintegration complexes containing discontinuous plus strands are competent to integrate in vitro. J. Virol. 69:3938–44

Miller MD, Warmerdam MT, Gaston I, Greene WC, Feinberg, MB. (1994). The human immunodeficiency virus-1 nef gene product: a positive factor for viral replication in primary lymphocytes and macrophages. J. Exp. Med. 179, 101-113.

Moarefi I, LaFevre-Bernt M, Sicheri F, Huse M, Lee CH, et al. 1997. Activation of the Src-family tyrosine kinase Hck by SH3 domain displacement. Nature 385:650–53

Modiano JF, Domenico J, Szepesi A, Lucas JJ, Gelfand EW, Nomura N, Zhao MJ, Nagase T, Maekawa T, Ishizaki R, Tabata S, Ishii S. 1994. Differential requirements for interleukin-2 distinguish the expression and activity of the cyclin-dependent kinases Cdk4 and Cdk2 in human T cells. J Biol Chem. 269, 32972-8.

Moore CB, John M, James IR, Christiansen FT, Witt CS, Mallal SA. 2002. Evidence of HIV-1 adaptation to HLA-restricted immune responses at a population level. Science. 296, 1439-43.

Morellet N, Jullian N, De Rocquigny H, Maigret B, Darlix JL, Roques BP. 1992. Determination of the structure of the nucleocapsid protein NCp7 from the human immunodeficiency virus type 1 by 1H NMR. EMBO J. 11:3059–65

Muramatsu M, Kinoshita K, Fagarasan S, Yamada S, Shinkai Y, Honjo T. 2000. Class switch recombination and hypermutation require activation-induced cytidine deaminase (AID), a potential RNA editing enzyme. Cell 102, 553-63.

HIV-EP2, a new member of the gene family encoding the human immunodeficiency virus type 1 enhancer-binding protein. (1991). Comparison with HIV-EP1/PRDII-BF1/MBP-1. J Biol Chem. 266, 8590-4.

Nagaoka H, Muramatsu M, Yamamura N, Kinoshita K, Honjo T. 2002. Activation-induced deaminase (AID)-directed hypermutation in the immunoglobulin Smu region: implication of AID involvement in a common step of class switch recombination and somatic hypermutation. J Exp Med. 195, 529-34.

Oberlin E, Amara A, Bachelerie F, Bessia C, Virelizier JL, et al. 1996. The CXC chemokine SDF-1 is the ligand for LESTR/fusin and prevents infection by T-cell-line-adapted HIV-1. Nature 382:833–35

O'Keeffe B, Fong Y, Chen D, Zhou S, Zhou Q. (2000). Requirement for a kinase-specific chaperone pathway in the production of a Cdk9/cyclin T1 heterodimer responsible for P-TEFb-mediated tat stimulation of HIV-1 transcription. J Biol Chem. 275, 279-87.

Oravecz T, Pall M, Norcross MA. 1996. Beta-chemokine inhibition of monocytotropic HIV-1 infection. Interference with a postbinding fusion step. J. Immunol. 157:1329–32

Oude Essink BB, Das AT, Berkhout B. 1996. HIV-1 reverse transcriptase discriminates against non-self tRNA primers J. Mol. Biol. 264:243–54

Paillart JC, Skripkin E, Ehresmann B, Ehresmann C, Marquet R. 1996. A loop-loop "kissing" complex is the essential part of the dimer linkage of genomic HIV-1 RNA.Proc.Natl. Acad. Sci. USA 93:5572–77

Parada CA, Roeder RG. 1996. Enhanced processivity of RNA polymerase II triggered by Tat-induced phosphorylation of its carboxy-terminal domain. Nature. 384, 375-8.

Park SH, Zarrinpar A, Lim WA. 2003. Rewiring MAP kinase pathways using alternative scaffold assembly mechanisms. Science. 299, 1061-4.

Peliska JA, Benkovic SJ. 1992. Mechanism of DNA strand transfer reactions catalyzed by HIV-1 reverse transcriptase. Science 258:1112–18

Petersen-Mahrt SK, Harris RS, Neuberger MS. 2002. AID mutates E. coli suggesting a DNA deamination mechanism for antibody diversification. Nature. 418, 99-103

Perelson AS, Essunger P, Ho DD. 1997. Dynamics of HIV-1 and CD4+ lymphocytes in vivo. AIDS. 11 Suppl A:S17-24.

Poignard P, Sabbe R, Picchio GR, Wang M, Gulizia RJ, Katinger H, Parren PW, Mosier DE, Burton DR. 1999. Neutralizing antibodies have limited effects on the control of established HIV-1 infection in vivo. Immunity. 10, 431-8.

Poon DT, Wu J, Aldovini A. 1996. Charged amino acid residues of human immunodeficiency virus type 1 nucleocapsid p7 protein involved in RNA packaging and infectivity. J. Virol. 70:6607–16

Popovic M, Sarngadharan MG, Read E, Gallo RC. 1984. Detection, isolation, and continuous production of cytopathic retroviruses (HTLV-III) from patients with AIDS and pre-AIDS. Science. 224, 497-500.

Price DA, Goulder PJ, Klenerman P, Sewell AK, Easterbrook PJ, Troop M, Bangham CR, Phillips RE. 1997. Positive selection of HIV-1 cytotoxic T lymphocyte escape variants during primary infection. Proc Natl Acad Sci U S A. 94, 1890-5.

Puglisi JD, Tan RY, Calnan BJ, Frankel AD, Williamson JR. 1992. Conformation of the TAR RNA-arginine complex by NMR spectroscopy.Science 257, 76–80.

Rabbi MF, Saifuddin M, Gu DS, Kagnoff MF, Roebuck KA. (1997). U5 region of the human immunodeficiency virus type 1 long terminal repeat contains TRE-like cAMP-responsive elements that bind both AP-1 and CREB/ATF proteins. Virology 233, 235-45.

Relogio A, Schwager C, Richter A, Ansorge W, Valcarcel J. 2002. Optimization of oligonucleotide-based DNA microarrays. Nucleic Acids Res. 30, e51.

Ren JS, Esnouf R, Garman E, Somers D, Ross C, et al. 1995. Crystals of HIV-1 reverse transcriptase diffracting to 2.2 A resolution. Nat. Struct. Biol. 2:293–302

Renkema GH, Manninen A, Mann DA, Harris M, Saksela K. (1999). Identification of the nef associated kinase as p21 activated kinase 2. Current Biology 9, 1407-1410.

Rey-Cuille MA, Berthier JL, Bomsel-Demontoy MC, Chaduc Y, Montagnier L, 1998. Hovanessian AG, Chakrabarti LA. Simian immunodeficiency virus replicates to high levels in sooty mangabeys without inducing disease.
J Virol. 72, 3872-86.

Rice P, Craigie R, Davies DR. 1996. Retroviral integrases and their cousins. Curr. Opin. Struct. Biol. 6:76–83

Ridky T, Leis J. 1995. Development of drug resistance to HIV-1 protease inhibitors. J. Biol. Chem. 270:29621–23

Rimsky LT, Shugars DC, Matthews TJ. 1998. Determinants of human immunodeficiency virus type 1 resistance to gp41-derived inhibitory peptides. J Virol. 72, 986-993.

Roberts JD, Bebenek K, Kunkel TA. 1988. The accuracy of reverse transcriptase from HIV-1. Science. 242, 1171-3.

Rodgers DW, Gamblin SJ, Harris BA, Ray S, Culp JS, et al. 1995. The structure of unliganded reverse transcriptase from the human immunodeficiency virus type

1 Proc. Natl. Acad. Sci. USA 92:1222–26

Rosen CA, Sodroski JG, Campbell K, Haseltine WA. (1986). Construction of recombinant murine retroviruses that express the human T-cell leukemia virus type II and human T-cell lymphotropic virus type III trans activator genes. J Virol. 57, 379-84.

Ross TM, Oran AE, Cullen BR. (1999). Inhibition of HIV-1 progeny virion release by cell-surface CD4 is relieved by expression of the viral Nef protein. Curr Biol. 9, 613-21.

Rouillard JM, Herbert CJ, Zuker M. 2002. OligoArray: genome-scale oligonucleotide design for microarrays. Bioinformatics. 18, 486-7.

Saifuddin M, Roebuck KA, Chang Ch, Ting JP, Spear GT. (2000) Cutting edge: activation of HIV-1 transcription by the MHC class II transactivator. J Immunol. 164, 3941-5.

Saksela K, Cheng G, Baltimore D. (1995). Proline rich (PXXP) motifs in HIV-1 Nef bind to SH3 domains in a subset of src kinases and are required for the enhanced growth of nef + viruses but not for downregulation of CD4. EMBO J. 14, 484-491.

Sanchez-Pescador R, Power MD, Barr PJ, Steimer KS, Stempien MM, Brown-Shimer SL, Gee WW, Renard A, Randolph A, Levy JA, et al (1985). Nucleotide sequence and expression of an AIDS-associated retrovirus (ARV-2). Science. 227, 484-92.

Saphire EO, Parren PW, Pantophlet R, Zwick MB, Morris GM, Rudd PM, Dwek RA, Stanfield RL, Burton DR, Wilson IA2001. Crystal structure of a neutralizing human IGG against HIV-1: a template for vaccine design. Science. 293, 1155-9.

Schock HB, Garsky VM, Kuo LC. 1996. Mutational anatomy of an HIV-1 protease variant conferring cross-resistance to protease inhibitors in clinical trials. Compensatory modulations of binding and activity. J. Biol. Chem. 271:31957–63

Schrager JA, Marsh JW. (1999). HIV-1 Nef increases T cell activation in a stimulus-dependent manner. Proc Natl Acad Sci U S A. 96, 8167-72.

Schwartz O, Marechal V, Le Gall S, Lemonnier F, Heard JM. (1996). Endocytosis of major histocompatibility complex class I molecules is induced by the HIV-1 Nef protein. Nat Med. 2, 338-42.

Senger K, Merika M, Agalioti T, Yie J, Escalante CR, Chen G, Aggarwal AK, Thanos D. (2000). Gene Repression by Coactivator Repulsion. Mol Cell 6, 931-937.

Shannon, M.F. & Rao, S. 2002. Transcription. Of chips and ChIPs. Science 296, 666–669.

Sieweke MH, Tekotte H, Jarosch U, Graf T. (1998). Cooperative interaction of ets-1 with USF-1 required for HIV-1 enhancer activity in T cells. EMBO J. 17, 1728-39.

Simon JH, Malim MH. 1996. The human immunodeficiency virus type 1 Vif protein modulates the postpenetration stability of viral nucleoprotein complexes. J. Virol. 70:5297–305

Smith BL, Krushelnycky BW, Mochly-Rosen D, Berg P. (1996). The HIV nef protein associates with protein kinase C theta. J Biol Chem. 271, 16753-7.

Spiegel H, Herbst H, Niedobitek G, Foss HD, 1992. Follicular dendritic cells are a major reservoir for human immunodeficiency virus type 1 in lymphoid tissues facilitating infection of CD4+ T-helper cells. Am J Pathol. 140, 15-22.

Srinivasakumar N, Hammarskjold ML, Rekosh D. 1995. Characterization of deletion mutations in the capsid region of human immunodeficiency virus type 1 that affect particle formation and Gag-Pol precursor incorporation. J. Virol. 69:6106–14

Summers MF, Henderson LE, Chance MR, Bess JW Jr, South TL, et al. 1992. Nucleocapsid zinc fingers detected in retroviruses: EXAFS studies of intact viruses and the solution-state structure of the nucleocapsid protein from HIV-1. Protein Sci. 1:563–74

Swingler S, Mann A, Jacque J, Brichacek B, Sasseville VG, Williams K, Lackner AA, Janoff EN, Wang R, Fisher D, Stevenson M. (1999). HIV-1 Nef mediates lymphocyte chemotaxis and activation by infected macrophages. Nat Med. 9, 997-103.

Tantillo C, Ding J, Jacobo-Molina A, Nanni RG, Boyer PL, et al. 1994. Locations of anti-AIDS drug binding sites and resistance mutations in the three-dimensional structure of HIV-1 reverse transcriptase. Implications for mechanisms of drug inhibition and resistance. J. Mol. Biol. 243:369–87

Tiganos E, Yao XJ, Friborg J, Daniel N, Cohen EA. 1997. Putative alpha-helical structures in the human immunodeficiency virus type 1 Vpu protein and CD4 are involved in binding and degradation of the CD4 molecule. J. Virol. 71:4452–60

Ullman KS, Powers MA, Forbes DJ. 1997. Nuclear export receptors: from importin to exportin. Cell 90:967–70

Valentin A, Lu W, Rosati M, Schneider R, Albert J, Karlsson A, Pavlakis GN. (1998) Dual effect of interleukin 4 on HIV-1 expression: implications for viral phenotypic switch and disease progression. Proc Natl Acad Sci U S A 95, 8886-91.

Van Gelder, R.N. et al. 1990. Amplified RNA synthesized from limited quantities of heterogeneous cDNA. Proc. Natl Acad. Sci. USA 87, 1663–1667.

Van Lint C, Amella CA, Emiliani S, John M, Jie T, Verdin E. (1997). Transcription factor binding sites downstream of the human immunodeficiency virus type 1 transcription start site are important for virus infectivity.J Virol. 71, 6113-27.

Wainberg Z, Oliveira M, Lerner S, Tao Y, Brenner BG. (1997). Modulation of stress protein (hsp27 and hsp70) expression in CD4+ lymphocytic cells following acute infection with human immunodeficiency virus type-1. Virology. 233, 364-73.

Wang JK, Kiyokawa E, Verdin E, Trono D. (2000). The Nef protein of HIV-1 associates with rafts and primes T cells for activation. Proc Natl Acad Sci U S A. 97, 394-9.

Wang J, Smerdon SJ, Jager J, Kohlstaedt LA, Rice PA, et al. 1994. Structural basis of asymmetry in the human immunodeficiency virus type 1 reverse transcriptase heterodimer. Proc. Natl. Acad. Sci. USA 91:7242–46

Weissenhorn W, Dessen A, Harrison SC, Skehel JJ, Wiley DC. 1997. Atomic structure of the ectodomain from HIV-1 gp41. Nature 387:426–30

Wild CT, Shugars DC, Greenwell TK, et al. 1994. Peptides corresponding to a predictive alpha-helical domain of human immunodeficiency virus type 1 gp41 are potent inhibitors of virus infection. Proc Natl Acad Sci USA. 91, 9770-9774.

Wilson JD, Ogg GS, Allen RL, Davis C, Shaunak S, Downie J, Dyer W, Workman C, Sullivan S, McMichael AJ, Rowland-Jones SL. 2000. Direct visualization of HIV-1-specific cytotoxic T lymphocytes during primary infection. AIDS. 14, 225-33.

Wlodawer A, Erickson JW. 1993. Structure-based inhibitors of HIV-1 protease. Annu. Rev. Biochem. 62:543–85

Xu XN, Laffert B, Screaton GR, Kraft M, Wolf D, Kolanus W, Mongkolsapay J, McMichael AJ, Baur AS. (1999). Induction of Fas ligand expression by HIV involves the interaction of Nef with the T cell receptor zeta chain. J Exp Med. 189, 1489-96.

Xu XN, Screaton GR, Gotch FM, Dong T, Tan R, Almond N, Walker B, Stebbings R, Kent K, Nagata S, Stott JE, McMichael AJ. (1997). Evasion of cytotoxic T lymphocyte (CTL) responses by nef-dependent induction of Fas ligand (CD95L) expression on simian immunodeficiency virus-infected cells. J Exp Med. 186, 7-16.

Yang, Y.H. et al. 2002. Normalization for cDNA microarray data: a robust composite method addressing single and multiple slide systematic variation. Nucleic Acids Res. 30, e15.

Yang X, Gold MO, Tang DN, Lewis DE, Aguilar-Cordova E, Rice AP, Herrmann CH. (1997).TAK, an HIV Tat-associated kinase, is a member of the cyclin-dependent family of protein kinases and is induced by activation of peripheral blood lymphocytes and differentiation of promonocytic cell lines. Proc Natl Acad Sci U S A 94, 12331-6.

Yang X, Goncalves J, Gabuzda D. 1996. Phosphorylation of Vif and its role in HIV-1 replication J. Biol. Chem. 271:10121–29

Yang XZ, Herrmann CH, Rice AP. 1996. The human immunodeficiency virus Tat proteins specifically associate with TAK in vivo and require the carboxyl-terminal domain of RNA polymerase II for function. J. Virol. 70:4576–84

Zhou M, Halanski MA, Radonovich MF, Kashanchi F, Peng J, Price DH, Brady JN. 2000. Tat modifies the activity of CDK9 to phosphorylate serine 5 of the RNA polymerase II carboxyl-terminal domain during human immunodeficiency virus type 1 transcription. Mol Cell Biol. 20, 5077-86.

Zhou QA, Sharp PA. 1996. Tat-SF1: cofactor for stimulation of transcriptional elongation by HIV-1 Tat. Science 274:605–10

Zhu Y, Pe'ery T, Peng J, Ramanathan Y, Marshall N, Marshall T, Amendt B, Mathews MB, Price DH. (1997). Transcription elongation factor P-TEFb is required for HIV-1 tat transactivation in vitro. Genes Dev.11, 2622-32.

Ziauddin, J. & Sabatini, D.M. 2001. Microarrays of cells expressing defined cDNAs. Nature 411, 107–110 (2001).

Zybarth G, Carter C. Domains upstream of the protease (PR) in human immunodeficiency virus type 1 Gag-Pol influence PR autoprocessing.1995. J. Virol. 69:3878–84

APPENDIX

Table 1. Genes upregulated by Nef over 24 hours

Encoded Protein	GenBank Accession Number	Cluster classification	Previous association with HIV	Previous association with T cell activation
LUCA2	U09577	B		
ARK1	D84212	A		
SAS	U01160	B		
LUCA 15	U23946	A		
ETS-1	J04101	A	yes	yes
Tyro3	D17517	B		
CDC2	X05360	A	yes	yes
CDK9	AF045161	A	yes	yes
BRCA2	U43746	B		
ezrin	X51521	A	yes	
BSP1	U57456	B		
Jun-D	X56681	A	yes	
c-abl	M14752; M14753; M14754	A	yes	
CDK4	M14505	A	yes	
P16-INK4	L27211	B		
P78 putative serine /threonine kinase	M80359	A		
ABL2	M35296	A		
CDK6	X66365	B		yes
DP2	U18422	A		
Mdm2	Z12020; M92424	A		
Prohibitin	S85655; U17179	B		
c-fos	K00650	B	yes	yes
Ets related protein tel	U11732	B		
shb	X75342	A		
TIAM 1	U16296	B		
geminin	AF067855	A		
c-myb	M15024	B	yes	
ERBB-3	M29366; M34309	B		
Diaphanous 1	AF051782	A		
PTEN	U92436	A		
ERBB4	L07868	A		
CBL-B	U26710	A		
Bub1	AF053305	A		

NEK2	U11050	A		
CLK1	L29222	B		
CDC25A	M81933	A		
CCK4	U33635 + U40271	A		
ILK	U40282	A		
JNK1	L26318	A		
GLYT-1	S70609	B		
Tnk1	U43408	A		
HEK	M83941	B		
NET	M65105	B		
PLC beta 3	Z16411	B		
Sodium/potassium -transporting ATPase	D00099	B		
Alpha-fetoprotein	V01514	B		
IL6 receptor beta subunit	M57230	A		
Rapamycin target protein	L34075	A		
BAD	U66879	A		
RalGDSB	U14417	A		
CD47	Y00815 + X69398	A		
Adenylate cyclase type 1	L05500	A		
Protein phosphatase 2B	D21878	A		
ATM	U33841	B		
Serine/threonine phosphatase 2B	L14778	B		
IRF1	X14454	A		
Ras p21 protein activator	M23379	B		
Protein phosphatase 2C alpha	S87759	B		
DNA ligase III	X84740	B		
DNA-repair protein complementing XP-C cells	D21089	A		
XRCC1	M36089	B		
5-HT-3	D49394	A		
DP1	L23959	B		
YL-1	D43642	A		
IRF2	X15949	A		
BTF2p44	Z30094	A		
NF-κB p100;p52	X61498	A	yes	yes
GABP-alpha	D13316	B	yes	
AREB6	D15050	B		
BARD1	U76638	B		
SMBP-2	L14754	B		
GLRB	U33267	B		
JNKK2	AF022805	B		
NFATc	U08015	B	yes	yes
NERF2	U43188	B		
Cadherin 5	X79981; X59796	B		
CD106	M30257	A		
HOXB7	M16937	B		
Stem cell protein	M29038	B		
PUR alpha	M96684	B	yes	
EBI3	L08187	B		
MIP 1-beta	J04130	A	yes	yes

Puramycin sensitive aminopeptidase	Y07701	A		
Heat shock related 70kd protein 2	L26336	B	yes	
Glutathione peroxidase	Y00483; M21304	B		
70Kd HSP 1	M11717	B	yes	
TGF beta	X02812; J05114	B	yes	yes
MIP 1-alpha	M23452	B	yes	yes
Estrogen sulfotransferase	U08098	B		
Insulin protease	M21188	A		
IL4 precursor	M13982	B	yes	yes
TALLA-1	D10653	A		
IRF2	X15949	A		
PEBP2aC1	Z35278	A		
HOX-D4	X04706; X17360	A		
HEX	L16499	A		
HIV-EP2	M60119	B	yes	yes
PAX-4	AB008913	B		
SOX-3	X71135	B		
MIZ-1 protein	Y09723	A		
GLI3	M57609	B		
CIITA	X74301	A	yes	yes
Insulin gene enhancer protein ISL1	U07559	B		
centrin	U03270	A		yes
TRANCE	AF013171	A		
Granzyme H precursor	M36118	A		
Defensin alpha 1	M21130	B		
NUP-98	U41815	A	yes	
Ectropic viral integration site protein 2A	M55267	B		
CYP1A1 and CYP1A2	K03191 + M55053; M38504	A		
HUT2	X96969	B		
Lumican precursor	U18728	A		
Annexin IV	X05908	B		
Beta'-COP	X70476	B	yes	
SNAP-25	L19761	A		
RAB-GDI beta	D13988	B		
Man9-alpha-mannosidase	X74837	A		
Phosphofructokinase 1	D25328	A		yes
Aldehyde dehydrogenase E3 isozyme	U34252	B		
PGAM	J04173	B		
Apo-D	J02611	B		
Ferritin heavy chain	M97164	B		yes
ALDH2	Y00109	A		
Ubiquitously expressed nuclear receptor	U07132	A		
Pregnane X receptor	AF061056	A		
TGF-beta 4	U81523	A		yes
GDF8	AF019627	B		
Natriuretic peptide precursor B	M25296	B		

STAM	U43899	A		yes
MAPKAP kinase 2	U12779	B		yes
GRK4	L03718	B		
PP2AB	M64929	A		
Dual-specificty protein phosphatase HVH2	U21108	A		yes
Regulator of G protein signaling 6	L40394	A		
Regulator of G protein signaling 16	U70426	A		
PLC-delta-1	U09117	B		
14-3-3 protein theta	X56468	A		
EBV-induced G-protein coupled receptor 2	L08177	A		
BD73	L31785	A		
Dynamin-1	L07807	A		
MTBT1	J03778	B		
Transmembrane protein 1	U19252	B		
mucin	AF007194	A		yes
BST-2	D28137	A		
SMCY	U52191	A		
Tetraspan net-5	AF089749	A		
RNA pol II (RPB3)	J05448	A	yes	
RNA pol II (RPB2)	X63563	A	yes	
RNA pol II (RPB6)	Z27113	B	yes	
Zinc finger protein 76	M91592	A		
NF-E2 related factor 2	S74017	A		
Zinc finger protein 133	U09366	A		
Zinc finger protein 140	U09368	A		
Zinc finger protein 139	U09848	A		
Zinc finger protein C2H2-25	U38904	B		
Zinc finger protein 33A	X68687	A		
TAFII-28	X83928	B	yes	
Zinc finger HSAL2	X98834	A		
Zinc finger (fragment)	L32164	A		
E74-like factor 5	AF049703	A		
H-2K binding factor-2	D14041	A		
EFP	D21205	A		
HKF-1	D76444	B		
Transcription factor SL1	L39059	B		
TAT-SF1	U76992	A	yes	
HPX-42B	AF068006	A		
TFECL	D43945	A		
RNA polymerase II terminaton factor	AF073771	B		
RNPL	U28686	A		
HS-II-T1	D50495	A		
mitochondrial RNA helicase	AF042169	B		
HA0659	X79538	B		
CSTF 64KD subunit	M85085	A		
TRA-2 alpha	U53209	A		
U1 SNRNP A protein	X06347	A	yes	
HU-antigen C	L26405	B		
RBP56	X98893	A		
TOB4 protein	D64109	B		
CUL-4A	U58090	B		
TP beta and TP gamma	U09087	B		

DEL-1	U70312	A		
Microfibril associated glycoprotein 4	L38486	B		
P22 phagocyte B-cytochrome	M21186	B		
Inositol 1,4,5-triphopshate receptor type 1	L38019	A		yes
NK-tumour recognition protein	L04288	B		
FKBP25	M90309	B		
SCCE	L33404	A		
bomapin	U35459	B		
mRNA encoding C4.4 like	AJ223603	A		
Polycomb 2 homolog	AF013956	B		
HSP86	X15183	B		
Yolk sac permease like 3	AF058317	A		
HVDAC2	L06328	B		
HPCN1	M55513	B		
EC3.6.1.36	U02076	B		
Chloride channel protein	AF026004	B		
Two pore domain potassium channel	AF084830	A		
Ca-activated potassium channel	U02632	B		
Type 2 INSP3 receptor	D26350	A		yes
Procollagen I N-proteinase	AJ003125	A		
Collagen alpha chain 5	M31115	A		
SKD1 homolog	AF038960	A		
Syntaxin 6	AJ002078	B		
adipophilin	X97324	B		
NASP	M97856	A		
TOM1-like protein	AJ010071	A		
SRP14	X73459	A		
Synaptotagmin VII fragment	AF038535	B		
Angiogenin precursor	M11567	A		
Sia alpha2,3galbeta1,4glcnAcalpha 2,8-sialtransferase	AF004668	B		
ATPase protein 9	D13119	B		
Malate dehydrogenase	D55654	B		
Alpha-ETF	J04058	B		
EC 1.9.3.1	J04823	B		
COX VIIA-M	M83186	B		
Complex I-B17	AF035840	A		
CTP:phosphocholine cytidylyltransferase b.	AF052510	A		
TPST1	AF038009	B		
alpha-ketoglutarate dehydrogenase complex dihydoelipoylsuccinyltransferase.	S72422	B		
MTHFS	L38928	B		
cyclohydrolase mitochondrial precursor	X16396	B		
Delta-ala synthetase	X56352	B		
Prostatic acid phosphatase	X56352	B		
PAM	M24902	B		
glutaminyl cyclase	M37721	B		
spermine synthase	X71125	B		
Nitrilase homolog 1	Z49099	B		
Carbonate dehydratase VI	AF069987	B		

ASF	M57892	B		
Acyl-CoA desaturase	X97868	A		
CYP-60	L77701	A		
Ribophorin II	U37220	A		
H-SCO1	Y00282	A		
40s ribosomal protein S17	M13932	A		
TAR binding protein	M60801	A	yes	
60S ribosomal protein L35A	M15661	A		
EF-1-beta	X60656	B		
P43	L38995	B		
EIF-2-beta	M29536	A		
Statin S1	X70940	B		
ARGRS	S80343	A		
Proline tRNA ligase	X54326	A		
TGF beta receptor assoc protein	AF022795	A		
DHP1	U62647	A		
ZAP-1	X99699	A		
Splicing factor	L10911	B		
U2 small ribonucleoprotein auxilllary factor	D49676	B		
SNRPN	D49676	A		
Nuclear riboprotein R	AF000364	A		
RNASEP protein P30	U77665	B		
DIM1P homolog	AF023612	B		
H2A.X.	X14850	B		
Heat stable enterotoxin receptor	L30117	B		
BMP 11	AF100907	B		
SNT-2	AF036718	B		
Serine/threonine kinase	AB015982	A		
CAMK	L07044	A		
SEC14-like protein	U79284	B		
AS-like phosphodiesterase	Y08134	A		
TRAP delta	X90583	B		
Myosin RLC	J02854	B		
MLC3F	M20643	B		
Dysferlin	AF075575	B		
PDZ domain containing protein	AF012281	B		
TRIP10	L40379	B		
MP78	U29366	B		
Ubiquitin conjugating enzyme E2 G1	D78514	B		
Ubiquitin conjugating enzyme E2	AF031141	B		
P26S4	AF031141	B		
Gastrointestinal peptide	AF048700	B		
Motor protein	D21092	B		
plectin	U53204	A		
P60 katanin	AF056022	B		
MUTS homolog 4	U89293	B		
TSPAN-2	AF054839	B		
MYLE	AF108145	A		
SPOP	AJ000644	A		
DGS-A	L77571	B		
Pinch protein	U09284	B		
POM-ZP3	U10099	B		

KIAA0209	D86964	B		

Table 2. Genes induced after CD28 activation over 24 hours

Encoded Protein	GenBank Accession Number
LUCA2	U09577
SAS	U01160
ETS-1	J04101
tyro3	D17517
CDC2	X05360
CDK9	L25676
BRCA2	U43746
BSP1	U57456
CDK4	M14505
p16-INK4	L27211
p78 putative serine/threonine-protein kinase	M80359
mdm2 protein	Z12020; M92424
c-myb	M15024
ERBB-3	M29366; M34309
PTEN	U92436
bub1	AF053305
Golgi 4-transmembrane spanning transporter; MTP	D14696
leukocyte surface CD47 antigen precursor	Y00815 + X69398
adenosine A1 receptor	S56143
ATM	U33841
serine/threonine protein phosphatase 2B catalytic subunit alpha isoform	L14778
ras p21 protein activator	M23379
DNA ligase III	X84740
BTF2p44	Z30094
ADA2-like protein	AF069732
SMBP-2	L14754
GADD45 gamma	AF078078
cadherin 5	X79981; X59796
CD106	M30257
PUR alpha	M96684
PAI1; PLANH1	X04429; M14083
TGF-beta	X02812; J05114
estrogen sulfotransferase	U08098
CD53	M37033
CD21 antigen	M26004

HEX	L16499
HOMEOBOX PROTEIN EMX1	X68879
PAX-4	AB008913
MIZ-1 PROTEIN	Y09723
interleukin enhancer binding factor 2 (ILF2)	U58197
INSULIN GENE ENHANCER PROTEIN ISL1	U07559
centrin	U03270
TRANCE	AF013171
DEFENSIN, ALPHA 1	M21130
lymphocyte cytosolic protein 1	M22300
ETV1	U17163
nucleoporin NUP98	U41815
ectropic viral integration site 2A	M55267
CYP1A1 + CYP1A2	K03191 + M55053; M38504
(CYP51) + CYP51P1 +CYP51P2	U23942 + U36926 + U40053
sodium- & chloride-dependent creatine transporter 1 (CT1)	L31409
Golgi antigen gcp372	D25542
annexin IV	X05908
beta'-COP	X70476
SNAP-25	L19761
ras-related protein RAB-11A	X53143
RAB GDI beta	D13988
glycerol kinase	L13943
ALDH7 or ALDH4	U34252
apo-D	J02611
nonsecretory ribonuclease precursor	M28129
ubiquitously expressed nuclear receptor	U07132
pregnane X receptor (PXR)	AF061056
GDF8	AF019627
natriuretic peptide precursor B	M25296
tyrosine-protein kinase syk	L28824
MAPKAP kinase 2	U12779
dual-specificity protein phosphatase HVH2	U21108
dynamin-1	L07807
transmembrane protein 1	U19252
BST-2	D28137
SMCY.	U52191
TETRASPAN NET-5.	AF089749
CD39 ANTIGEN-LIKE 1	U91510
RNA POLYMERASE II (RPB7).	U20659
BN51 PROTEIN.	M17754

ZINC FINGER PROTEIN 76.	M91592
ZINC FINGER PROTEIN 140.	U09368
ZINC FINGER PROTEIN 137.	U09414
ZINC FINGER PROTEIN 139 (FRAGMENT).	U09848
ZINC FINGER PROTEIN C2H2-25	U38904
ZINC FINGER PROTEIN CLONE 647 (FRAGMENT).	X16282
TRANSCRIPTION INITIATION FACTOR TFIID 28 KD SUBUNIT	X83928
HKF-1.	D76444
TRANSCRIPTION FACTOR SL1.	L39059
HPX42B.	AF068006
NASCENT POLYPEPTIDE ASSOCIATED COMPLEX ALPHA SUBUNIT.	X80909
HA0659	X79538
TRA-2 ALPHA	U53209
HU-ANTIGEN C	L26405
CUL-4A	U58090
TP BETA AND TP GAMMA	U09087
FKBP25	M90309
BOMAPIN	U35459
POLYCOMB 2 HOMOLOG.	AF013956
EC 3.6.1.36	U02076
CALCIUM-ACTIVATED POTASSIUM CHANNEL	U02632
TYPE 2 INSP3 RECEPTOR	D26350
PROCOLLAGEN I N-PROTEINASE	AJ003125
COLLAGEN ALPHA 5 CHAIN PRECURSOR.	M31115
ADIPOPHILIN	X97324
TOM1-LIKE PROTEIN.	AJ010071
Homo sapiens putative 13 S Golgi transport complex 90kD subunit	AF058718
ANGIOGENIN PRECURSOR	M11567
SIA ALPHA2,3GALBETA1,4GLCNACALPHA 2,8-SIALYLTRANSFERASE	AF004668
MALATE DEHYDROGENASE	D55654
UBIQUINOL-CYTOCHROME C REDUCTASE COMPLEX CORE PROTEIN 2 PRECURSOR	J04973
COX VIIA-M	M83186
ATPASE PROTEIN 9	U09813
COMPLEX I-B17	AF035840
CTP:PHOSPHOCHOLINE CYTIDYLYLTRANSFERASE B.	AF052510
TPST1	AF038009
ALPHA-KETOGLUTARATE DEHYDROGENASE COMPLEX DIHYDROLIPOYL SUCCINYLTRANSFERASE.	S72422
URO-D	M14016
DELTA-1-PYRROLINE-5-CARBOXYLATE DEHYDROGENASE PRECURSOR	U24266
MTHFS	L38928

BIFUNCTIONAL METHYLENETETRAHYDROFOLATE DEHYDROGENASE/CYCLOHYDROLASE, MITOCHONDRIAL PRECURSOR	X16396
PROSTATIC ACID PHOSPHATASE	M24902
PAM	M37721
SPERMINE SYNTHASE	Z49099
ASF	X97868
H-SCO1.	AF026852
ELONGATION FACTOR 1-BETA (EF-1-BETA).	X60656
MULTIFUNCTIONAL AMINOACYL-TRNA SYNTHETASE [INCLUDES: GLUTAMYL-TRNA SYNTHETASE (EC 6.1.1.17) (GLUTAMATE--TRNA LIGASE); PROLYL-TRNA SYNTHETASE (EC 6.1.1.15) (PROLINE--TRNA LIGASE)].	X54326
XIAP ASSOCIATED FACTOR-1 (ZAP-1).	X99699
SPLICING FACTOR.	L10911
DIM1P HOMOLOG.	AF023612
HISTONE H2A.X.	X14850
heat-stable enterotoxin receptor	L30117
LDL RECEPTOR RELATED PROTEIN 105.	AB009462
CAMK	L07044
MLC3F	M20643
PDZ DOMAIN CONTAINING-PROTEIN.	AF012281
UBIQUITIN CARBOXYL-TERMINAL HYDROLASE 12	U44839
UBIQUITIN-CONJUGATING ENZYME E2 G1	D78514
26S PROTEASOME SUBUNIT S5B .	S79862
P26S4	L02426
GASTROINTESTINAL PEPTIDE.	AF048700
MOTOR PROTEIN.	D21092
P60 KATANIN.	AF056022
MUTS HOMOLOG 4.	U89293
RAD51-INTERACTING PROTEIN	AF006259

Table 3. Genes induced after CD3/CD28 stimulation of Nef expressing cells over 24 hours

Encoded Protein	GenBank Accession Number
LUCA2	U09577
ARK1	D84212
SAS	U01160
LUCA 15	U23946
ETS-1	J04101
Tyro3	D17517
CDC2	X05360
CDK9	AF045161
BRCA2	U43746
BSP1	U57456
ezrin	X51521
BSP1	U57456
Jun-D	X56681
c-abl	M14752; M14753; M14754
CDK4	M14505
P16-INK4	L27211
P78 putative serine /threonine kinase	M80359
ABL2	M35296
CDK6	X66365
DP2	U18422
Mdm2	Z12020; M92424
Prohibitin	S85655; U17179
c-fos	K00650
Ets related protein tel	U11732
shb	X75342
TIAM 1	U16296
geminin	AF067855
c-myb	M15024
ERBB-3	M29366; M34309
Diaphanous 1	AF051782
PTEN	U92436
ERBB4	L07868
CBL-B	U26710
Bub1	AF053305
Golgi 4-transmembrane spanning transporter; MTP	D14696
NEK2	U11050
CLK1	L29222
CDC25A	M81933
CCK4	U33635 + U40271
ILK	U40282
JNK1	L26318
GLYT-1	S70609
Tnk1	U43408
HEK	M83941
NET	M65105
PLC beta 3	Z16411

Sodium/potassium -transporting ATPase	D00099
Alpha-fetoprotein	V01514
IL6 receptor beta subunit	M57230
Rapamycin target protein	L34075
BAD	U66879
RalGDSB	U14417
adenosine A1 receptor	S56143
CD47	Y00815 + X69398
Adenylate cyclase type 1	L05500
CD95	M67454
Protein phosphatase 2B	D21878
ATM	U33841
Serine/threonine phosphatase 2B	L14778
IRF1	X14454
Ras p21 protein activator	M23379
Protein phosphatase 2C alpha	S87759
DNA ligase III	X84740
DNA-repair protein complementing XP-C cells	D21089
XRCC1	M36089
5-HT-3	D49394
DP1	L23959
YL-1	D43642
IRF2	X15949
BTF2p44	Z30094
ADA2-like protein	AF069732
NF-κB p100;p52	X61498
GABP-alpha	D13316
AREB6	D15050
BARD1	U76638
SMBP-2	L14754
GADD45 gamma	AF078078
GLRB	U33267
JNKK2	AF022805
NFATc	U08015
NERF2	U43188
Cadherin 5	X79981; X59796
CD106	M30257
IL3 precursor	M14743
Il2 receptor alpha precursor	X01057
HOXB7	M16937
Stem cell protein	M29038
PUR alpha	M96684
EBI3	L08187
MIP 1-beta	J04130
Il2 precursor	A14844
Puramycin sensitive aminopeptidase	Y07701
Heat shock related 70kd protein 2	L26336
Glutathione peroxidase	Y00483; M21304
70Kd HSP 1	M11717
TGF beta	X02812; J05114
MIP 1-alpha	M23452
Estrogen sulfotransferase	U08098
CD53	M37033

CD21 antigen	M26004
Insulin protease	M21188
IL4 precursor	M13982
TALLA-1	D10653
IRF2	X15949
PEBP2aC1	Z35278
HOX-D4	X04706; X17360
HEX	L16499
HIV-EP2	M60119
PAX-4	AB008913
SOX-3	X71135
MIZ-1 protein	Y09723
GLI3	M57609
CIITA	X74301
Insulin gene enhancer protein ISL1	U07559
centrin	U03270
TRANCE	AF013171
Granzyme H precursor	M36118
Defensin alpha 1	M21130
lymphocyte cytosolic protein 1	M22300
ETV1	U17163
NUP-98	U41815
Ectropic viral integration site protein 2A	M55267
CYP1A1 and CYP1A2	K03191 + M55053; M38504
(CYP51) + CYP51P1 +CYP51P2	U23942 + U36926 + U40053
sodium- & chloride-dependent creatine transporter 1 (CT1)	L31409
Golgi antigen gcp372	D25542
HUT2	X96969
Lumican precursor	U18728
Annexin IV	X05908
Beta'-COP	X70476
SNAP-25	L19761
ras-related protein RAB-11A	X53143
RAB-GDI beta	D13988
Man9-alpha-mannosidase	X74837
Phosphofructokinase 1	D25328
Aldehyde dehydrogenase E3 isozyme	U34252
PGAM	J04173
Apo-D	J02611
nonsecretory ribonuclease precursor	M28129
Ferritin heavy chain	M97164
ALDH2	Y00109
Ubiquitously expressed nuclear receptor	U07132
Pregnane X receptor	AF061056
TGF-beta 4	U81523
GDF8	AF019627
Natriuretic peptide precursor B	M25296
STAM	U43899
MAPKAP kinase 2	U12779
tyrosine-protein kinase syk	L28824

GRK4	L03718
PP2AB	M64929
Dual-specificty protein phosphatase HVH2	U21108
Regulator of G protein signaling 6	L40394
Regulator of G protein signaling 16	U70426
PLC-delta-1	U09117
14-3-3 protein theta	X56468
EBV-induced G-protein coupled receptor 2	L08177
BD73	L31785
Dynamin-1	L07807
MTBT1	J03778
Transmembrane protein 1	U19252
mucin	AF007194
BST-2	D28137
SMCY	U52191
Tetraspan net-5	AF089749
RNA pol II (RPB3)	J05448
RNA pol II (RPB2)	X63563
RNA pol II (RPB6)	Z27113
RNA POLYMERASE II (RPB7).	U20659
BN51 PROTEIN.	M17754
Zinc finger protein 76	M91592
NF-E2 related factor 2	S74017
Zinc finger protein 133	U09366
Zinc finger protein 140	U09368
Zinc finger protein 139	U09848
Zinc finger protein C2H2-25	U38904
Zinc finger protein 33A	X68687
ZINC FINGER PROTEIN CLONE 647 (FRAGMENT).	X16282
TAFII-28	X83928
Zinc finger HSAL2	X98834
Zinc finger (fragment)	L32164
E74-like factor 5	AF049703
H-2K binding factor-2	D14041
EFP	D21205
HKF-1	D76444
Transcription factor SL1	L39059
TAT-SF1	U76992
HPX-42B	AF068006
TFECL	D43945
RNA polymerase II terminaton factor	AF073771
RNPL	U28686
HS-II-T1	D50495
mitochondrial RNA helicase	AF042169
NASCENT POLYPEPTIDE ASSOCIATED COMPLEX ALPHA SUBUNIT.	X80909
HA0659	X79538
CSTF 64KD subunit	M85085
TRA-2 alpha	U53209
U1 SNRNP A protein	X06347
HU-antigen C	L26405
RBP56	X98893
TOB4 protein	D64109
CUL-4A	U58090

TP beta and TP gamma	U09087
DEL-1	U70312
Microfibril associated glycoprotein 4	L38486
P22 phagocyte B-cytochrome	M21186
Inositol 1,4,5-triphopshate receptor type 1	L38019
NK-tumour recognition protein	L04288
FKBP25	M90309
SCCE	L33404
bomapin	U35459
mRNA encoding C4.4 like	AJ223603
Polycomb 2 homolog	AF013956
HSP86	X15183
Yolk sac permease like 3	AF058317
HVDAC2	L06328
HPCN1	M55513
EC3.6.1.36	U02076
Chloride channel protein	AF026004
Two pore domain potassium channel	AF084830
Ca-activated potassium channel	U02632
Type 2 INSP3 receptor	D26350
Procollagen I N-proteinase	AJ003125
Collagen alpha chain 5	M31115
SKD1 homolog	AF038960
Syntaxin 6	AJ002078
adipophilin	X97324
NASP	M97856
TOM1-like protein	AJ010071
SRP14	X73459
Synaptotagmin VII fragment	AF038535
Homo sapiens putative 13 S Golgi transport complex 90kD subunit	AF058718
Angiogenin precursor	M11567
Sia alpha2,3galbeta1,4glcnAcalpha 2,8-sialtransferase	AF004668
ATPase protein 9	D13119
Malate dehydrogenase	D55654
Alpha-ETF	J04058
EC 1.9.3.1	J04823
UBIQUINOL-CYTOCHROME C REDUCTASE COMPLEX CORE PROTEIN 2 PRECURSOR	J04973
COX VIIA-M	M83186
ATPASE PROTEIN 9	U09813
Complex I-B17	AF035840
CTP:phosphocholine cytidylyltransferase b.	AF052510
TPST1	AF038009
alpha-ketoglutarate dehydrogenase complex dihydoelipoylsuccinyltransferase.	S72422
URO-D	M14016
DELTA-1-PYRROLINE-5-CARBOXYLATE DEHYDROGENASE PRECURSOR	U24266
MTHFS	L38928
cyclohydrolase mitochondrial precursor	X16396
Delta-ala synthetase	X56352
Prostatic acid phosphatase	X56352
PAM	M24902
glutaminyl cyclase	M37721

spermine synthase	X71125
Nitrilase homolog 1	Z49099
Carbonate dehydratase VI	AF069987
ASF	M57892
Acyl-CoA desaturase	X97868
CYP-60	L77701
Ribophorin II	U37220
H-SCO1	Y00282
40s ribosomal protein S17	M13932
TAR binding protein	M60801
60S ribosomal protein L35A	M15661
EF-1-beta	X60656
P43	L38995
EIF-2-beta	M29536
Statin S1	X70940
ARGRS	S80343
Proline tRNA ligase	X54326
TGF beta receptor assoc protein	AF022795
DHP1	U62647
ZAP-1	X99699
Splicing factor	L10911
U2 small ribonucleoprotein auxilllary factor	D49676
SNRPN	D49676
Nuclear riboprotein R	AF000364
RNASEP protein P30	U77665
DIM1P homolog	AF023612
H2A.X.	X14850
Heat stable enterotoxin receptor	L30117
BMP 11	AF100907
SNT-2	AF036718
Serine/threonine kinase	AB015982
LDL RECEPTOR RELATED PROTEIN 105.	AB009462
CAMK	L07044
SEC14-like protein	U79284
AS-like phosphodiesterase	Y08134
TRAP delta	X90583
Myosin RLC	J02854
MLC3F	M20643
Dysferlin	AF075575
PDZ domain containing protein	AF012281
TRIP10	L40379
MP78	U29366
UBIQUITIN CARBOXYL-TERMINAL HYDROLASE 12	U44839
Ubiquitin conjugating enzyme E2 G1	D78514
Ubiquitin conjugating enzyme E2	AF031141
26S PROTEASOME SUBUNIT S5B .	S79862
P26S4	AF031141
Gastrointestinal peptide	AF048700
Motor protein	D21092
plectin	U53204
P60 katanin	AF056022
MUTS homolog 4	U89293
RAD51-INTERACTING PROTEIN	AF006259

TSPAN-2	AF054839
MYLE	AF108145
SPOP	AJ000644
DGS-A	L77571
Pinch protein	U09284
POM-ZP3	U10099
KIAA0209	D86964